

Advanced Deep Learning and Large Language Models: Comprehensive Insights for Cancer Detection

Yassine Habchi^a, Hamza Kheddar^b, Yassine Himeur^c, Adel Belouchrani^d, Erchin Serpedin^e, Fouad Khelifi^f and Muhammad E.H. Chowdhury^g

^aInstitute of Technology, University Center Salhi Ahmed, Naama, Algeria

^bLSEA Laboratory, Electrical Engineering Department, Faculty of Technology, University of Medea, 26000, Algeria

^cCollege of Engineering and Information Technology, University of Dubai, Dubai, UAE

^dEcole Nationale Polytechnique/ LDCCP lab., El Harrach, Algiers, Algeria

^eECEN Department, Texas A&M University, College Station TX 77843-3128 USA

^fDepartment of Computer Science and Digital Technologies, Engineering and Environment, Northumbria University at Newcastle

^gDepartment of Electrical Engineering, Qatar University, Doha 2713, Qatar

ARTICLE INFO

Keywords:

Cancer diagnosis
Federated learning
Transfer learning
Reinforcement learning
Transformer-based learning
Large language models.

ABSTRACT

In recent years, the rapid advancement of machine learning (ML), particularly deep learning (DL), has revolutionized various fields, with healthcare being one of the most notable beneficiaries. DL has demonstrated exceptional capabilities in addressing complex medical challenges, including the early detection and diagnosis of cancer. Its superior performance, surpassing both traditional ML methods and human accuracy, has made it a critical tool in identifying and diagnosing diseases such as cancer. Despite the availability of numerous reviews on DL applications in healthcare, a comprehensive and detailed understanding of DL's role in cancer detection remains lacking. Most existing studies focus on specific aspects of DL, leaving significant gaps in the broader knowledge base. This paper aims to bridge these gaps by offering a thorough review of advanced DL techniques, namely transfer learning (TL), reinforcement learning (RL), federated learning (FL), Transformers, and large language models (LLMs). These cutting-edge approaches are pushing the boundaries of cancer detection by enhancing model accuracy, addressing data scarcity, and enabling decentralized learning across institutions while maintaining data privacy. TL enables the adaptation of pre-trained models to new cancer datasets, significantly improving performance with limited labeled data. RL is emerging as a promising method for optimizing diagnostic pathways and treatment strategies, while FL ensures collaborative model development without sharing sensitive patient data. Furthermore, Transformers and LLMs, traditionally utilized in natural language processing (NLP), are now being applied to medical data for enhanced interpretability and context-based predictions. In addition, this review explores the efficiency of the aforementioned techniques in cancer diagnosis, it addresses key challenges such as data imbalance, and proposes potential solutions. It aims to be a valuable resource for researchers and practitioners, offering insights into current trends and guiding future research in the application of advanced DL techniques for cancer detection.

1. Introduction

Researchers and clinicians face the formidable challenge of combating cancer, a leading cause of death globally. The World Health Organization has issued warnings about the anticipated increase in cancer-related deaths if effective solutions are not developed [1]. Consequently, early detection of cancer has become crucial for saving numerous lives. However, the traditional process of diagnosing cancer through manual inspection of medical images is error-prone and time-consuming, highlighting the urgent need for more accurate and efficient detection methods. The computer-aided diagnosis (CAD) systems have aided physicians by enhancing the accuracy and efficiency of medical image analysis, a task where feature extraction is crucial and heavily reliant on machine learning (ML) techniques [2]. While various feature extraction methods have been explored for different types of cancer, these approaches face inherent limitations that ML strives to overcome. Deep learning (DL), a subset of ML algorithms, has gained significant prominence due to its layered structure, which makes it highly effective in medical fields, particularly in response to the increasing patient numbers, rapid technological advancements, and the exponential growth of medical data [3]. The use of DL in medical diagnostics has broadened to cover a wide range of cancer types, including breast [4], lung [5], kidney [6], skin [7], leukemia [8], thyroid [9], brain cancer [10], among others. By leveraging its multi-layered architecture, DL outperforms traditional neural networks (Figure 1). The capability of DL algorithms to effectively extract diverse features from data underscores their importance, particularly in cancer detection. The architecture of convolutional neural networks (CNN), a prominent class of DL, mirrors the structure of the human visual cortex and is composed of multiple layers, including convolutional, pooling, and fully connected (FC) layers. CNNs excel at learning features directly from raw data without requiring human intervention, allowing them to develop hierarchical data representations that are highly valuable in image analysis [11].

* Dr. Hamza Kheddar is the corresponding author.

✉ habchi@cuniv-naama.dz (Y. Habchi); kheddar.hamza@cuniv-medea.dz (H. Kheddar); yhimeur@ud.ac.ae (Y. Himeur); adel.belouchrani@g.enp.edu.dz (A. Belouchrani); eserpedin@tamu.edu (E. Serpedin); fouad.khelifi@northumbria.ac.uk (F. Khelifi); chowdhury@qu.edu.qa (M.E.H. Chowdhury)

ORCID(s):

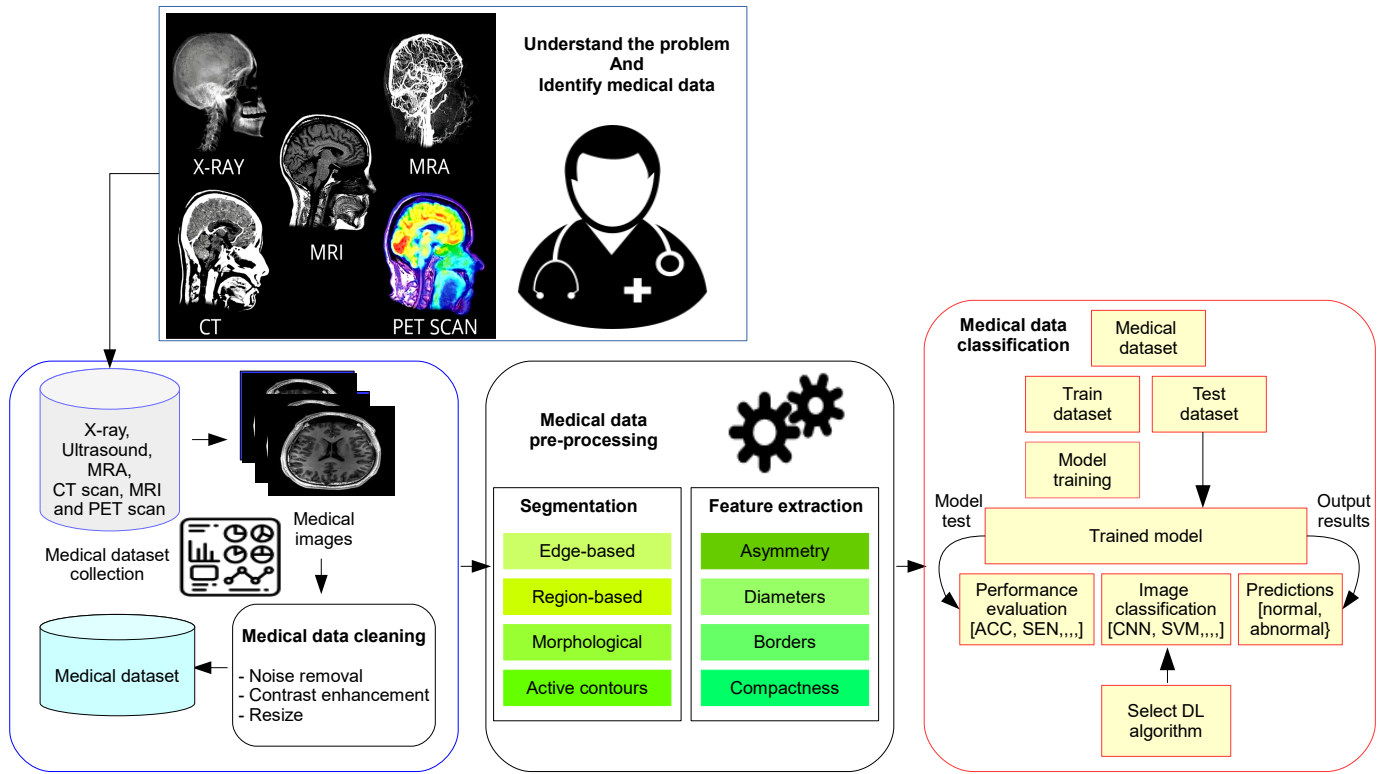


Figure 1: The general process of cancer detection via DL

Many methods are designed to efficiently classify diseases despite data imbalance. For example, the ENTAIL framework [12] demonstrates strong robustness on an unbalanced dataset, achieving high accuracy and sensitivity. However, limited dataset sizes and imbalanced data are particularly significant challenges in the field of medical cancer research. Collecting comprehensive cancer datasets is often constrained by privacy regulations, ethical considerations, and the high cost and complexity of medical procedures. Consequently, the available datasets tend to be small, especially for rare types of cancer, which can hinder the development of robust and generalizable ML models. This limitation can lead to overfitting, where models perform well on training data but fail to generalize to new, unseen data. Additionally, imbalanced data is a prevalent issue, as certain types of cancer are much more common than others. This imbalance can cause models to become biased towards the majority class, reducing their ability to accurately detect and diagnose less common cancers.

To address these issues, techniques such as data augmentation where synthetic data generation can be utilized to expand the size of training datasets, and transfer learning (TL) can be used [13, 14]. Moreover, federated learning (FL) offers a promising solution by enabling the training of ML models on decentralized datasets distributed across various institutions without the need to share sensitive patient data [15]. This will encourage patients to accept participating in gathering their own private data. This approach not only preserves privacy but also increases the diversity of data used in model training, which enhances the model robustness and generalizability. In addition, reinforcement learning (RL) can be employed in clinical decision-making, where models are trained to optimize treatment plans and diagnostic pathways by learning from their interactions with the environment [16, 17]. This adaptive learning strategy allows the system to continuously improve and personalize recommendations based on real-time data.

The emergence of Transformer-based models and large language models (LLMs) has further advanced the fields of computer vision and natural language processing (NLP) [18], and found applications in the analysis of medical data [19]. Unlike conventional DL models such as CNNs and recurrent neural networks (RNNs), which rely on localized feature extraction and sequential dependencies, Transformers introduce self-attention mechanisms that enable them to capture long-range dependencies and global contextual relationships across large datasets. This capability is particularly crucial in cancer diagnostics, where heterogeneous data sources—including medical images, electronic health records, and genomic sequences—must be analyzed holistically to improve diagnostic precision.

Transformers excel at processing sequential data and can be applied to medical records, imaging data, and genomics, providing enhanced interpretability and context-aware predictions [20]. Furthermore, LLMs, with their ability to process vast amounts of unstructured medical text, extend these capabilities by enabling automated medical reasoning and decision support. By leveraging large-scale textual and multimodal data, LLMs facilitate tasks such as medical literature review, patient history analysis, and clinical decision-making, surpassing traditional methods that primarily rely on structured data inputs. On the other side, traditional resampling methods, cost-sensitive learning, and ensemble techniques can help mitigate the effects of data imbalance, ensuring that ML models are more accurate and reliable across different types of cancer. By effectively integrating advanced techniques such as

FL, RL, Transformers, and LLMs alongside traditional methods, the performance and generalizability of artificial intelligence (AI) models in cancer diagnosis and treatment can be significantly improved.

Despite numerous reviews [3, 21], this coverage of ML in cancer detection often lacks depth, leading to an incomplete understanding of its challenges. This paper proposes to cover this gap by offering a comprehensive review of DL in cancer detection, discussing the key challenges, current applications, and most recent AI models. Our contribution includes an in-depth examination of the aforementioned algorithms TL, RL, FL, and Transformers, which are considered as the state-of-the-art DL tools, and highlight their key features. In addition, this paper overviews the contributions of DL in early detection of cancer as well as in improving the diagnosis and outcome prediction. Unlike other reviews that focus on specific aspects such as FL or TL [22, 23], this paper delves into a broader spectrum, including emerging techniques like RL, vision transformers (ViTs), and LLMs. While some reviews limit their discussion to particular cancers, such as lung or breast cancer [24, 25], this review offers a thorough analysis of multiple cancer types, showcasing the versatility of DL models across various domains. Additionally, other reviews such as [26] focuses solely on Transformers or omit certain advanced algorithms. In contrast, our review integrates these advanced algorithms alongside FL, RL, and LLMs, providing a more holistic view of their contributions to the detection of many types of cancer, including *skin, brain, thyroid, liver, kidney, pancreas, lung, leukemia, breast, cervical, ovarian, stomach, bladder, and colorectal* cancer. Furthermore, this review addresses critical gaps by exploring challenges such as data privacy, model scalability, and dataset limitations, topics that other reviews often overlook. By covering evaluation metrics, model performance, and the role of advanced architectures, our survey bridges the gaps in existing literature and offers valuable insights into the future potential of DL for improving cancer diagnosis and treatment planning. Table 1 presents a summary of the topics covered, highlighting the similarities and differences compared to existing reviews. It also identifies important topics often overlooked in the literature by current reviews, which our paper seeks to cover.

Table 1: Comparison with existing advanced DL-based cancer diagnosis. The markers \blacklozenge and \diamond signify that a specific topic has been addressed or ignored, respectively.

Ref	Year	The similarity with our review	Differentiate from our review	DL	RL	FL	TL	ViT	LLM
[22]	2023	The work highlights FL for disease detection, emphasizing its impact on diagnostic accuracy, data privacy, and model effectiveness.	This paper explores, in a general manner, various models for disease detection using FL alone. However in our paper, the disease type is identified as cancer.	\blacklozenge	\diamond	\blacklozenge	\diamond	\diamond	\diamond
[23]	2023	This study examines TL in medical image analysis, detailing its methods, applications, source and target data, and the use of public or private imaging datasets.	Compared to our work, it lacks exploration of other advanced DL techniques and fails to highlight the significance of these methods in cancer image analysis.	\blacklozenge	\diamond	\diamond	\blacklozenge	\diamond	\diamond
[27]	2024	In this work, RL has emerged as a dynamic and transformative paradigm in the field of AI, offering the promise of intelligent decision making, especially in robotics and healthcare.	Although RL is discussed, this work does not review its application in the context of cancer diagnosis. Moreover, it only presents a comparative study of RL algorithms, excluding others like LLMs and ViTs.	\blacklozenge	\blacklozenge	\diamond	\diamond	\diamond	\diamond
[28]	2024	The review offers a comprehensive analysis of the use of advanced AI models in healthcare.	The survey emphasizes the evolution of LLMs and their performance metrics in the biomedical domain, without mentioning the other methods used to detect cancer.	\blacklozenge	\diamond	\diamond	\diamond	\diamond	\blacklozenge
[24]	2024	This review highlights the DL techniques for lung cancer diagnosis. This study emphasizes the high performance of these models compared to traditional methods.	The review focuses on DL techniques such as CNN for lung cancer. It covers public datasets and addresses challenges in deploying models clinically, but did not examine the role of advanced DL in the diagnosis of several type of cancers.	\blacklozenge	\diamond	\diamond	\diamond	\diamond	\diamond
[26]	2024	This work explores Transformer models in healthcare, focusing on their application to complex data.	The provided work offers a broad overview types of Transformer applications in various healthcare settings, including surgical outcomes and drug synthesis, without delving into specific models or datasets related to cancer.	\blacklozenge	\diamond	\diamond	\diamond	\blacklozenge	\diamond
[25]	2024	The focus is on the application of DL techniques to breast cancer imaging.	This work explores discusses only DL techniques for cancer detection and focuses exclusively on applications for diagnosing of the breast cancer.	\blacklozenge	\diamond	\diamond	\diamond	\diamond	\diamond
[29]	2024	This article illustrates the importance of ViT for cancer diagnosis.	A comprehensive study on the application of ViTs in addressing intractable diseases is lacking, and other relevant algorithms have not been thoroughly explored either.	\blacklozenge	\diamond	\diamond	\diamond	\blacklozenge	\diamond
Ours	2024	This paper reviews the DL tools for cancer diagnosis by highlighting their key features and applications.	This survey first presents the conventional DL tools. Our survey first presents the background of conventional DL techniques, followed by advanced approaches for cancer diagnosis, including RL, FL, TL, LLMs, and ViTs. It examines their effectiveness, challenges, datasets, evaluation metrics, and potential to enhance detection, classification, and treatment.	\blacklozenge	\blacklozenge	\blacklozenge	\blacklozenge	\blacklozenge	\blacklozenge

The remaining of the paper is structured to provide a comprehensive review of DL in cancer detection. Section 2 offers background information on DL fundamentals. Section 3 overviews various DL training modes. Section 4 delves into the most commonly used advanced DL networks for cancer detection, namely TL, RL, FL, and Transformers. Section 5 discusses existing computational approaches. Section 6 addresses research challenges and future directions. Finally, Section 7 concludes this paper. Figure 2 illustrates the road-map structure of this review in terms of sections and subsections.

2. Background

This section presents the basics of DL, covering the necessary layers for building models in medical image recognition, such as convolutional, pooling, and FC layers. It also discusses the concepts of activation function activation functions (AFs), regularization, hyper-parameter optimization, training, and other essential components required to construct efficient DL models.

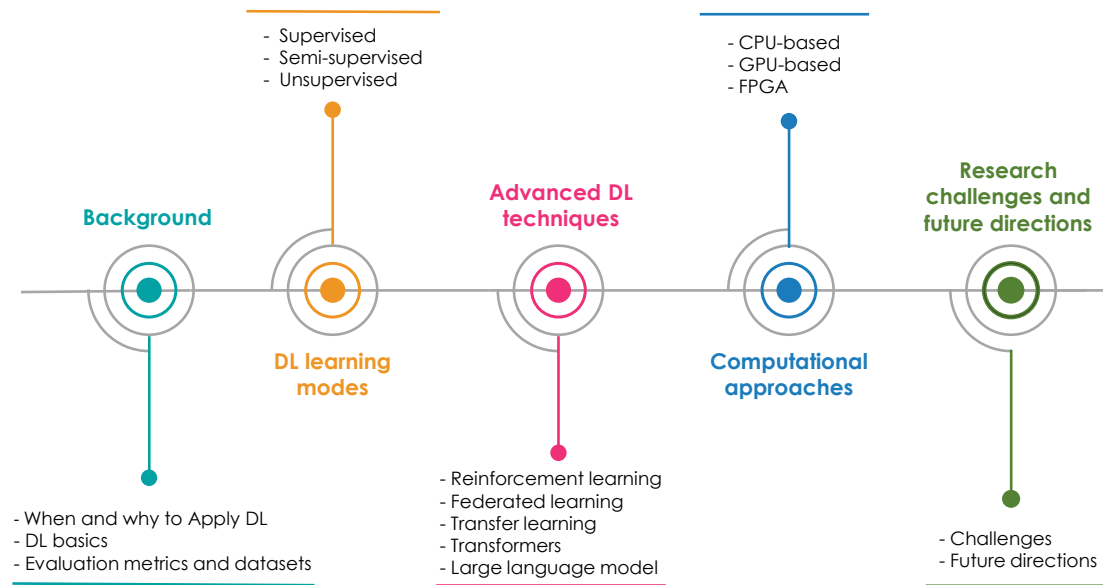


Figure 2: Road-map outlining the structure of the review.

2.1. When and why applying DL in the medical domain

DL is applied in the medical field when addressing complex tasks that require advanced data processing and interpretation. One key area is medical imaging, where DL models are used for classifying, segmenting, and detecting abnormalities in images, such as detecting tumors and diagnosing diseases from radiological scans. It plays a critical role in interpreting magnetic resonance imaging (MRI) and computed tomography (CT) scans to identify irregularities [30]. DL is also instrumental in disease diagnosis and prognosis by being capable to analyze vast datasets of medical records and images, providing more precise predictions and enabling personalized treatments for patients. In drug discovery and development, DL accelerates the process by analyzing molecular data to identify potential drug candidates, predict their effectiveness, and model their interactions with biological systems. Additionally, DL supports electronic health records (EHR) analysis by parsing large datasets to generate clinical insights, predict outcomes, and identify disease patterns. Genomics and precision medicine benefit from DL by analyzing genetic data to identify anomalies and predict disease risks, while NLP applications in healthcare aid in extracting information from unstructured medical texts [31].

DL is favored in the medical domain because of its ability to handle large-scale and complex data, such as medical images, genomic data, and electronic health records. Its capacity for feature extraction and representation learning allows it to automatically learn meaningful features from raw medical data, which is particularly useful for tasks like medical image analysis. DL models also provide improved accuracy and predictive power, often outperforming traditional methods and even surpassing human performance in certain diagnostic tasks. Another advantage is in personalized medicine, where DL leverages extensive patient data to customize treatment plans, improving disease management and treatment outcomes. Moreover, DL enhances efficiency by automating routine tasks, thus alleviating the workload on medical professionals and allowing them to focus on patient care. In research and drug discovery, DL accelerates the discovery process and helps reduce the cost and time involved in clinical trials. Finally, DL models continually improve their performance with more data, making them highly adaptable to the evolving needs of the medical field. Figure 3 summarizes the benefits of DL in the healthcare domain [32].

2.2. DL and CNN basics

DL has revolutionized medical image analysis by enabling automated feature extraction and hierarchical representation learning. Unlike traditional ML approaches that require handcrafted feature engineering, DL models, particularly CNNs, learn patterns directly from raw medical images, improving accuracy and diagnostic reliability. These models leverage multiple layers, including convolutional layers for spatial feature extraction, pooling layers for dimensionality reduction, and fully connected layers for classification. Regularization techniques and optimization strategies further enhance model generalization and performance.

CNNs have been widely applied in *cancer detection*, excelling in tumor segmentation, classification, and localization. Their hierarchical structure allows them to capture intricate patterns within medical images, making them highly effective for tasks such as identifying malignant lesions in radiology scans. Table 2 summarizes the main CNN components and their roles in cancer detection. Unlike traditional ML-based CAD systems, CNNs automatically extract tumor-related features without requiring manual selection, streamlining the diagnostic process and improving efficiency. Table 3 summarizes the most frequently used activation, loss, and pooling functions in DL, particularly in CNN-based approaches.

2.3. Evaluation metrics and datasets

When evaluating the performance of DL, Transformers, and LLM models, selecting an appropriate metric is of paramount importance. Numerous metrics have been proposed and employed across various DL applications [33, 34]. Table 4 presents a concise summary of commonly used metrics that are particularly suited for assessing the performance of AI algorithms in cancer

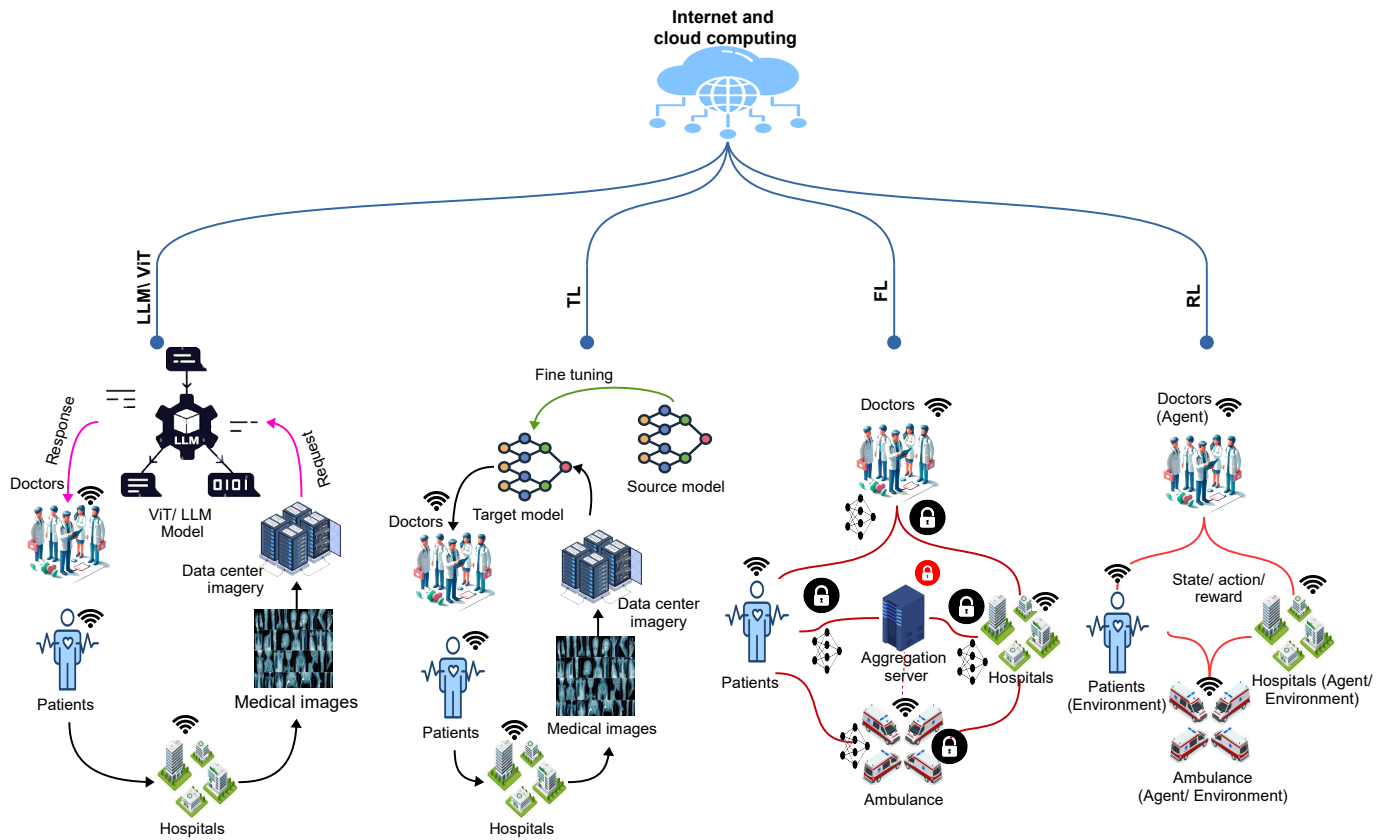


Figure 3: Application of advanced DL methods in healthcare, showcasing technologies such as RL, FL, TL, ViT, and LLMs. It highlights scenarios like real-time decision-making, privacy-preserving model training, and personalized treatment. The ecosystem integrates agents like hospitals, doctors, and ambulances with cloud computing, pretrained models, and aggregation servers. Key use cases include optimizing resource allocation, enhancing diagnostic accuracy, and improving scalability. Advanced DL solutions address challenges such as data privacy, limited labeled datasets, and computational efficiency, ultimately supporting accurate, efficient, and personalized patient care [32].

Table 2
Key CNN components for cancer detection.

Component	Function	Relevance to cancer detection
Convolutional layer	Extracts spatial features by applying filters to input images.	Detects tumor patterns and abnormal tissue structures.
Pooling layer	Reduces feature map size, preserving key information.	Enhances computational efficiency without losing critical features.
Activation function	Introduces non-linearity to improve model learning.	Helps differentiate between cancerous and non-cancerous regions.
Fully connected layer	Aggregates extracted features for final classification.	Used to distinguish between cancer types or stages.
Regularization (Dropout, Batch norm.)	Prevents overfitting by stabilizing learning.	Improves model generalization to unseen medical data.

detection. Additionally, several datasets have been employed in recent years across various medical domains to evaluate performance and accelerate progress. Table 5 lists the most widely used datasets in different medical applications.

¹<http://cimalab.intec.co/?lang=en&mod=project&id=31>

²<http://homes.di.unimi.it/scotti/all/>

³https://archive.ics.uci.edu/ml/datasets/chronic_kidney_disease

⁴<https://web.inf.ufpr.br/vri/databases/breast-cancer-histopathological-database-breakhis/>

⁵<https://dataverse.harvard.edu/dataset.xhtml?persistentId=doi:10.7910/DVN/DBW86T>

⁶<https://luna16.grand-challenge.org/>

⁷<https://www.cancerimagingarchive.net/collection/prostatex/>

⁸<https://www.cancerimagingarchive.net/collection/stageii-colorectal-ct/>

⁹<https://paip2019.grand-challenge.org/Dataset/>

¹⁰<https://www.synapse.org/Synapse:syn51156910>

¹¹<https://cdas.cancer.gov/datasets/plco/10/>

Table 3

Types of functions used in CNN-based cancer detection.

	Function	Mathematical formula	Role overview
Activation functions	Sigmoid	$f(x) = \frac{1}{1 + e^{-x}}$	The input is real numbers, while the output is between "0" and "1".
	Tanh	$f(x) = \frac{e^x - e^{-x}}{e^x + e^{-x}}$	Its input is real numbers, and the output is between -1 and 1.
	ReLU	$f(x) = \max(0, x)$	It converts the input values to positive numbers and presents low computational complexity. Is characterized with lower computational load.
	Leaky ReLU	$f(x) = \begin{cases} x, & x > 0 \\ m.x, & x \leq 0 \end{cases}$	It has a small slope for negative values. It is employed to overcome the Dying ReLU problem. m: the leak factor.
	Noisy ReLU	$f(x) = \max(x + Y)$	It employs a Gaussian distribution $Y \sim N(0, \sigma(x))$ to create ReLU noisy.
	Parametric linear units	$f(x) = \begin{cases} x, & x > 0 \\ a.x, & x \leq 0 \end{cases}$	It is similar to Leaky ReLU, but it differs in that the leak factor is updated during the model training process. a: learnable weight.
Loss functions	SLF	$H(p, y) = -\sum_i y_i \log(p_i),$	Is employed for measuring the performance. $P_i = \frac{e^{a_i}}{\sum_{k=1}^N e_k^a}, i \in [1, N]$ Its output is the probability $p \in [0, 1]$.
	ELF	$H(p, y) = \frac{1}{2N} \sum_{i=1}^N (p_i - y_i)^2$	It is called mean square error and is used in regression problems.
	HLF	$H(p, y) = \sum_{i=1}^N \max(0, m - (2y_i - 1)p_i)$	It is employed in binary classification problems; this is important for SVMs.
Pooling functions	Max pooling	$y = \max(x_i)$	Retains the most significant feature by selecting the maximum activation in each pooling region. Preserves texture details.
	Average pooling	$y = \frac{1}{n} \sum_{i=1}^n x_i$	Averages the activations in each pooling region. Helps retain background information.
	Global pooling	$y = \frac{1}{N} \sum_{i=1}^N x_i$	Reduces feature maps to a single value per channel, helping in model regularization. Often used in fully convolutional architectures.
	Stochastic pooling	$P(x_i) = \frac{x_i}{\sum_j x_j}$	Randomly selects activation based on a probability distribution. Helps prevent overfitting.
	Rank-based pooling	$y = \text{Rank}(x_i)$	Ranks the activations instead of selecting absolute values. Offers stronger robustness in noisy environments.
	Ordinal pooling	$\text{Sort}(x_1, x_2, \dots, x_n)$	Sorts activations in ascending or descending order to retain structured information. Speeds up training.

3. Training modes in DL

DL techniques can be trained using three primary modes: supervised learning (SL), semi-supervised learning (SSL), and unsupervised learning (USL). A detailed explanation of each mode is provided below, along with examples relevant to their respective category. Table 7 provides an overview of state-of-the-art studies employing these DL training modes for various cancer detection applications. Table 6 provides an overview of these modes, their applications in cancer detection, and their key limitations.

3.1. Deep SL

Deep SL is a specialized branch of ML that trains algorithms to predict or make decisions based on labeled data sets. The primary objective of deep SL is to develop a function that maps inputs to outputs by identifying patterns within the data. The "deep" aspect of SL pertains to the application of deep neural networks (DNN), which are characterized by multiple hidden layers. Training involves iterative adjustments of the network's weights and biases to reduce the disparity between its predictions and the actual labels, usually employing a loss function (LF) to measure this difference. Back-propagation is used to update parameters and incrementally enhance performance.

In the context of image processing, SL can be further divided into two sub-categories: fully-supervised DL and weakly-supervised DL algorithms. Fully-supervised DL algorithms require segmentation—either manual or automated and cropping of the region of interest (ROI) before inputting the data into classifiers. In contrast, weakly-supervised DL algorithms do not require image annotation of the lesion's ROI. Instead, they leverage class activation maps generated by incorporating a global average pooling (GAP) layer into the final convolutional layer to visualize detected regions. Figure 4 illustrates a comparison between weakly-supervised and fully-supervised DL algorithms for breast mass classification and localization.

Many studies employing advanced DL rely on SL. For example, in [48], the authors explore the use of TL and SL techniques to enhance the classification of breast cancer histopathology images. The proposed approach aims to automate the differentiation between benign and malignant tissue by employing various feature extractors and classifiers, addressing challenges associated with image analysis. Moreover, in [49], the authors examine how FL can facilitate the detection of boundaries in rare cancers using big data. This research highlights the integration of FL with SL techniques to enhance the accuracy and effectiveness of cancer boundary detection while protecting patient privacy. At the same time, it enables the use of diverse datasets to improve the model's performance in detecting rare cancer types. Moving forward, the study [50], proposes a two-stage transformer-based

Table 4

Summary of metrics used in evaluating DL, Transformers, and LLM-based cancer detection.

Task type	Metric	Description
Classification	$Acc = \frac{T_p + T_N}{T_p + F_p + T_N + F_N}$	Gives the correct percent of the total number of positive and negative predictions.
Classification	$Spe = \frac{T_N}{T_N + F_p}$	It is the ratio of correctly predicted negative samples to the total negative samples.
Classification	$Sen = \frac{T_p}{T_p + F_N}$	It is a quantifiable measure of real positive cases predicted as true positive cases.
Classification	$P = \frac{T_p}{T_p + F_p} 100\%$	Measures the proportion of true positive predictions made by the model, out of all positive predictions.
Classification	$F1 = 2 \times \frac{Precision \times Recall}{Precision + Recall}$	It is the harmonic mean of precision and sensitivity of the classification.
Classification	$NPV = \frac{T_N}{T_N + F_N}$	The proportion of negative results in diagnostic tests; a higher value indicates better diagnostic accuracy.
Similarity	$JSC = \frac{ A \cap B }{ A \cup B } = \frac{T_p}{T_p + F_p + F_N}$	Proposed by Paul Jaccard to gauge the similarity and variety in samples.
Error rate	$FPR = \frac{F_p}{F_p + T_N} = 1 - SP$	Measures the proportion of negative samples incorrectly classified as positive by the model.
Correlation (ViT and LLM)	$MCC = \frac{T_p \cdot T_N - F_p \cdot F_N}{\sqrt{(T_p + F_p)(T_p + F_N)(T_N + F_p)(T_N + F_N)}}$	Assesses binary classification by balancing true/false positives and negatives across varying class sizes.
Adversarial robust (ViT and LLM)	$FR = \frac{\text{Number of samples with changed predictions}}{\text{Total number of adversarial samples}}$	Measures misclassified samples after adversarial manipulation, crucial for attack evaluation.
Anomaly detection (ViT and LLM)	$AS = \frac{\text{Score} - \text{Max baseline score}}{\text{Baseline standard deviation}}$	Assesses anomaly deviations from normal activity, adjusting thresholds to balance false positives and negatives.

Abbreviations: Accuracy (Acc); Alert score (AS); Specificity (Spe); Sensitivity (Sen); Fooling rate (FR); Matthew's correlation coefficient (MCC); Fallout or False positive rate (FPR); Jaccard similarity index (JSI); Negative predictive value (NPV); F1 score (F1); Precision (P).

Table 5

Summary of the most commonly used datasets in different cancer type.

Datasets	Available?	Format	Bit per pixel	Resolution	N of images	Type of images	Application	Related work
DDTI	Yes ¹	JPG	8-bit	-	134	Ultrasound images	Thyroid	[35]
ALL-IDB	Yes ²	JPG	24-bit	2592x1944	108	Microscope images	Leukemia	[36]
TCGA	Yes ³	TIFF, DICOM	16-bit	1000x1000	-	Histopathological, radiology	Kidney	[37]
BreakHis	Yes ⁴	JPEG	8-bit	700x460	7,909	Histopathological	Breast	[38]
HAM10000	Yes ⁵	JPEG	8-bit	600x450	10,015	Dermatoscopic	Skin	[39]
LUNA16	Yes ⁶	-	16-bit	512x512	1,200	Lung CT	Lung	[40]
ProstateX	Yes ⁷	DICOM	16-bit	384x384	1,000	Prostate MRI	Prostate	[41]
TCIA - Colorectal Histology	Yes ⁸	PNG	8-bit	150x150	5,000	Histopathological	Colorectal	[42]
PAIP 2019	Yes ⁹	TIFF	16-bit	20kx20k	100	Histopathological	Liver	[43]
BraTS 2023 dataset	Yes ¹⁰	NIFTI	16-bit	240x240x155	15,000	MRI	Brain	[44]
NIH Pancreatic	Yes ¹¹	DICOM	16-bit	512x512	100+	MRI	Pancreatic	[45]

weakly SL framework, called SSRViT, to support histo-pathological diagnosis of lung cancer. Due to the large size of whole-slide images and the difficulty of obtaining precise annotations, SSRViT aims to leverage weak labels for efficient learning. The framework uses a Shuffle-remix ViT to extract discriminative local features, which are then aggregated for slide-level classification via a simple transformer-based classifier. The method demonstrates superior performance in distinguishing between lung adenocarcinoma, pulmonary sclerosing pneumocytoma, and normal lung tissue. Sushil et al. [51] explored the use of LLMs to reduce the need for extensive data annotation in breast cancer pathology. A manually labeled dataset of 769 reports with 13 categories was used to compare the zero-shot classification performance of generative pretrained transformer (GPT)-4 and GPT-3.5 with traditional supervised models like random forests, long short-term memory (LSTM)-Attention, and UCSF-bidirectional encoder representations from transformers (BERT). GPT-4 performed as well as or better than the best SL models, particularly in handling imbalanced label tasks. The findings suggest that LLMs can significantly reduce the labor-intensive data labeling process, advancing cancer diagnosis without sacrificing accuracy.

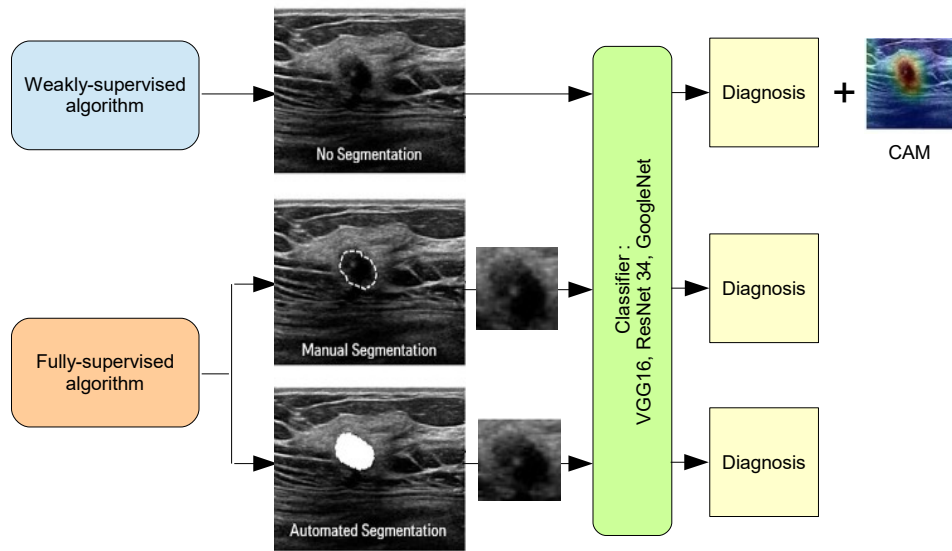
3.2. Deep USL

Deep USL is a branch of ML where neural networks are trained on large datasets without specific guidance or supervision. Unlike SL, which use labeled data, USL aims to identify inherent patterns and structures in the data autonomously. A prevalent

Table 6

Overview of DL training modes for cancer diagnosis.

Training mode	Key characteristic	Application in cancer diagnosis	Limitations
SL	Requires labeled data for training	Used in cancer image classification, tumor segmentation, and disease diagnosis with well-annotated datasets [46].	High labeling cost; performance depends on dataset quality; limited generalization to unseen data.
SSL	Uses a mix of labeled and unlabeled data	Reduces the reliance on labeled data, making it useful for medical imaging where obtaining labeled samples is costly. Applied in histopathology and radiology [20].	Performance is sensitive to the proportion of labeled data; risk of learning incorrect patterns from noisy unlabeled data.
USL	Extracts patterns from unlabeled data	Used in clustering cancer subtypes, anomaly detection in medical images, and identifying novel biomarkers [19].	Lack of ground truth validation; difficult to interpret results; risk of overfitting to irrelevant patterns.

**Figure 4:** SL for ultrasound diagnosis of breast cancer images using both fully-supervised and weakly-supervised DL algorithms [47].

technique in deep USL is the use of auto-encoder (AE)s, which are designed to compress data into a lower-dimensional space before reconstructing it to its original form, thereby learning the essential structures and features without labels. Other significant methods in deep USL include generative adversarial networks (GANs), which learn to create new data mimicking the original by understanding its distribution. Clustering is another common unsupervised strategy. Deep USL's primary benefit is its ability to reveal critical data features that are not readily visible, aiding in tasks such as image recognition where it can uncover crucial visual patterns like edges and textures. This insight can improve the accuracy and robustness of models for tasks like object recognition. However, deep USL presents several challenges: (1) *Interpretability*: The complexity of deep USL models makes it difficult to interpret how decisions are made or to diagnose errors effectively. (2) *Data requirements*: Deep USL requires large datasets for effective learning; insufficient data may hinder accurate pattern recognition. (3) *Model complexity*: Deep USL models, often consisting of numerous layers and parameters, can complicate training and demand significant computational resources and time. (4) *Fine-tuning issues*: While deep USL excels at learning general features, adapting these models to specific tasks remains challenging. (5) *Noise sensitivity*: These models are vulnerable to noise, which can mislead the learning process and obscure relevant patterns. (6) *Pattern bias*: Deep USL may introduce bias towards certain patterns or data points, potentially reducing diversity in the learned features [52, 53].

In this context, numerous studies have been proposed in the literature, with many schemes adopting AE as the primary unsupervised approach, as depicted in Figure 5. For example, the study [55] employed USL and TL to assess epidermal growth factor receptor mutation status in lung cancer using CT images. A convolutional AE was developed to reconstruct images and extract features from three ROI: the nodule, the lung containing the nodule, and both lungs. By leveraging TL, the model improved feature extraction and analysis. The study found that analyzing beyond the nodule captured more relevant information, enhancing prediction accuracy. Bercea et al. [56] introduce FedDis, a novel FL approach that integrates USL to address data heterogeneity in medical imaging. FedDis disentangles model parameters into shape and appearance components, sharing only the shape parameters among clients. This method leverages the assumption that anatomical structures in brain MRI images are consistent across institutions, improving anomaly detection, such as cancer identification. By utilizing healthy brain scans from various sources, FedDis segments abnormal structures in pathological databases, including Glioblastoma cases. Similarly, Stember et al. [57] propose a method that combines USL (clustering) with RL to segment brain lesions in MRI scans. Initially, clustering generates candidate lesion masks for each image. Users then select the best mask for a subset of images, which is subsequently used to train an RL algorithm to identify the optimal masks. This approach was compared to a U-net SL network. While the SL model suffered from overfitting

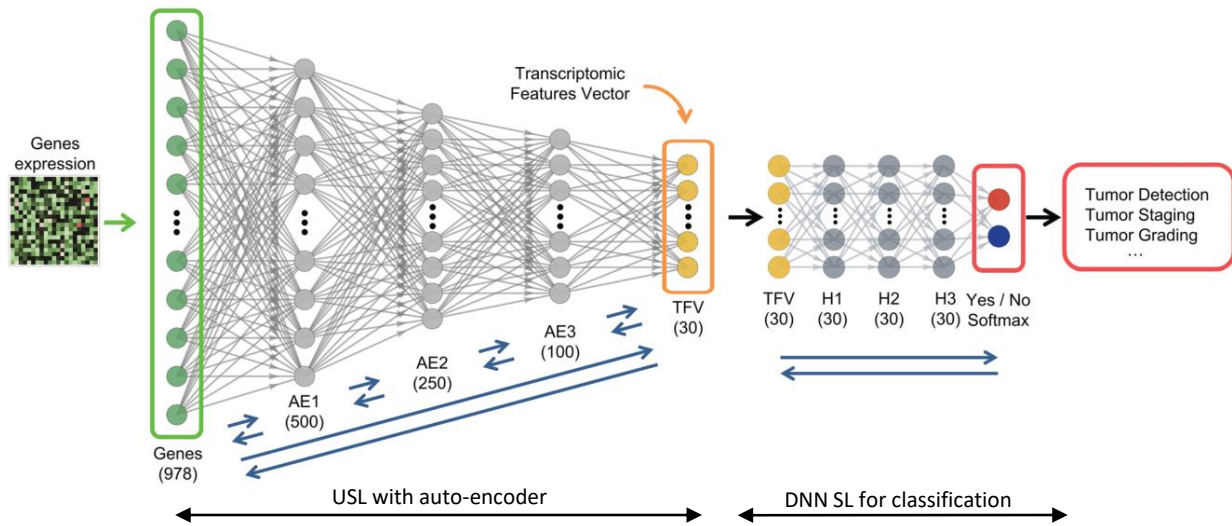


Figure 5: An example on USL for cancer diagnosis using AE [54]. A 5-layer AE is trained in an USL manner to extract features from high-dimensional gene expression data, compressing them into a 30-dimensional transcriptomic feature vector. These feature vectors are subsequently used for supervised training in a fully connected deep softmax classifier, which distinguishes between normal and tumor samples and classify tumors by grade and stage.

and performed poorly, the combined USL and RL approach achieved a high Dice score, demonstrating its effectiveness in lesion segmentation with minimal radiologist input. Additionally, Pina's study [58] addresses the challenges of digital pathology image analysis for breast cancer, focusing on the variability in histopathological slides and differences in staining techniques. The manual annotation of large datasets across different stains (Estrogen receptor, progesterone receptor, human epidermal growth factor receptor 2, and Ki-67 protein) is highly labor-intensive. To overcome this, the study applies USL combined with domain adaptation techniques and ViT to enhance cell detection tasks. By leveraging adversarial feature learning, the research improves pipelines for CAD, significantly boosting diagnostic accuracy across various staining methods. Moving forward, the study [59] presents a comprehensive exploration of USL techniques, which were employed using topic modeling methods such as latent Dirichlet allocation (LDA), non-negative matrix factorization (NMF), and combined topic models (CMT). These unsupervised methods were applied to analyze and categorize large volumes of text data from the Web of Science and LexisNexis concerning discussions on LLMs. The use of USL enabled the study to evaluate topic coherence and diversity across different models, with BERTopic emerging as a top performer in both metrics [60].

3.3. Deep SSL

Deep SSL is a strategy that merges the strengths of SL and USL. In SL, models are trained with labeled data, while USL involves training with unlabeled data. Deep SSL use a mix of a small set of labeled data with a significantly larger batch of unlabeled data, enhancing the training process under conditions where labeled data is scarce or costly to acquire. This hybrid approach allows the labeled data to steer the learning while the unlabeled data aids in discerning broader data attributes. However, several challenges impact its effectiveness: (1) *Data quality and quantity*: The efficacy of a deep SSL model is highly reliant on the volume and quality of the available unlabeled data. Insufficient or non-representative unlabeled data can degrade model performance. (2) *Data distribution*: Performance can also suffer from disparities in the distribution between labeled and unlabeled data, especially if labeled data represents limited classes. (3) *Hyperparameter selection*: Deep SSL requires careful tuning of numerous hyperparameters such as the amount of labeled versus unlabeled data, the strength of regularization, and learning rates, which can be complex and time-consuming to optimize. (4) *Model interpretability*: The complexity of DNN architectures in deep SSL makes it challenging to interpret how decisions are made or to pinpoint which data features are most influential in those decisions. (5) *Adversarial vulnerability*: Deep SSL models are susceptible to adversarial attacks, where manipulated inputs can lead the model to incorrect outputs [73]. Figure 6 illustrates a colorectal cancer study where SSL and SL are applied to labeled and unlabeled image patches from 70% of Dataset-PATT, generating models. Patient-level tests and human-AI competitions classify subjects as cancerous if clusters of positive patches are detected in whole slide images.

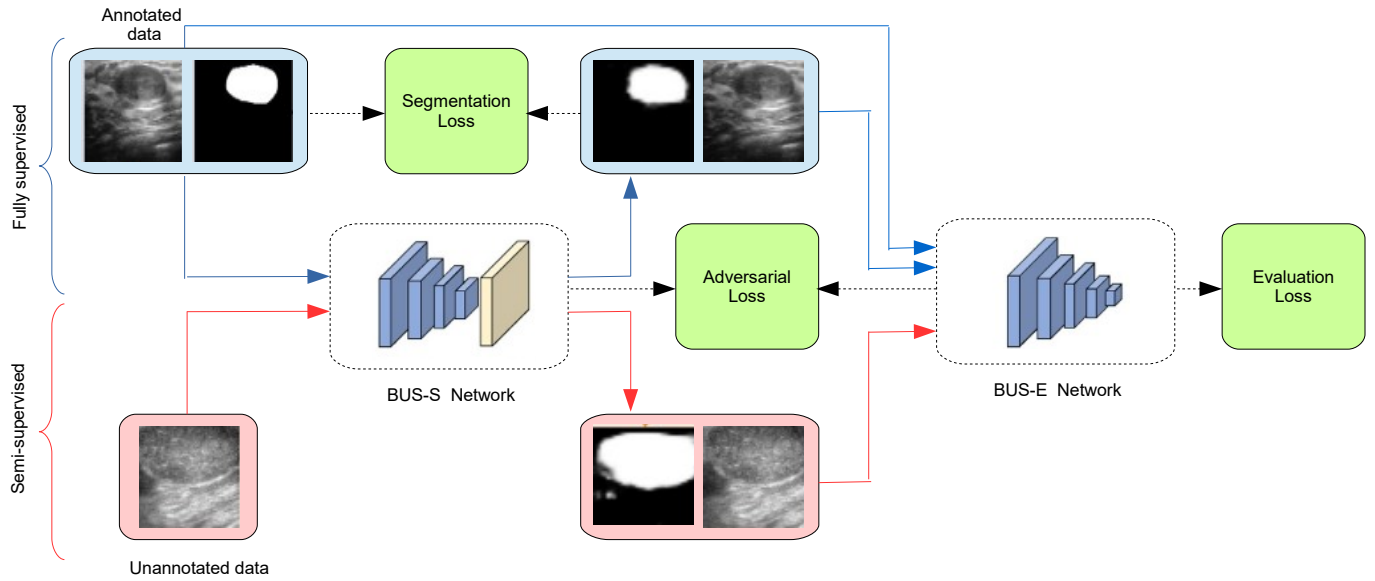
The study [69], proposes SDTL framework for diagnosing benign and malignant pulmonary nodules. By utilizing TL and an iterated feature-matching-based SSL method, the model benefits from both a pre-trained classification network and a large dataset of unlabeled nodules. The SDTL framework gradually incorporates unlabeled samples to optimize the classification network. Experimental results show that TL and SSL significantly improve diagnostic accuracy, highlighting the framework's potential as an effective tool in clinical practice for lung nodule diagnosis. In addition, Bdair et al. [74], introduces FedPerl, a semi-supervised FL method for skin cancer detection that addresses the challenge of limited annotated data. FedPerl integrates peer learning and ensemble averaging to improve pseudo label accuracy by fostering collaboration among distributed clients. Unlike previous methods, [75] introduces DGARL, a novel approach for end-to-end semi-supervised segmentation of medical images, including cancer detection. DGARL combines deep RL with GANs, improving both tumor detection and segmentation tasks simultaneously.

Table 7

Summary of classification examples employing various training modes in different medical domains.

Ref.	Year	C	Algo.	Disease	Dataset	Modality	Metrics					
							Acc.	F1	FPR	AUC	Pre.	Sens.
[50]	2024	DSL	ViT	Lung Cancer	TCGA-LUAD	Whole Slide Images	96.90	–	–	99.60	–	–
[51]	2024	DSL	LLM	Breast cancer	BreaKHis	Pathology Images	–	83.00	–	–	–	–
[55]	2021	DUSL	TL	Lung cancer	LIDC-IDRI	Chest CT Images	–	–	–	68.00	–	–
[61]	2024	DSL	LLM	Multiple cancers	TCGA PatchCamelyon	Histopathology	90.00	–	80.00	–	–	–
[62]	2023	DSL	TL	Lung cancer	LIDC-IDRI	DICOM	96.00	–	–	95.84	–	–
[63]	2022	DSL	TL	Lung cancer	LIDC-IDRI, LUNA16	CT Scans	91.10	81.50	–	95.80	84.9	–
[64]	2020	DSL	TL	Breast cancer	INbreast, DDSM	Mammography	89.77	88.91	–	–	–	83.78
[65]	2023	DSL	FL	Multiple Cancers	Histopath. images	JPEG, PNG	96.66	96.64	–	–	97.14	–
[66]	2023	DSL	FL	Lung Cancer	LUNA16	CT Scans	83.41	83.40	–	88.38	83.41	83.38
[67]	2023	DSL	FL	Breast Cancer	VINDR-MAMMO, CMMD, INbreast	Mammography	95.00	–	–	–	–	–
[68]	2023	DSL	ViT	Breast cancer	Thermal dataset	Thermal Images	95.78	–	–	–	–	–
[69]	2021	DSSL	TL	Pulmonary nodules	LUNA16	Chest CT Images	88.30	–	–	91.00	–	–
[70]	2023	DSSL	TL	Skin cancer	Custom dataset	2D Dermoscopy	98.00	98.00	–	–	–	98.00
[71]	2023	DSSL	TL	Prostate cancers	Custom dataset	PET/CT 3D PET/CT	83.00	–	–	86.00	–	–
[72]	2024	DSSL	ViT	Breast cancer	BreakHis	Histopath. Images	98.12	98.41	–	–	98.17	–

Abbreviations: Category (C);

**Figure 6:** An example on recognition of breast cancer with SSL [47].

This method incorporates a task-joint GAN with two discriminators to link detection outcomes with segmentation performance, enabling mutual optimization. Furthermore, a bidirectional exploration RL technique is employed to address challenges associated with unlabeled data. Experiments conducted on datasets of brain, liver, and pancreas tumors demonstrate that DGARL enhances segmentation accuracy, underlining its potential effectiveness in cancer diagnosis. Wang et al. [72] propose a SSL framework for breast cancer detection using the ViT, which has demonstrated superior performance compared to traditional CNNs across various tasks. While CNNs have been extensively studied for breast cancer detection, the use of ViT in this domain has been relatively limited. Nonetheless, validation on ultrasound and histopathology datasets reveals that this method consistently outperforms CNN baselines across multiple tasks. Kumari et al. [76] introduce LLM-SegNet, a SSL model for 3D medical image segmentation, including cancer imaging, that reduces the reliance on extensive voxel-level annotations. By incorporating a LLM into its co-training framework, LLM-SegNet improves learning from unannotated samples, enhancing the model's ability to identify cancerous regions.

Table 8

Comprehensive comparison of advanced DL techniques for cancer diagnosis.

DL method	Scalability	Real-world implementation	Computational complexity	Accuracy	Privacy considerations	Research gaps
RL	Moderate (limited scalability due to need for interactions with environment and reward structure complexity)	Used for tumor segmentation, automated lesion localization, and personalized treatment planning by continuously refining predictions based on rewards [18].	High (trial-and-error learning requires significant computational resources)	High (if well-defined reward functions are used)	Low (centralized data required for training)	Limited application in cancer detection; requires large datasets for effective learning.
FL	High (scalable across institutions without data sharing)	Trains models across decentralized datasets from different hospitals, enhancing generalizability while ensuring patient data confidentiality [20].	Moderate (network bandwidth and encryption overhead affect performance)	Comparable to centralized models (when sufficient data diversity exists)	High (data remains decentralized, improving security)	Model divergence, communication delays, and potential security risks in distributed learning.
TL	High (leverages pre-trained models for adaptation)	Fine-tunes pre-trained models on cancer imaging datasets, improving accuracy with minimal labeled data [19].	Low (reduces training time by reusing pre-trained models)	High (if source and target domains are well-matched)	Moderate (requires labeled data, but training can be privacy-preserving)	Domain shift challenges when applied to different datasets.
Transf.	High (well-suited for large-scale datasets)	Improves feature extraction in cancer histopathology, radiology, and genomics by leveraging self-attention mechanisms [77].	Very (self-attention computations expensive)	High (state-of-the-art performance in medical imaging tasks)	Low (requires centralized data for training)	Overfitting in small medical datasets; high resource requirements.
LLM	Moderate (requires fine-tuning for specific medical applications)	Assists in clinical decision-making by analyzing patient histories, summarizing pathology reports, and automating medical literature reviews [46].	Very (pretraining inference computationally demanding)	High (excellent for text-based analysis, but needs domain adaptation)	Low (requires centralized data for pre-training, posing privacy risks)	Ethical concerns, hallucination issues, and regulatory challenges in healthcare applications.

Experimental results on multiple datasets demonstrate that LLM-SegNet outperforms existing models in terms of segmentation accuracy.

4. Advanced DL techniques

To improve cancer diagnosis, various advanced DL techniques have been integrated into medical applications. This section summarizes key proposed techniques, emphasizing their effectiveness. Table 8 presents an overview, detailing their advantages and specific applications in cancer detection.

4.1. Reinforcement learning

RL is a ML paradigm in which an agent learns to make decisions by interacting with an environment, aiming to maximize cumulative rewards over time. The agent selects actions based on a policy (π) that maps states (s) to actions (a), receiving feedback in the form of rewards (r) from the environment. RL problems are typically modeled as Markov decision processes (MDPs), where the agent's objective is to learn an optimal policy that maximizes long-term returns. Various types of RL have been explored in the literature (Figure 7), with a summary of their key findings presented in Table 9. While most RL approaches have already been reviewed in [78], the most commonly employed types in cancer diagnosis include:

4.1.1. Q-learning and DQN

Aims to find the optimal action-selection policy by maximizing cumulative rewards in a given environment. However, Q-learning struggles to handle large state spaces where storing a Q-table becomes inefficient. To address this, the deep Q-network (DQN) algorithm extends Q-learning by using neural networks to approximate the Q-values, solving problems with large, discrete action spaces. DQN introduces experience replay and target networks, which decouple the target and learned Q-values, stabilizing learning. This approach is particularly useful in environments where exploration is critical. The key functions associated with the DQN are [75, 81]: (i) The Q-function approximates the expected cumulative reward of taking an action a in a given state s and following the policy afterward, $Q(s, a) = \mathbb{E}[R_t | s_t = s, a_t = a]$, where, $Q(s, a)$ is the Q-value (action-value), s is the state, and a is the action and R_t is the cumulative reward from time t onward. (ii) The update rule for DQN based on the Bellman equation is:

$$Q(s, a) \leftarrow Q(s, a) + \alpha \left(r + \gamma \max_{a'} Q(s', a') - Q(s, a) \right) \quad (1)$$

Where r is the reward received after taking action a in state s , s' is the next state and γ is the discount factor, and α is the learning rate. (iii) The loss function minimizes the difference between the target and predicted Q-values:

$$L(\theta) = \mathbb{E} \left[\left(r + \gamma \max_{a'} Q(s', a'; \theta^-) - Q(s, a; \theta) \right)^2 \right] \quad (2)$$

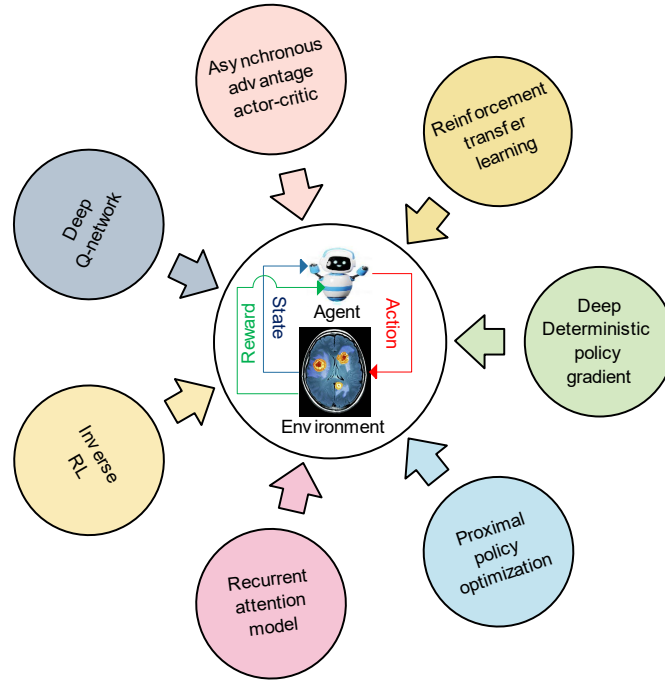


Figure 7: RL types used in cancer diagnosis. DQN [79, 80, 81]; RAN [82]; PPO [83]; DDPG [84]; IRL [85, 86]; A3C [87]; RTL [88, 89].

Where, θ and θ^- represent the parameters of the Q-network and target Q-network. Many studies related to DQN-based cancer detection have been proposed in the literature. For example, [79] focuses on enhancing the localization of malignant cervical cells, a key aspect of detecting tumors. It employs a DQN algorithm to fine-tune bounding boxes around cancerous nuclei to improve localization accuracy through reward-based reinforcement. This method addresses DL overfitting issues by incorporating randomness, leading to successful and competitive localization performance compared to existing techniques. Similarly, [80] addresses the inefficiencies of manual lung nodule detection methods and proposes the LLC-QE model, which integrates ensemble learning with DQN. The model is pre-trained using the artificial bee colony algorithm to avoid local optima. It employs multiple CNNs to extract and combine feature vectors for classification. Trained on the LIDC-IDRI dataset, the model tackles dataset imbalance by using RL to prioritize accurate classification of underrepresented classes. Moving on, Dahdouh in [81], proposes an advanced model for early skin cancer detection by integrating DL and DQN. The approach uses the watershed algorithm for segmentation to isolate affected areas. A deep CNN classifies the lesions into seven categories: actinic keratosis, basal cell carcinoma, benign keratosis, dermatofibroma, melanocytic nevi, melanoma, and vascular skin lesions. The model is further refined using the DQN algorithm, which optimizes performance through RL. Likewise, Tao [90], contributes by proposing SeqSeg framework, a novel method for reliable carcinoma segmentation in MRI. SeqSeg addresses background dominance issues at two scales: instance level and feature level. It uses a DQN-based model to focus attention on the tumor and reduce segmentation background scale, and employs high-level semantic features to guide FL. Evaluated on a large dataset, SeqSeg outperforms state-of-the-art methods and demonstrates superior performance across multi-device and multi-center datasets. Praneeth et al. [91], presents RL2NdgsNet, a DL network enhanced by RL for diagnosing mediastinal lymph nodes and distinguishing between benign and malignant cases. The proposed approach leverages radiological modalities like X-ray, ultrasound, CT, and MRI, which are non-invasive and painless. The RL2NdgsNet network incorporates a custom DQN policy to optimize its performance. Various state-of-the-art AFs and exploration fractions were tested to refine the network's capabilities. The results demonstrate that the RL2NdgsNet achieves superior diagnostic performance, improving upon existing DL-based methods for medical imaging and offering a promising alternative to traditional invasive procedures. The reference [92] explores the potential of deep RL in lung cancer detection, emphasizing its integration with medical big data from the medical Internet of Things (IoT). This work discusses the use of DQN and its variants, such as double DQN and hierarchical DQN.

4.1.2. Proximal policy optimization (PPO)

Is another popular type of RL algorithm designed to balance exploration and exploitation. It improves training stability by updating policies using clipped objective functions within a trust region to avoid large updates, ensuring smoother policy updates. The key functions involved in PPO are: (i) The policy $\pi_\theta(a|s)$ represents the probability of taking action a given state s , parameterized by θ . (ii) The advantage function \hat{A}_t which represents how much better a particular action is compared to the average action taken at state s_t where:

$$\hat{A}_t = R_t - V(s_t) \quad (3)$$

The R_t is the cumulative reward at time step t and $V(s_t)$ is the value function, representing the expected cumulative reward from state s_t . The objective is to maximize:

$$L(\theta) = \mathbb{E}_t [\min(r_t(\theta)\hat{A}_t, \text{clip}(r_t(\theta), 1 - \epsilon, 1 + \epsilon)\hat{A}_t)] \quad (4)$$

Where $r_t(\theta)$ is the probability ratio of the new policy to the old policy, \hat{A}_t is the advantage estimate at time step t , ϵ is a small hyper-parameter that defines the clipping range and $\text{clip}(r_t(\theta), 1 - \epsilon, 1 + \epsilon)$ limits the policy update to be within a trusted region.

Within the class of PPO-based cancer detection methods, the study [93] introduces a RL-based neural architecture search method to automate the development of DL models for cancer data. This approach streamlines the creation of predictive models by incorporating domain-specific characteristics and reducing reliance on manual trial-and-error methods. Custom building blocks are designed to cater to the specific needs of cancer data, leading to the discovery of DNN architectures with fewer trainable parameters and shorter training times, while achieving comparable or superior accuracy to manually designed models. Similarly, [83] presents RLogist, a deep RL method based on the PPO algorithm designed to improve the efficiency of whole-slide image analysis in computational pathology. Unlike traditional methods that require extensive sampling of high-magnification patches, RLogist emulates the diagnostic process of human pathologists to strategically identify valuable regions for observation. This approach reduces the need for dense, high-magnification patch analysis by learning to select representative features from multiple resolution levels. Evaluated on tasks such as detecting metastases in lymph node sections and subtyping lung cancer, RLogist demonstrates competitive performance and provides interpretable decision-making pathways, potentially offering educational and assistive benefits for pathologists.

4.1.3. Deep deterministic policy gradient (DDPG)

Is a type of RL used to handle problems with continuous action spaces. It is an actor-critic (AC) method, which means it combines two networks: an actor network that suggests actions and a critic network that evaluates them. DDPG is an off-policy algorithm, meaning it learns the value function from actions taken by a behavior policy different from the target policy [94]. DDPG consists of two neural networks:

(i) **Actor network:** outputs a deterministic action given the state. The deterministic policy function is defined as: $a_t = \mu(s_t|\theta^\mu)$ where s_t is the current state, $\mu(s_t)$ is the learned policy, and θ^μ are the parameters of the actor network. The actor network is updated using the deterministic policy gradient (DPG):

$$\nabla_{\theta^\mu} J \approx \mathbb{E} [\nabla_a Q(s, a|\theta^Q) | a = \mu(s) \nabla \theta^\mu \mu(s|\theta^\mu)]$$

This update ensures that the actor selects actions that maximize the critic's estimated Q-values.

(ii) **Critic network:** estimates the Q-value (expected return) for state-action pairs. The action-value function is approximated as:

$$Q(s, a|\theta^Q) = \mathbb{E} [r_t + \gamma Q(s_{t+1}, \mu(s_{t+1}|\theta^\mu) | \theta^Q)] \quad (5)$$

where, r_t is the reward at time t , γ is the discount factor, and θ^Q are the parameters of the critic network. The loss function for updating the critic network is:

$$L(\theta^Q) = \mathbb{E} [(y_t - Q(s_t, a_t|\theta^Q))^2], \quad (6)$$

where $y_t = r_t + \gamma Q(s_{t+1}, \mu(s_{t+1}|\theta^\mu) | \theta^Q)$. This minimizes the error between the predicted Q-value and the target Q-value. As an example, [94] employed DDPG as RL method for skin lesion segmentation. The method mimics physicians' delineation of ROI, training an agent to refine segmentation through continuous actions using the DDPG algorithm.

4.1.4. Other RL methods

Many other types of RL methods have been investigated in the field of cancer detection, including:

- **Asynchronous advantage actor-critic (A3C):** optimizes policy parameters using the advantage function, which reduces variance in gradient estimation. The policy gradient update is given by:

$$\nabla_{\theta} J = \mathbb{E} [\nabla_{\theta} \log \pi_{\theta}(a|s) A(s, a)] \quad (7)$$

where $A(s, a) = Q(s, a) - V(s)$ is the advantage function, and $\pi_{\theta}(a|s)$ is the stochastic policy parameterized by θ . Unlike standard AC methods, A3C runs multiple agents asynchronously, reducing training time and preventing correlation in training samples. For example, [87] addresses the challenge of skin cancer diagnosis by developing an automated system using a novel deep RL technique based on asynchronous advantage A3C. This assumes multiple independent CNN agents that interact. These agents interact with skin images to perform segmentation, guided by policies that maximize rewards and minimize errors.

- **Residual attention network (RAN):** integrates attention mechanisms (cf. Section 4.4) into RL, where an agent sequentially focuses on informative regions of an observation, and it is formulated as:

$$g_t = f_g(s_t, l_t; \theta_g) \quad (8)$$

where g_t represents the extracted features at time step t , s_t is the state, l_t is the attention location, and θ_g are the learnable parameters. The agent optimizes its policy to select l_t such that the accumulated reward is maximized. This is particularly effective in image-based RL tasks, reducing computation by selectively processing high-information regions. For example, [82] employed RAN to enhance cancer detection by guiding neural networks to focus on lesions in chest radiographs. RL penalizes irrelevant areas, while attention improves lesion localization for accurate classification.

- **Reinforcement transfer learning (RTL):** Leverages pre-trained policies to accelerate learning in new environments. The knowledge transfer objective is:

$$J_{TL} = \mathbb{E}_{s,a} [\lambda Q_{source}(s,a) + (1 - \lambda)Q_{target}(s,a)] \quad (9)$$

where $Q_{source}(s,a)$ is the action-value function from a pre-trained model, and $Q_{target}(s,a)$ is the value function for the new task. The parameter λ controls the influence of the transferred knowledge. This approach is effective in robotics, where motor skills learned in simulated environments can be transferred to real-world applications. For instance, Xu et al. [89] have employed RTL to improve the quality of MRI images and extract significant tumor features. The aim is to improve the early detection of brain tumors through the use of advanced DL networks for segmentation and classification. The proposed method employed a specific type of RL called AC, with U-Net and ResNet architectures for multi-classification of brain tumors. This approach leverages these models to extract significant features from MRI slices, thereby improving diagnostic accuracy and efficiency.

- **Inverse reinforcement learning (IRL):** Infers a reward function $R(s,a)$ from expert demonstrations. The optimal reward function is estimated by solving:

$$\max_R \sum_t \gamma^t R(s_t, a_t) - \lambda ||\nabla R||^2 \quad (10)$$

where γ is the discount factor, and $\lambda ||\nabla R||^2$ is a regularization term to prevent overfitting. IRL enables learning human-like policies by inferring implicit goals from observed expert behavior, making it a powerful tool in imitation learning applications. In [86], IRL enhances cancer screening by deriving reward functions from expert decisions. Utilizing maximum entropy IRL, partially observable Markov decision process (MDP) models optimize screening strategies, achieving expert-level recommendations for breast and lung cancer detection. Furthermore, IRL improves specificity, reduces false positives, and enhances early cancer detection while maintaining expert-level accuracy.

Table 9: Summary of RL in cancer diagnosis.

Ref	Model(s) used	Image dataset	Contribution	Best result (%)	Limitation
[80]	RL-EL	Lung nodule	Combines RL and ensemble learning (EL) improve for lung nodule detection.	F1: 89.80 Pre: 87.70	Increased computational demands limit scalability.
[81]	CNN-DQN	HAM10000	Combining CNN and DQN for accurate skin cancer classification.	Acc: 80.00	Reliance on one dataset limits model's coverage.
[84]	Attention-RL	Skin lesion	RL for skin lesion segmentation with attention mechanism.	Acc: 97.10	Computational complexity of attention-guided model.
[87]	AC-CNN	PH2, ISIC	Deep RL for skin cancer localization.	Acc: 98.80	Increased computational complexity with CNN agents.
[88]	RL-DBN	3D Brain tumor	Automated brain tumor segmentation using RL models.	Acc: 97.57 Pre: 97.15 AUC: 69.59	Preprocessed data may miss tumor variations.
[89]	SKT-RL	Liver tumor	Liver tumor detection without contrast agents using spatiotemporal knowledge teacher student (SKT)-RL.	Acc: 97.35 Rec: 74.60 Spe: 98.44	High computational resources required.
[90]	DQL-RANet	nasopharyngeal carcinoma	SeqSeg framework for carcinoma segmentation.	Dice: 80.32 Rec: 87.57	High computational complexity of SeqSeg.
[91]	DL-RL	Lymph nodes	RL for benign and malignant lymph node diagnosis.	Acc: 98.20 Sen: 98.03 AUC: 98.19	Complexity of RL increases demands.
[94]	DDPG	ISIC, PH2, HAM10000	Deep RL for skin lesion segmentation.	Acc: 96.33 Spe: 98.60 Sen: 96.79	Requires accurate annotations and high computational demands.
[95]	RL-Attention	Breast DCE-MRI	Post-hoc breast cancer screening using RL.	AUC: 91.00	Challenges with convergence and dataset consistency.
[96]	Customized reward	Breast ultrasound video	RL for keyframe extraction in breast ultrasound videos.	AUC: 84.15	Requires extensive data for class imbalance.
[97]	TL-RL	Lung cancer	Adaptive RL for early lung cancer detection.	Acc: 92.00	Substantial computational resources required.
[98]	TL-RL	Thyroid nodule	RL for thyroid nodule feature extraction and localization.	Acc: 98.32 Rec: 93.84	Complexity and computational constraints for implementation.
[99]	DQN-CNN	Lung cancer	DQN for non-small cell lung cancer prognosis.	Pre: +12.5	Computational complexity of integrating multiple techniques.

Ref	Model(s) Used	Image dataset	Contribution	Best result (%)	Limitation
[100]	Attention-CNN-RL	Breast cancer	RL-based CNN for early breast cancer detection.	Acc: 99.35 FNR: 0.34	Complexity limits practical clinical implementation.

4.2. Federated learning

FL is a distributed ML paradigm that allows multiple decentralized devices (clients) to collaboratively train a shared model while retaining their data locally, thereby enhancing privacy preservation. A central server orchestrates the training process by aggregating updates from individual clients without directly accessing their data [15]. FL encompasses various approaches, such as horizontal federated learning (HFL), vertical federated learning (VFL), and federated semi-supervised learning (FSSL). The overall FL process can be formally expressed as:

$$w^{t+1} = \sum_{i=1}^N \frac{|D_i|}{\sum_{j=1}^N |D_j|} w_i^t \quad (11)$$

Where w^{t+1} denotes the updated global model parameters after the aggregation in the $(t+1)$ -th round, w_i^t stands for local model parameters from client i after local training at round t and $|D_i|$ is the number of data samples at client i , and this determines the weight of each client's contribution to the global model. Figure 8 summarizes the most commonly used FL techniques in the context of cancer detection, including both well-established methods from the literature and approaches specific to certain schemes.

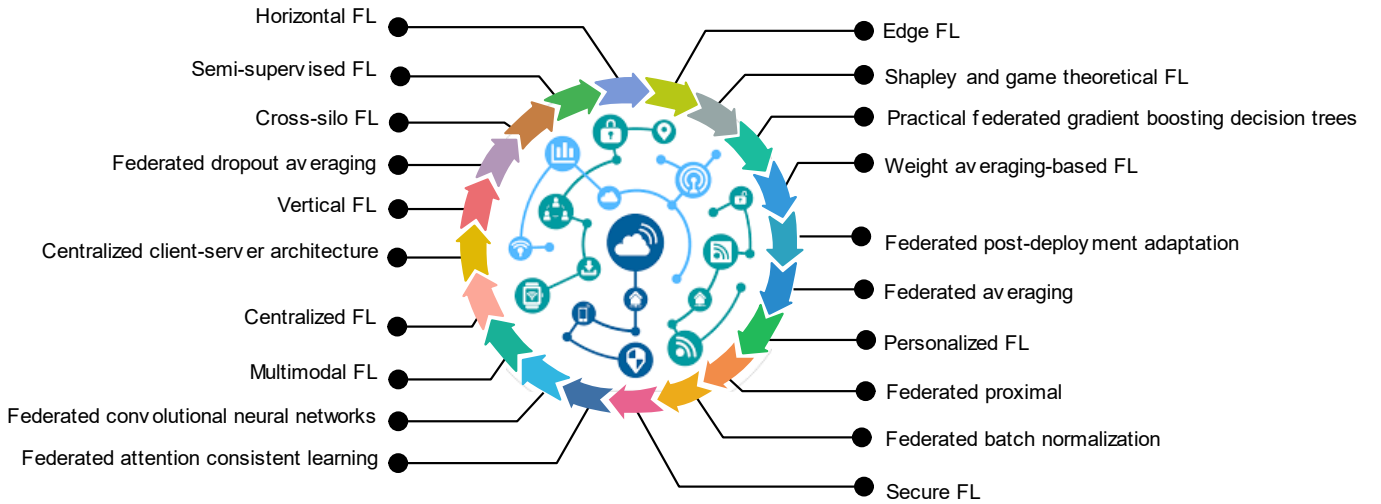


Figure 8: FL types used in the diagnosis of cancer. Cross-silo FL [101, 102]; FSSL [74]; HFL [103]; VFL [104]; Centralized client-server architecture [67]; Centralized FL [105]; Federated dropout averaging [106]; Federated averaging [107]; Federated-CNN [108]; Practical federated gradient boosting decision trees [109]; Shapley and game theoretical FL [110]; Weight averaging-based FL [111]; Edge FL [112]; Federated post-deployment adaptation [113]; personalized FL [114]; Federated proximal [115]; Secure FL [116]; Federated attention-consistent learning [117].

HFL, also known as sample-based federated learning, is a type of FL where the participants (e.g., clients or institutions) have datasets that share the same features (i.e., the same feature space) but represent different individuals or entities (i.e., different samples). In this scenario, all participants hold data about different people or entities, but the structure of the data (the features) is consistent across them [66]. However, VFL trains the models on datasets with identical sample spaces but different feature spaces. Participants collaborate by aligning data entities and sharing encrypted model updates, ensuring privacy while leveraging complementary features for improved performance [15]. FSSL is a specialized variation of FL designed to handle distributed datasets where some clients (devices or organizations) have labeled data while others have unlabeled or partially labeled data. FSSL combines the principles of FL and SSL to collaboratively train models without requiring all participants to have labeled data [118]. As shown in Figure 9, the proposed SSL-FL-BT pipeline enhances histopathological image classification by integrating SSL with FL. This approach improves feature extraction and model generalization, making it well-suited for cancer diagnosis.

In the context of cancer detection, numerous FL techniques have been recently reported. Reference [119, 120, 121, 122, 123, 124, 125, 126, 66] HFL as main technique for cancer detection. Study [119] introduced a distributed learning methodology for particle swarm optimization-based fuzzy cognitive maps that prioritizes data privacy. Applied to cancer detection, this approach demonstrates improved model performance through FL, achieving results comparable to those found in existing literature. Reference [120] introduced "Skin-net," a CNN model for skin cancer detection using progressively private HFL. This method ensures data confidentiality during training, achieving high performance while addressing privacy concerns in medical image analysis. [121]

proposed a knowledge-sharing model HFL using a Unet-based mask generator featuring classification-guided discriminator and an adversarial network for improved detection performance of pulmonary nodules. The paper [122] addressed the challenge of accessing large datasets for disease detection while ensuring data privacy. HFL is proposed as an alternative to conventional methods, using X-ray images for detecting lung cancer and tuberculosis. Reference [123] presented a HFL approach for predicting breast cancer while ensuring data privacy. The study [124] introduced the privacy-embedded lightweight and efficient automated (PLA) method for breast cancer diagnosis within the framework of internet of medical things (IoMT). This approach combines privacy-preserving techniques, efficiency, and automation. The PLA model utilizes a ViT backbone optimized for IoMT environments, ensuring lightweight classification and effective global information processing of breast cancer data. It also employs HFL to protect patient privacy and incorporates texture analysis as an auxiliary task alongside the primary classification task. The PLA framework achieves impressive performance metrics. The study [125], addressed the challenges in lung cancer detection caused by fragmented patient data across various medical institutions and privacy concerns that hinder centralized data analysis. HFL is proposed as a solution to train models on decentralized data and leveraging TL to set initial weights. The approach achieved a high accuracy in detecting lung cancer from medical images. Reference [126] tackled the challenge of detecting hepatocellular carcinoma by integrating 2D and 3D DL models within HFL framework for accurate liver and tumor segmentation in CT scans. Using 131 scans from the liver tumor segmentation challenge, the Hybrid-ResUNet model outperformed ResNet and EfficientNet models, achieving a high dice score and AUC. The horizontal FL approach ensures privacy and facilitates large-scale clinical trials, addressing data imbalances and demonstrating robust local model performance. Likewise, [66] proposed a HFL framework combined with a ResNet18-based dual path DL model for lung nodule detection. This approach addresses privacy issues while training a global model across multiple institutions. The dual path ResNet18 architecture improves feature extraction and detection accuracy. The method demonstrates effective lung nodule detection while preserving patient data privacy.

Reference [104] presents a new paradigm for cancer detection using a combination of VFL, AE, and XGBoost methods within a distributed fog computing environment. This approach addresses challenges in digital healthcare such as security, execution delay, and accuracy. The proposed multi-cancer multi-omics clinical dataset laboratories (MCMOCL) scheme integrates multi-omics data (RNA, miRNA, and methylation) for improved cancer prediction. The method achieved high accuracy, reduced processing delay, and enhanced security compared to existing models in heterogeneous fog cloud computing environments.

Cross-silo FL is another popular method that boost the boundary of cancer detection. For example, Heidari et al [101] propose a novel method for lung cancer detection, addressing challenges related to data privacy and inter-hospital collaboration by employing blockchain-based cross-silo FL. The proposed method employs capsule networks for local lung cancer classification and introduces a data normalization technique to handle variability in CT data. Extensive experiments demonstrated the effectiveness of this technique, achieving a high accuracy. Similarly, [127], contributes by proposing a novel memory-aware curriculum cross-silo FL approach for breast cancer classification using mammography images. This method addresses the challenge of imbalanced datasets, particularly the scarcity of positive samples in routine screenings, by controlling the order of training samples in the FL setting. This method prioritizes forgotten samples to improve local model consistency and overall global model performance. Additionally, the method incorporates unsupervised domain adaptation to handle domain shifts while ensuring privacy. Agbley et al. This study demonstrates that the FL model performed comparably to a centralized learning model, with only minor differences in F1-Score. Agbley et al [102] proposed a novel approach for breast tumor classification that integrates different magnification factors of histopathological images using a residual network and information fusion in a cross-silo FL framework. This method addresses the challenge of limited publicly available medical data by preserving privacy and enabling collaborative model training. The approach was evaluated using the BreakHis dataset, showing superior performance compared to centralized learning models. Additionally, visualizations for explainable AI were provided, and the models are intended for deployment in healthcare institutions' IoMT systems for timely diagnosis and treatment.

Other proposed methods are based on FSSL for identifying cancer. For instance, [74], suggested the FedPerl scheme, an FSSL method that enhances skin lesion classification using peer learning and ensemble averaging techniques. This approach addresses the challenge of limited annotated data in the medical field by allowing models to learn from each other through community-based peer learning and producing accurate pseudo labels. The peer anonymization technique preserves privacy and reduces communication costs without adding complexity.

Moreover, various aggregation techniques have been proposed and implemented to construct the global model on the central server within the FL framework. For example, [107] introduces a federated Averaging (FedAvg) aggregation approach for breast cancer detection along with CNN. This method addresses privacy concerns associated with sharing patient data and the challenge of training on limited, localized datasets. The approach is tested on many large-scale datasets, achieving a high detection accuracy. The study demonstrates that FedAvg can enhance detection accuracy while preserving data privacy, offering a robust and scalable solution for breast cancer diagnostics. The work in [106], introduced FedDropoutAvg, an aggregation approach for tumor detection in histology images that integrates dropout techniques into both client selection and federated averaging processes. This method leverages dropout to mitigate overfitting and improve model generalization. Another aggregation technique proposed in [113] employs federated post-deployment adaptation (FedPDA), which integrates FL to address distribution shifts in medical imaging models. This approach enables remote gradient exchange between the deployed model and source data by maximizing gradient alignment between source and target domains, facilitating more effective learning. FedPDA customizes the model for target domains, enhancing performance in cancer metastasis detection and skin lesion classification. Addition, the study in [115] addresses the challenge of developing accurate and private AI models for breast cancer detection using ultrasound imaging. It proposes leveraging FL to manage sensitive medical data while preserving privacy. To enhance model performance on non-independent and identically distributed (non-IID) datasets, the study incorporates the federated proximal (FedProx) aggregation method, combined with a modified U-Net model featuring attention mechanisms. FedProx mitigates heterogeneity in FL by introducing a proximal term

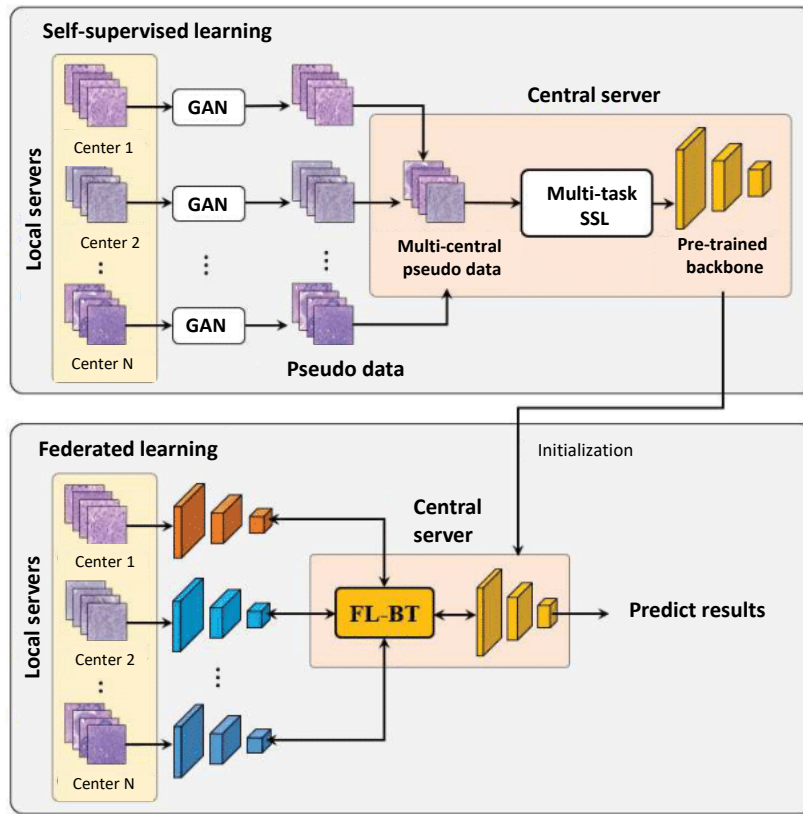


Figure 9: The proposed SSL-FL-BT classification pipeline is designed for histopathological image analysis, which is widely used in cancer diagnosis. The scheme consists of two main stages: the SSL stage and the FL stage. During the SSL stage, a specially designed multi-task SSL approach is applied to all pseudo images to pre-train the backbone network. In the FL stage, the pre-trained backbone serves as the initialization network for the FL-BT model [65].

into the local objective function, ensuring stability and improving convergence. This approach resulted in a global model with high accuracy for tumor segmentation, demonstrating the effectiveness of FedProx in addressing non-IID medical data and improving segmentation performance. Building on this, [128] explored leveraging genomic big data for stomach adenocarcinoma detection using AI and DL. The study introduces *Fed_ANN11*, an aggregation technique developed within a FL framework, integrating novel feature extraction methods based on Electro-Ion interaction pseudo-potential values and Kidera factors. *Fed_ANN11* demonstrates superior performance, achieving high testing accuracies in federated environments and showing significant improvements over existing methods, all while maintaining strong data privacy and security.

Researchers have suggested methods that combine both FL and TL have been reported in [111, 129]. The study [111] addresses the challenge of prostate cancer detection by proposing a FL-based approach that ensures data confidentiality while using weight averaging to detect anomalies. The performance of a customized basic CNN model with three Conv2D layers, along with VGG19 and Xception models, was compared in both centralized and decentralized (federated) settings. The results demonstrate that the decentralized method achieves accuracy comparable to state-of-the-art centralized models, effectively balancing data privacy with high detection performance. Similarly, [129] report a novel FL framework for breast cancer segmentation that addresses data inconsistencies and privacy concerns. It employs random ROI and bilinear interpolation to augment data, and a U-Net model with a pretrained VGG backbone. The Gaussian mixture model is applied to enhance segmentation quality by managing diverse data distributions and improving tumor detection. Experiments show that this approach, using FedAvg and federated batch normalization (BN), outperforms several state-of-the-art methods on five public breast cancer datasets.

Shapley values and game theory were utilized in [110] to develop a unique FL approach specifically designed for breast cancer prediction. Leveraging the Wisconsin Diagnostic Breast Cancer dataset, this approach enhances privacy and prediction accuracy by identifying key features and incentivizing high-performing clients.

In addition to the previously discussed types of FL, other variations are tailored to specific applications, such as IoT. For instance, [112] proposes a lightweight and scalable IoT framework for skin cancer detection, leveraging edge FL to enhance real-time processing and privacy at the edge. The framework supports integration with other computer vision models and features a mobile application that detects skin cancer.

Other FL approaches focus on securing the global model (aggregated model). For example, [116] investigated the integration of fully homomorphic encryption with secure FL using mammogram data from Belgian medical records. The research focuses on evaluating memory constraints when applying fully homomorphic encryption to sensitive medical data. Despite notable limitations in memory usage, the results demonstrate that fully homomorphic encryption maintains comparable performance in terms of ROC curves, showcasing its robustness in secure ML applications. This approach preserves data confidentiality and enhances the security

Table 10

Summary of FL in cancer diagnosis.

Ref	Model used	Images dataset	Contribution	Best (%)	perf.	Limitation
[101]	Blockchain-based FL	Chest CT	Proposed TL, Blockchain, FL, and CapsNets framework enhances lung cancer detection.	Acc: 99.69		Blockchain increases computational overhead.
[104]	FL, AE, XGBoost	Omics data	Integrates federated AE with XGBoost to detect multi-omics cancer.	Acc: 98.00		Scalability of the scheme unaddressed.
[105]	FL	Skin cancer	Presents a secure FL approach for skin cancer detection, mitigating data poisoning attacks.	Acc: 95.20 Pre: 94.80 Rec: 96.10		Scalability issues with larger datasets.
[107]	CNN-FL	Breast cancer	Introduces a FL using CNNs for breast cancer detection across diverse datasets.	Acc: 98.90 Sen: 95.00 Spe: 98.00		Data privacy management across federated networks.
[108]	CNN-FL	Lung cancer	Demonstrates FL with CNNs for scalable, privacy-preserving lung cancer severity diagnosis.	Acc: 95.76		Privacy and data integration issues.
[109]	GBDTMO-FL	Breast cancer	Gradient boosting decision tree-based mayfly optimization (GBDTMO) with FL for breast cancer diagnosis.	Acc: 94.47 Rec: 98.52 F1: 97.52 ROC: 96.32		Communication overhead, complexity in synchronization.
[110]	FL, Shapley values	Breast Cancer	Integrates shapley values, game theory, and horizontal FL to enhance breast cancer prediction.	Acc: 94.73 Pre: 95.28 Rec: 95.48 ROC: 98.97		Challenges scaling to larger datasets.
[115]	FL	Breast cancer	A novel FL integrates FedProx and Attention U-Net for precise breast cancer segmentation.	Acc: 96.07 Spe: 99.19 F1: 70.76		Computational overhead unaddressed.
[117]	FL-Attention	Prostate cancer	Federated attention-consistent learning integrates FL and attention consistency to enhance prostate cancer diagnosis and grading.	AUC: 97.18		FL adds communication overhead.
[120]	Skin-net with FL	Skin cancer	Skin-net CNN with privacy-preserving FL for skin cancer.	Acc: 98.30 Sen: 98.80 Spe: 97.90		Complexity of progressively private FL implementation.
[122]	FL	X-ray lung	Compares sequential and ensemble model (EM)s in FL and centralized approaches for disease detection.	Acc: 99.00		Sequential models add computational complexity.
[124]	FL-ViT	Breast dataset	Proposes a privacy-preserving, lightweight PLA model using ViT for breast cancer diagnosis.	Acc: 95.30 Rec: 99.80 Pre: 98.80		Dataset details lacking, scalability concerns.
[125]	FL-TL	Lung cancer	Developed a FL framework leveraging TL for robust lung cancer detection.	Acc: 91.03 Rec: 89.44 AUC: 98.55 Pre: 98.80		FL synchronization adds complexity.
[126]	DL-FL	Liver CT	Designed a robust Hybrid-ResUNet with FL for accurate liver tumor segmentation.	Dice: 94.33 AUC: 99.65		Communication overhead affects performance.
[127]	Memory-aware curriculum FL	Mammography	Integrated curriculum learning into federated settings for improved consistency, and multi-site breast cancer classification.	AUC: 79.00		Increased computational complexity.
[128]	Fed_ANN11	Stomach Adenocarcinoma	Integrates generative AI and FL for sequence-based stomach adenocarcinoma detection.	Acc: 99.00		Communication overhead and latency issues.
[130]	CNN-FL	Brain tumor	Proposed CNN-based FL for brain tumor detection.	Acc: 96.00		Data heterogeneity and communication overhead.
[131]	FL	Breast cancer	Federated YOLO-ResNet fusion ensures high-accuracy breast cancer detection.	Acc: 98.73 Pre: 98.73 Rec: 98.73		FL with multiple clients adds complexity.

of exchanges between participants and the central server. The study [108] incorporate CNN into FL to enhance lung cancer diagnosis. Reference [114] incorporates client-specific AEs and hierarchical clustering to address the challenges posed by non-independent and identically distributed data across clients. This framework aims to enhance the effectiveness of FL in heterogeneous medical data environments while preserving data privacy.

Distinct from other methods, [117] introduced a federated attention-consistent learning framework designed to advance AI in medical imaging by addressing challenges related to large-scale pathological images and data heterogeneity. Federated attention-consistent learning enhances model generalization by ensuring attention consistency between local clients and the central server model. To further safeguard data, differential privacy is incorporated by adding noise during parameter transfers. The framework was evaluated using a substantial dataset of prostate cancer images from various centers, demonstrating improved performance in cancer diagnosis and Gleason grading (aggressiveness of prostate cancer assessment) compared to existing methods. This approach offers a robust, privacy-preserving solution for training AI models in medical imaging.

4.3. Transfer learning

TL is a ML strategy designed to improve the performance of models on a target task by transferring knowledge from a related source task, especially when labeled data for the target task is scarce. This technique capitalizes on pre-trained models that have

Table 11

Comparison of various TL techniques.

TL type	D_S	D_T	Labels in D_T	Objective function
Inductive	Same/Diff	Same/Diff	Labeled	$\hat{\theta}_T = \arg \min_{\theta} \mathcal{L}_T(f_T(\theta, D_T), T_T)$
Transductive	Diff	Diff	Unlabeled	$\hat{\theta}_T = \arg \min_{\theta} \mathcal{L}_S(f_S(\theta, D_S), T_S) + \lambda \cdot \mathcal{L}_T(f_T(\theta, D_T), T_T)$
Unsupervised	Diff	Diff	Unlabeled	$\hat{\theta}_T = \arg \min_{\theta} \mathcal{L}_S(f_S(\theta, D_S), T_S) + \lambda \cdot \mathcal{L}_U(f_U(\theta, D_T))$

been developed using large and diverse datasets, which can then be fine-tuned to specific problems in domains with limited data such as medical imaging [132, 13], 3D data representation [133], and NLP [134] tasks. The rationale behind TL is that features learned from large-scale tasks, such as detecting edges, shapes, or general patterns in images, can be beneficial for smaller, related tasks without starting the learning process from scratch. The essential mathematical foundation of TL lies in the optimization of a loss function that allows the model to learn and adapt to new tasks. The general equation for loss function optimization in TL is given by Equation 12:

$$L(\theta) = \frac{1}{N} \sum_{n=1}^N L(y_i, f(x_i; \theta)) \quad (12)$$

Where N denotes the number of samples, θ represents the model parameters, y_i is the true label, and $f(x_i; \theta)$ is the model's prediction. This loss function is minimized using optimization algorithms like stochastic gradient descent (SGD), adjusting the model's weights for better generalization on the target task. TL encompasses various approaches, including inductive, transductive, and unsupervised TL, allowing models to generalize better to new tasks while improving training efficiency. Regularization techniques like dropout help mitigate overfitting during fine-tuning, and feature extraction methods utilize pre-trained models as fixed feature extractors for simpler models. Knowledge distillation further enhances efficiency by training smaller models to replicate the performance of larger ones [134, 14, 135, 133]. Table 11 provides a summary of the types of TL, including inductive, transductive, and unsupervised TL, highlighting their distinct characteristics and key differences. Table 12 summarizes several state-of-the-art studies in terms of the AI models used, datasets, contributions, limitations, and best performances achieved. Additionally, popular pre-trained models are comprehensively reviewed in [134, 14, 135]. Figure 11 illustrates an example of the proposed approach, which involves unsupervised pre-training of a convolutional autoencoder (CAE) to extract features from CT images, combined with the TL technique to enhance lung cancer prediction.

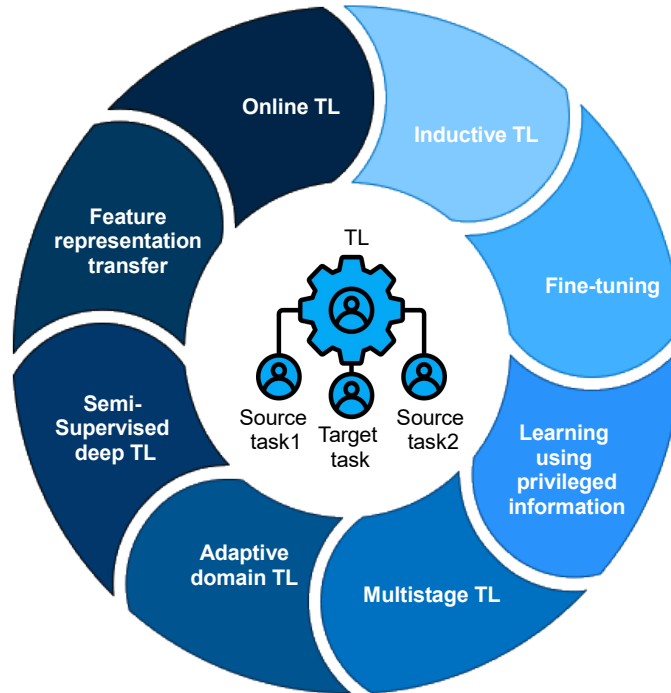


Figure 10: TL types used in the diagnosis of cancer and their respective related work. Inductive TL [136]; Fine-tuning [137, 138, 63]; Learning using privileged information [64]; Multistage TL [139]; Adaptive domain TL [140]; Semi-supervised deep TL [69]; Feature representation TL [141]; Online TL [142].

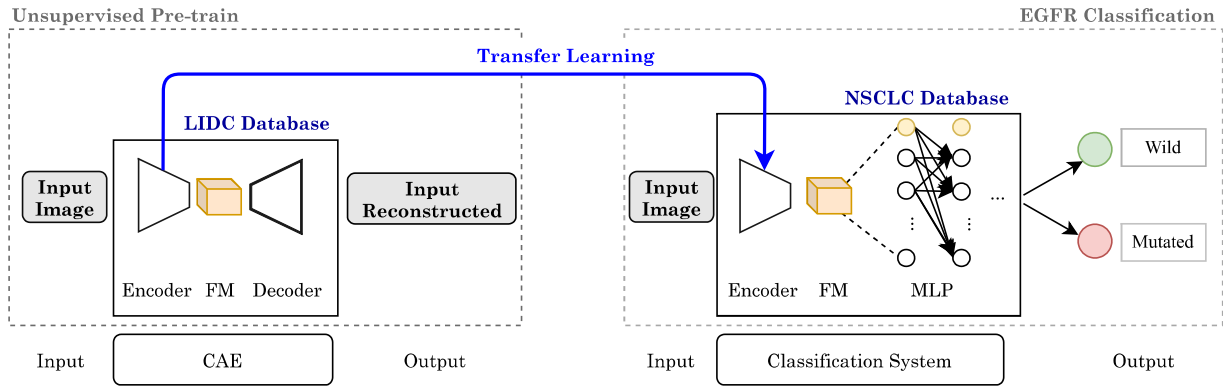


Figure 11: Example of a proposed approach, which involves unsupervised pre-training of a CAE to extract features from CT images, followed by an end-to-end classifier for predicting the mutation status of the EGFR. This latter is a transmembrane protein involved in cell signaling pathways that regulate cell proliferation, survival, and differentiation; mutations in this receptor are commonly associated with non-small cell lung cancer. TL enables the reuse of the encoder, pre-trained on unlabeled data from the *LIDC-IDRI* database, as a feature extractor for EGFR mutation classification in the *NSCLC-Radiogenomics* database [55].

Recently, numerous AI methods based on TL have been proposed to enhance cancer diagnosis and detection as summarized in Figure 10, with most relying on inductive learning and fine-tuning techniques. For instance in [136], the authors addressed the critical issue of breast cancer detection and classification by proposing a novel CAD method utilizing ResNet18, ShuffleNet, and Inception-V3Net in an inductive TL mode. The method is tested on the BreakHis dataset, with final image dimensions of 224×224 for ResNet18 and ShuffleNet, and 299×299 for Inception-V3Net. This approach demonstrates high accuracy in both binary and multi-class classification. Similarly, [143] proposed a novel DL framework for detecting and classifying breast cancer in cytology images using inductive TL. Pre-trained CNN architectures, including GoogLeNet, VGGNet, and ResNet, are employed for feature extraction, followed by classification of malignant and benign cells. Saber et al. [144] contributed by developing a DL model based on inductive TL to assist in the automatic detection and diagnosis of breast cancer. This study utilizes pre-trained CNN architectures such as Inception V3, ResNet50, VGG-19, VGG-16, and Inception-V2 ResNet and evaluates the model on the MIAS dataset. The findings demonstrate that VGG16 is the most effective architecture for breast cancer diagnosis using mammographic images. Reference [145] introduced a DL model for detecting skin cancer in its benign and malignant stages using inductive TL. The model builds upon the pre-trained VGG16 architecture by adding a flattened layer, two dense layers with LeakyReLU activation, and a final dense layer with sigmoid activation to improve accuracy. This model aims to assist dermatologists in early skin cancer diagnosis. Continuing diagnosis scheme cancer, [146], proposed an automatic detection system using the sparrow search algorithm (SpaSA) for hyperparameter optimization. This study employs five U-Net models (U-Net, U-Net++, Attention U-Net, V-net, Swin U-Net) for segmentation and eight pre-trained CNN models (VGG16, VGG19, MobileNet variants, NASNet variants) for classification. For segmentation, U-Net++ with DenseNet201 achieved the best results on “skin cancer segmentation and classification” dataset, while Attention U-Net with DenseNet201 performed best on the “PH2” dataset. MobileNet pre-trained models achieved the highest accuracy on the “ISIC 2019 and 2020 Melanoma” and “HAM10K” datasets, and MobileNetV2 excelled with the “skin diseases image” dataset. The proposed method is compared with 13 related studies, demonstrating its effectiveness in skin cancer diagnosis. A breast cancer diagnostic system that integrates deep TL with IoT and fog computing was proposed in [147]. Using mammography images from the Cancer Imaging Archive, the system employed ResNet50, InceptionV3, AlexNet, VGG16, and VGG19 architectures alongside a support vector machine (SVM) classifier. Fog computing played a crucial role in enhancing privacy, reducing server load, and improving overall system efficiency.

Reference [138] applies deep TL fine-tuning of a pre-trained model combined with hybrid optimization, using adaptive moment estimation (adam), RMSprop, and SGD optimizers, to improve detection and diagnosis of oral cancer. This study utilizes models such as ResNet50, MobileNetV2, VGG19, VGG16, and DenseNet on both real-time and histopathologic datasets. Image preprocessing techniques, including Gaussian blur and morphological operations, are used to prepare the data. Likewise, [63] presented a fine-tuned model to classify three widespread lung cancer types: Squamous cell carcinoma, large cell carcinoma, and Adenocarcinoma. The models used include VGG16, ResNet152V2, MobileNetV3 (small and large), InceptionResNetV2, and EfficientNetV2. InceptionResNetV2 emerged as the best model with the highest performance metrics (accuracy, precision, AUC, and F1-score) in classifying the lung cancers from normal samples. Study [148] presented a novel approach to skin lesion classification by combining VGG16 and VGG19 architectures into a modified AlexNet network. This combined model was fine-tuned on a dermatology dataset of 2,541 images without relying on data augmentation techniques. Dropout was used to address overfitting, and the model was evaluated using K-fold cross-validation. The proposed method achieved a significant improvement in classification accuracy. In a different study [149] contributed by proposing a real-time data augmentation-based fine-tuning TL model for breast cancer diagnosis using histopathological images. It compares two popular models, InceptionV3 and Xception, trained on the BreakHis dataset. The findings show that the Xception model, when trained using fine-tuning TL from ImageNet weights, achieved high accuracy, outperforming models trained from scratch and surpassing previous state-of-the-art results on the BreakHis dataset. Deepak et al. [150] suggested a brain tumor classification system using fine-tuning TL by employing a pre-trained

GoogLeNet to extract features from MRI images of glioma, meningioma, and pituitary tumors, and integrates proven classifiers for accurate classification.

Table 12: Summary of TL in cancer diagnosis.

Ref	Model(s) used	Image dataset	Contribution	Best result (%)	Limitation
[136]	DNN-TL	BreakHis	Fine-tuning multiple DNN models with TL for accurate breast cancer classification.	Acc: 97.81 Pre: 97.65 Sen: 97.65	Single dataset may cause overfitting.
[137]	ResNet-50	Herlev, UIC	TL enhances cervical cancer detection using Pap smear images.	Acc: 92.03	Requires significant computational power.
[138]	DL-TL	Oral cancerous, histopathologic	Efficient oral cancer diagnosis using DenseNet with fine-tuning and hybrid optimization.	Acc: 95.41 Loss: 0.70	Hybrid optimization adds computational complexity.
[139]	EfficientNetB2	Ultrasound breast cancer	Proposed multistage TL method significantly improves breast cancer ultrasound classification.	Acc: 99.00 F1: 98.90	Extensive pre-processing may introduce biases.
[141]	AlexNet	Histopathology	TL for lung and colon histopathology image classification.	Acc: 98.40	Contrast enhancement method limits class generalizability.
[142]	Online TL	Thyroid cancer	Online TL distinguishes thyroid nodules using ultrasound.	AUC: 98.00 Sen: 98.70 Spe: 98.80	Relies on specific datasets.
[143]	CNN-TL	Breast cancer	DL framework for breast cancer classification using TL.	Acc: 97.67	Requires substantial computational resources.
[144]	DL-CNN	Mammographic	TL for breast cancer detection using pre-trained CNNs.	Acc: 98.96 Sen: 97.83 AUC: 99.50	Relies on single dataset.
[145]	DL-TL	Skin cancer	Fine-tuned VGG16 with added layers, data augmentation, and hyperparameter optimization for skin cancer diagnosis.	Acc: 89.09	Model complexity increases training time.
[146]	U-Net	PH2, HAM10K	ISIC, Fine-tuning CNNs with SpaSA optimizer improves skin cancer segmentation, classification, and detection efficiency.	Acc: 98.83 AUC: 99.45	Model complexity adds challenges.
[147]	CNN-TL	Mammography	Integrates TL with fog computing for breast cancer diagnosis.	Acc: 97.99 Pre: 99.51 Spe: 80.08	High computational power needed.
[148]	VGG16, VGG19, TL	Dermatology dataset	Introduces a fine-tuned acTL approach combining VGG16/VGG19 architectures for superior melanoma detection.	Acc: 98.18	Dataset size limits generalization.
[149]	InceptionV3, Xception	BreakHis	Proposed a TL-based fine-tuning and real-time augmentation model for breast cancer classification.	Acc: 90.86 Sen: 92.51 Spe: 80.85	Limited data increases overfitting risk.
[150]	TL-CNN	MRI	TL for brain tumor classification using MRI.	Acc: 98.00	Dataset may not cover all tumor types.
[151]	TL-MLP-SVM	Breast cancer	Intelligent breast cancer diagnosis with ensemble TL models.	AUC: 94.70 Rec: 85.80	Data quality limits real-time use.
[152]	ResNet-50, DenseNet	Breast cancer	Automated breast cancer detection using TL.	Acc: 90.96 F1: 94.11	Larger dataset required for validation.
[153]	CNN-TL	Cervical histopathological	Proposed a fine-tuned deep TL framework for interpretable and automated cervical histopathological image diagnosis.	Acc: 97.42 Spe: 98.93 Sen: 95.88	Requires substantial computational resources.
[154]	TL	Mammogram	TL for breast lesion diagnosis with hybrid DL.	Acc: 98.80	Computational complexity due to the multi-step pipeline.
[155]	Hybrid TL	CE-MRI	TL model for brain tumor classification using contrast-enhanced (CE)-MRI.	Acc: 99.51 Sen: 98.90	Relies on specific CE-MRI dataset.
[156]	VGG16	JUMC	IVNet uses TL for breast cancer grading.	Acc: 97.00	Despite employing TL, the relatively small dataset size could still cause overfitting.

Another TL technique consist of multistage TL as suggested in [139] dedicated for ultrasound breast cancer image classification. It employs three pre-trained models EfficientNetB2, InceptionV3, and ResNet50—along with adam, Adagrad, and SGD optimizers. Study [140] employed domain adaptation TL techniques for early lung cancer diagnosis using multi-omics data. The approach combines CNNs and convolutional AEs to handle the challenges of high-dimensional, low-sample-size, and noisy omics data. The AEs reduce dimensionality to enhance migration learning, while the CNN model is trained on both the original and labeled datasets. The proposed method outperforms five other ML models, demonstrating superior performance in classifying and predicting lung cancer from gene datasets. Similarly in [157], where the domain adaptation approach have been used to address the issue of limited labeled data in medical imaging. Traditional TL methods, which often use pretrained models from datasets like ImageNet, may be ineffective due to feature mismatches between natural and medical images. To overcome this, the authors propose training DL models on large unlabeled medical image datasets before fine-tuning them on smaller labeled datasets. They also introduce a new deep CNN model that incorporates recent advancements in the field. The proposed method has been empirically validated through experiments on skin and breast cancer classification tasks, showing significant performance improvements.

The scheme proposed in [69] is a semi-supervised TL framework for diagnosing benign and malignant pulmonary nodules in chest CT images. This approach combines TL with a pre-trained classification network and an iterated feature-matching-based semi-supervised method to handle the challenge of limited and imbalanced pathological datasets. Unlabeled dataset contains 14,735 nodules from 4,391 subjects and are used by the semi-SL framework. However, the work in [154] proposed a TL-based feature extraction approach for breast lesion diagnosis using mammograms. It addresses two key challenges: enhancing input data by generating pseudo-colored images using CLAHE and pixel-wise intensity adjustment, and mitigating multicollinearity in high-level features through a novel LR-PCA method. The proposed system achieves high performance with accuracies demonstrating its effectiveness for breast cancer diagnosis.

4.4. Transformer-based learning

Transformers have revolutionized computer vision by modeling long-range dependencies through self-attention mechanisms [77], unlike CNNs, which rely on local receptive fields. Since cancer diagnosis is image-based, the Transformer architecture employed in this domain is ViT, which enables more effective feature extraction for tumor detection, segmentation, and classification. Various ViT architectures have been designed to address challenges such as computational complexity, spatial information loss, and multi-scale feature representation. ViT replaces traditional CNNs by dividing images into patches and processing them as sequences, similar to how words are handled in NLP [16, 20].

In general, ViT divides an image of size $H \times W \times C$ into $N = \frac{H \times W}{p^2}$ patches, where each patch is flattened into a vector and linearly transformed using a learnable embedding matrix $E \in \mathbb{R}^{(p^2 \cdot C) \times D}$, resulting in patch embeddings:

$$z_0^i = x^i \cdot E \quad (13)$$

for each i -th patch. To retain spatial information, positional encodings p_i are added:

$$z_0^i = z_0^i + p_i. \quad (14)$$

These embeddings pass through the Transformer encoder, which applies the multi-head self-attention (MHSA) mechanism:

$$\text{Attention}(Q, K, V) = \text{softmax}\left(\frac{QK^T}{\sqrt{d_k}}\right)V \quad (15)$$

where Q, K, V represent the query, key, and value matrices, and d_k is the dimension of the keys. The MHSA operation aggregates multiple attention heads, such that: $\text{MHSA}(X) = \text{Concat}(\text{head}_1, \dots, \text{head}_h)W^O$. A feed-forward network (FFN) is applied to each token:

$$\text{FFN}(x) = \max(0, x \cdot W_1 + b_1) \cdot W_2 + b_2, \quad (16)$$

where W_1, W_2 are learnable weight matrices and b_1, b_2 are biases. A special classification token (CLS token) is added to the patch sequence, and after the final Transformer layer, the CLS token is passed to a multi-layer perceptron (MLP) classifier:

$$y = \text{MLP}(z_L^{\text{CLS}}), \quad (17)$$

where z_L^{CLS} is the processed CLS token.

While the standard ViT structure has shown competitive performance, several variants have been developed to enhance efficiency, improve local and global feature extraction, and incorporate convolutional priors. Table 13 summarizes key ViT variants, their advantages, applications in cancer diagnosis, and limitations. These variants address some of the computational and structural challenges of ViT, making them more suitable for tasks such as medical image analysis, where feature locality and efficiency are critical. A comprehensive overview of these architectures can be found in [20, 77].

Among the types of ViT, there is a swin transformer, which is a type of ViT designed to efficiently handle high-resolution visual data and complex vision tasks. Unlike the original ViT, which treats an entire image as a sequence of patches, the swin Transformer introduces a hierarchical structure and operates on non-overlapping windows (patches). This structure progressively increases the model's ability to capture both local and global contextual information [58]. The compact ViT is another variant of the ViT designed to address some limitations of the original ViT, particularly its need for large amounts of data and lack of inductive biases commonly found in CNNs. The compact ViT introduces mechanisms like sequence pooling and multi-scale features to improve the model's efficiency and performance, especially when working with smaller datasets or when computational resources are limited [158]. Figure 12 provides the taxonomy of different types of ViT, including some commonly used models and others proposed in specific studies.

Many suggested strategies for cancer detection are based on Transformers. In particular, the study in [169] compares different ViT models including pooling-based vision transformer (PiT), convolutional vision transformer (CvT), CrossFormer, CrossViT, NesT, MaxViT, and separable vision transformer (SepViT) for classifying breast cancer in digital histopathology images. MaxViT was identified as the best-performing model. [170] proposed a ViT model designed for the detection and classification of prostate cancer by first extracting patches from ROI in the whole slide images and then applying the ViT model for classification. The classified patches are subsequently scored and graded according to the Gleason system. Mali et al [158] investigate the use of ViT

Table 13

Comparison of ViT variants in cancer diagnosis.

ViT variant	Advantages	Use case	Limitations
Self-Supervised ViT	Learns representations without labeled data, improves generalization	Detects rare cancer types with limited labeled data	Requires extensive computational resources for pretraining
Multi-Axis ViT	Processes spatial axes separately for better feature extraction	Enhances tumor boundary delineation in histopathology images	Increased model complexity affects real-time processing
Swin Transformer	Uses shifted windows to reduce computation and improve efficiency	Efficient large-scale whole-slide image analysis	Limited ability to model global dependencies
Tokens-to-Token ViT	Preserves spatial relationships via progressive tokenization	Improves segmentation of tumor regions in MRI scans	Higher memory requirements due to hierarchical tokenization
Convolutional ViT (CvT)	Incorporates convolutional layers for local feature extraction	Better texture recognition for skin and breast cancer detection	Partially loses global receptive field advantage of ViTs
CrossFormer & Cross ViT	Multi-scale feature fusion improves robustness	Enhances multi-modal imaging (e.g., PET-CT fusion for cancer staging)	Computationally intensive due to cross-scale processing
Separable ViT	Reduces computational complexity by factorizing attention	Speeds up inference for real-time cancer detection systems	Trade-off in accuracy due to reduced interaction between features
Multi-View ViT	Aggregates different perspectives for robust representations	Assists in multi-angle breast cancer mammography analysis	High data requirements for multi-view learning
Boosted ViT	Applies ensemble principles to enhance prediction accuracy	Improves classification of rare cancer subtypes	Training complexity increases significantly
Local-Global ViT	Balances fine-grained and high-level feature extraction	Helps identify tumor microenvironments in histopathology	Computationally expensive for large images
Pooling-Based ViT	Reduces dimensionality using pooling mechanisms	Speeds up processing in large-scale cancer imaging datasets	May lose fine-grained spatial information
Nested Hierarchical Transformer	Multi-level feature extraction enhances contextual understanding	Improves differentiation of overlapping cell structures in pathology	Increased model depth leads to high training time

focusing on data preprocessing and the Transformer models are utilized for detecting colorectal cancer. This study implements three transformer-based models ViT, CvT, and compact convolutional Transformer (CCT) to classify histopathological images, exploring the impact of different patch sizes and model configurations, demonstrating that ViTs outperform traditional methods in accuracy. It provides insights into optimization techniques specific to colorectal cancer detection. Similarly, the research in [171], explored the use of an ensemble of ViT for classifying brain tumors from MRI scans. Pretraining and fine-tuned four ViT models is performed on ImageNet. The dataset comprised T1-weighted contrast-enhanced MRI slices with meningiomas, gliomas, and pituitary tumors. It shows that combining multiple ViT models enhances classification accuracy and reliability compared to single ViT models and traditional methods. Pachetti et al [172] evaluate the effectiveness of 3D ViT in predicting prostate cancer aggressiveness. It demonstrates that 3D ViTs can effectively capture and analyze spatial information in 3D medical images, potentially outperforming traditional 2D approaches and 3D CNN. This study optimized 3D Vision Transformer models for prostate cancer aggressiveness prediction by selecting five key MRI slices per lesion, harmonizing pixel dynamics, and rescaling and center-cropping images to focus on the prostate gland. Ayana et al. [162] investigated the use of a novel type of Transformer called ViTCol, a boosted vision Transformer model specifically designed for classifying endoscopic pathological findings. Additionally, they proposed PUTS, a Swin-Unet transformer-based model for polyp segmentation. Both models represent significant advancements in classification and segmentation tasks, which are critical for early CRC diagnosis. Their findings demonstrate that these enhanced ViTs can significantly improve detection performance and provide valuable insights in pathology. Sun et al. [173] propose thyroid cancer-ViT, which integrates contrastive learning to enhance the classification accuracy of thyroid nodules in ultrasound images. The main issue addressed is the lack of distinguishing features between benign nodules, particularly those classified as TI-RADS level 3 and malignant nodules, which can lead to diagnostic inconsistencies, overdiagnosis, and unnecessary biopsies. The thyroid cancer-ViT model leverages ViT's capability to capture global features and contrastive learning to reduce the representation distance between nodules of the same category, improving the consistency of global and local feature representations. Similarly, Chen et al. [174] demonstrated that transformer-based models improve breast cancer diagnosis by utilizing unregistered multi-view mammograms (CC and MLO) from both sides (right and left breasts). The outputs are concatenated and processed through global Transformer blocks to jointly learn patch relationships across the four images. The model was trained and evaluated on a balanced dataset of mammogram sets, comprising malignant and normal cases, and showed that this approach significantly outperforms traditional methods in handling unregistered images.

Several studies [175, 176, 177, 178, 179] have combined ViT with TL to enhance cancer detection. Yang et al. [175] developed a model for skin cancer classification, where the network was pretrained on the ImageNet dataset and fine-tuned on the HAM10000 dataset. Ayana et al. [176] focused on breast cancer mass classification, introducing three ViT-based TL architectures pretrained on ImageNet and evaluating their performance using ultrasound and mammogram datasets. The comparative analysis demonstrated that ViT-based TL achieved superior performance. Similarly, Nejad et al. [177] proposed a hybrid DL framework combining ViTs and CNNs with TL for improved lung cancer detection. Their hybrid ViT model effectively addressed the challenges of lung nodule detection by extracting features from chest CT images to classify nodules as normal, benign, or malignant. Tested on a dataset of CT images, the model achieved high accuracies in training, validation, and testing, demonstrating superior performance compared to existing methods. Hossain et al. [178] explored advanced methods for brain tumor detection and classification using MRI images. The study addressed the challenges of inconsistent diagnostic results among specialists and emphasized the need for reliable multi-class tumor classification. It evaluated several DL architectures, including VGG16, InceptionV3, VGG19, ResNet50, InceptionResNetV2, and Xception. A new TL-based model, IVX16, was proposed by combining features from the best-performing

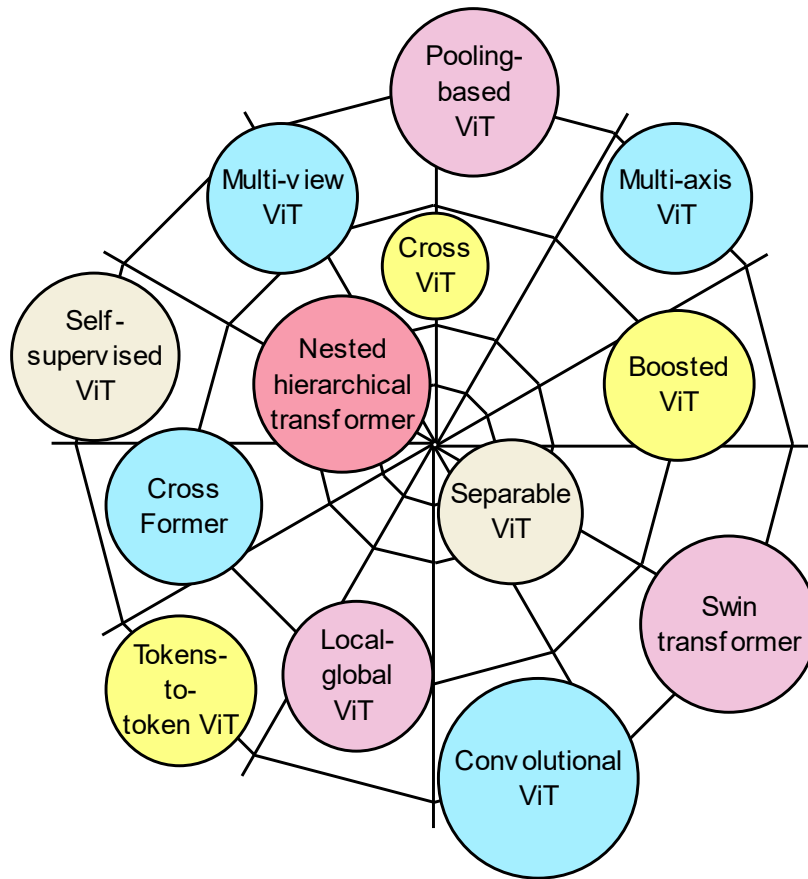


Figure 12: ViT types used in the diagnosis of cancer. Separable ViT [159]; Cross-validation ViT [160]; Multi-Axis ViT [161]; Boosted ViT [162]; Swin Transformer [163]; Tokens-to-token ViT [164]; Local-global ViT [165]; Self-supervised ViT [166]; CNN-ViT [167]; CrossFormer [168]; CrossViT [169]; and nested hierarchical Transformer [169].

architectures. Tested on a dataset of 3264 images, the model demonstrated improved classification performance. Additionally, explainable AI (XAI) was employed to assess model performance, while ViT models were compared with other TL methods and EMs, highlighting their effectiveness.

Several frameworks combined ViT with CNN as an efficient solution for detecting various types of cancer. Zhou et al. [180] introduced a hybrid architecture, RFIA-Net, for classifying stage I multi-modality oesophageal cancer images. RFIA-Net leveraged the local modeling capabilities of CNNs and the global information extraction of ViTs, enhanced by a structural reparameterization strategy. The architecture included a feature extraction module and a feature enhancement module, which exchanged information between branches to improve performance. An asymmetric fusion module further strengthened feature relationships through spatial translation and channel swapping. Tested on the XJMU-XJU dataset, RFIA-Net achieved high performance. Xin et al. [181] proposed an enhanced ViT model, SkinTrans, for classifying skin cancer from dermoscopic images. Traditional CNN-based methods, while effective, struggled to extract features from large, critical regions in images. To address this, SkinTrans utilized self-attention mechanisms to focus on significant features while suppressing noise. The model incorporated multi-scale patch embedding, overlapping sliding windows, and contrastive learning to enhance classification accuracy. Similarly, Zhang [182] developed multi-stage hybrid transformer (MSHT), a hybrid model that combined the local spatial feature extraction capabilities of CNNs with the global feature capture and long-range dependency handling of Transformers. The MSHT architecture integrated a CNN backbone to extract multi-scale local features, guiding the Transformer in capturing global features. This approach enabled the model to effectively leverage both local and global information. Lastly, Tabatabaei et al. [167] explored an advanced framework for classifying brain tumors in MRI images using a hybrid architecture combining self-attention units and CNNs. Their proposed model enhanced classification accuracy by combining local features extracted by CNNs with global features captured by Transformers through a cross-fusion strategy. Additionally, the study introduced an improved CNN architecture, iResNet, optimized for distinguishing tumor features in MRI images.

Tokens-to-token vision transformers (T2T-ViT) also attracted significant attention from researchers in the field of cancer diagnosis. For instance, Yin et al. [183] introduced a novel lightweight architecture, Pyramid T2T-ViT, to address challenges in classifying histopathological thyroid images. Traditional methods using CNNs struggled with high-resolution whole slide images due to increased model parameters and computational complexity. The Pyramid T2T-ViT combined T2T-ViT with an image pyramid approach to balance local and global features effectively while reducing computational demands. The model incorporated a feature extractor to minimize parameters and employed multiple receptive fields to enhance classification accuracy. In the same manner,

Zhao et al. [164] tackled the challenges of cervical cancer screening, such as limited public datasets, imbalanced class distribution, and varying image quality. They proposed a cervical cell image generation model, CCG-taming Transformers, to create high-quality, balanced datasets. The researchers enhanced the model's encoder with SE-blocks and multi-Res-blocks for improved feature extraction and introduced a normalization layer to optimize data processing. Additionally, SMOTE-Tomek links were used to balance the dataset, and T2T-ViT combined with TL was employed for classification. The model was validated on three public datasets, demonstrating its effectiveness.

Table 14: Summary of Transformer-based cancer diagnosis.

Ref	Model(s) used	Image dataset	Contribution	Best result (%)	Limitation
[162]	ViT	Colorectal pathology	Enhanced ViT improves colorectal cancer early detection.	AUC: 99.99 MCC: 90.48	Model complexity increases computational demands.
[164]	T2T-ViT	Cervical cancer	Hybrid T2T-ViT model improves cervical cancer classification.	Acc: 99.98 Sen: 98.34	High computational complexity.
[167]	ATM-CNN	Brain tumor MRI	Combines attention Transformers and CNN for brain tumor classification.	Acc: 99.30	High computational resource requirements.
[169]	ViT	Breast cancer histopathology	ViT models compared for breast cancer classification.	Acc: 92.12	Study only compares ViT models.
[170]	ViT	Prostate tissue slides	ViT improves prostate cancer detection from slide images.	Pre: 99.00 F1: 94.00	High computational resources needed.
[171]	ViT	Brain tumor MRI scans	Ensemble ViTs improve brain tumor classification accuracy.	Acc: 98.70 Sen: 97.78	Ensemble models increase computational complexity.
[172]	3D ViT	3D MRI prostate scans	3D ViT improves prostate cancer aggressiveness prediction.	AUC: 77.50 Spe: 75.00	High computational cost for training.
[173]	ViT-CL	Thyroid nodule ultrasound	Combines ViT with contrastive learning (CL) for thyroid classification.	Acc: 86.90	High computational demands for CL.
[174]	Multi-view ViT	Breast cancer	Multi-view ViT improves feature management in cancer diagnosis.	AUC: 81.40 Pre: 79.70	Depends on availability of multi-view data.
[175]	ViT-TL	Skin cancer	ViT-TL enhances skin cancer classification.	Acc: 80.5	Requires significant computational resources.
[176]	ViT-TL	Breast mass	ViT-TL improves breast mass classification.	AUC: 100	Depends on diverse diagnostic modalities.
[177]	ViT-TL	Lung cancer	Hybrid ViT-TL improves lung cancer diagnosis accuracy.	Acc: 99.09	Hybrid model increases computational complexity.
[178]	ViT-EM-TL	Brain tumor	Ensemble ViTs improve brain tumor classification accuracy.	Acc: 96.94	Requires diverse imaging data.
[180]	ViT-CNN	Oesophageal cancer	Enhances oesophageal cancer diagnosis using ViT + CNN.	Acc: 99.02 AUC: 99.73	Complex model increases computational demands.
[181]	SkinTrans	Skin cancer	Improved Transformer network enhances skin cancer classification.	Acc: 94.30	High computational demands.
[182]	MSHT	Pancreatic cancer	MSHT improves pancreatic cancer diagnosis using Transformers.	Acc: 95.68 Spe: 96.95 NPV: 96.35	Increased computational complexity.
[184]	ViT	Colorectal histology	ViT predicts biomarkers from colorectal histology images.	Sen: 99.00	Limited applicability to other data types.
[185]	ViT-DeiT	Breast histopathology	ViT + data-efficient image transformers (DeiT) improve breast cancer classification.	Acc: 98.17 Pre: 98.18 F1: 98.12	High computational resources required.
[186]	ViT-CNN	Skin lesion	Compares ViT and CNN for skin lesion segmentation.	Acc: 92.11 Dice: 89.84	High computational demands for both methods.
[187]	ViT-CNN	Mammography	Integrating ViT with CNN improves breast cancer detection.	Acc: 99.22	Increased computational complexity.
[188]	LCDEiT	Brain tumor MRI	linear complexity data-efficient image transformer (LCDEiT) reduces Transformer model complexity in brain classification.	Acc: 98.11 F1: 93.69	Requires extensive tuning for optimal results.
[189]	YOLOv8-DeiT	Brain tumor	Combines you only look once version 8 (YOLOv8) and DeiT for brain tumor detection.	Acc: 100 F1: 100	High computational demands.
[190]	Swin	Skin lesion	Swin Transformer improves multiclass skin lesion classification accuracy.	Acc: 97.20 Spe: 98.00	Requires extensive computational resources.
[191]	Swin -MLP	Brain tumor MRI	Hybrid swin Transformer and multilayer perceptron (MLP) improves brain tumor diagnosis.	Acc: 99.92 Rec: 99.92	Significant computational resource requirements.
[192]	Ensemble swins	Breast histopathology	BreaST-Net uses swin Transformers for breast cancer classification.	Acc: 99.60 MCC: 98.90	Single dataset limits generalization.
[193]	ViT-LSTM	Breast histopathology	ViT and LSTM improves breast cancer classification accuracy.	Acc: 99.20	Complexity increases computational demands.
[194]	RMTE-Net	Brain tumor MRI	residual mix transformer fusion network (RMTE-Net) improves brain tumor segmentation accuracy.	Dice: 93.50	Limited to 2D imaging scenarios.
[195]	RadFormer	Gallbladder cancer	RadFormer improves gallbladder cancer detection using global attention.	Acc: 92.10 Spe: 96.10	The complexity of the attention mechanisms.

The study [163], introduces a novel approach for segmenting cholangiocarcinoma histopathological images using hyperspectral imaging. Hyperspectral imaging offers richer spectral information compared to RGB imaging, which can enhance segmentation

performance. The study proposes a swin-spectral Transformer network, which integrates spectral and spatial features more effectively. The network employs a spectral multi-head self-attention mechanism to handle the spectral dimension as a sequence, rather than treating it as an additional spatial dimension. The swin-spectral Transformer combines spectral-multi-head self-attention with shifted window-based multi-head self-attention to capture both spectral and spatial features. Additionally, a spectral aggregation token is introduced for effective dimensional reduction, producing a 2D segmentation result. The experimental results demonstrate that the proposed method significantly outperforms existing techniques.

Swin Transformer uses a hierarchical feature maps and shifted windows for efficient image modeling and scalability. In particular, [190] proposed a Swin Transformer model for multi-class skin lesion classification, leveraging the strengths of both Transformers and CNNs. This model benefits from end-to-end learning capabilities and does not require prior knowledge. To address class imbalance, this approach uses a weighted cross-entropy loss, enhancing the model's performance in dealing with imbalanced datasets. The proposed method was evaluated on the skin lesion imaging. This study demonstrates that the Swin Transformer model outperforms many existing state-of-the-art methods, showing superior balanced accuracy and effectiveness in multiclass skin lesion classification. In contrast [191] addressed the critical need for accurate and timely brain tumor diagnosis. This study introduces an advanced DL approach using the Swin Transformer model as depicted in Figure 13. Key innovations include hybrid shifted windows, multi-head self-attention modules and a residual-based MLP integrated into the swin Transformer. The Res-MLP replaces the traditional MLP to further improve accuracy, training speed, and parameter efficiency. The proposed-swin model was evaluated on the publicly available brain MRI dataset. The model benefits from TL and data augmentation techniques. This approach offers a novel and robust diagnostic tool, supporting radiologists in achieving timely and accurate brain tumor diagnoses. The study [196] addresses the challenge of distinguishing benign from malignant colorectal adenomas. The proposed method, multiple instance learning network (MIST), leverages the swin Transformer as its backbone for feature extraction. This approach utilizes self-supervised contrastive learning and integrates a dual-stream multiple instance learning network to classify whole slide images based solely on slide-level labels, eliminating the need for labor-intensive manual annotation. MIST was trained and validated on a dataset of 666 whole slide images from 480 patients, encompassing six common types of colorectal adenomas. Reference [192], explored the use of swin Transformers for classifying breast cancer subtypes from histopathological images.

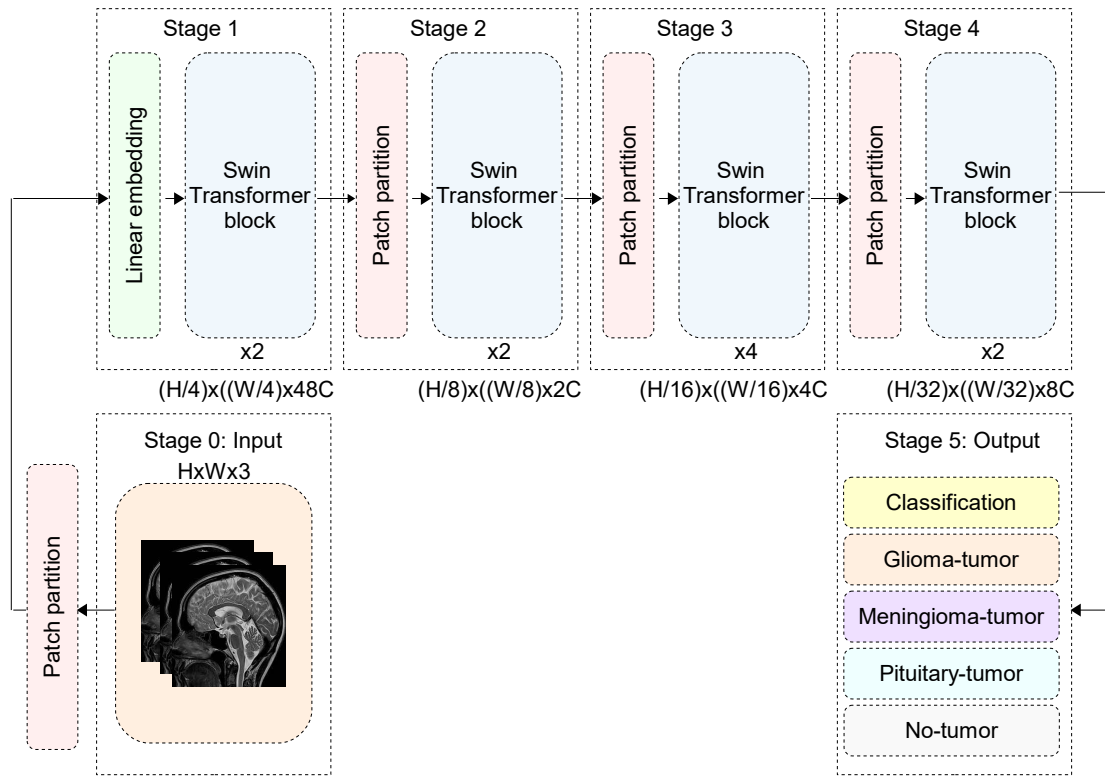


Figure 13: An example of the structure of Swin Transformer architecture for brain tumor diagnosis [191]. The Swin Transformer architecture comprises essential blocks for brain tumor diagnosis. The input module, preprocesses brain scans by normalizing and resizing them. The Patch partitioning block, divides images into fixed-size patches, embedding them into tokens. The Swin Transformer blocks, employ hierarchical learning with shifted window attention, ensuring efficient local-global feature extraction while multi-head self-attention identifies critical regions. Feature Aggregation, progressively reduces spatial dimensions, consolidating key features. The classification head, maps aggregated features to tumor classes using fully connected layers and softmax. Finally, the output delivers diagnostic results, excelling in capturing spatial hierarchies for accurate brain tumor detection.

Other proposed Transformers included the multi-axis ViT introduced by Pacal et al. [161], an advanced architectural framework designed to enhance the early detection of cervical cancer using Pap smear images. The multi-axis ViT was specifically adapted for Pap smear data, featuring a lightweight structure that improved both accuracy and inference speed. [197] replaced MBConv

blocks in the MaxViT architecture with ConvNeXtv2 blocks and MLP blocks with gated residual network gated residual network (GRN)-based MLPs. These modifications significantly reduced the number of parameters and enhanced the model's generalization capabilities. The proposed method was rigorously evaluated on the SIPaKMeD and Mendeley LBC Pap smear datasets, utilizing 106 DL models—53 CNNs and 53 ViT models for each dataset. Barzekar et al. [198] presented a novel DNN architecture, MultiNet, designed to improve the multiclass classification of medical images with a focus on cancer diagnosis. This study integrated Transformers within a multiclass framework to enhance data representation and improve classification accuracy. The proposed MultiNet ViT model was evaluated on publicly available datasets, employing various assessment metrics to ensure reliability. Results demonstrated that MultiNet significantly improved cancer diagnosis accuracy through image classification, potentially reducing the reliance on costly and time-consuming manual analyses by radiologists and pathologists. This approach offered a scalable solution for large-scale biological image classification, paving the way for more efficient and effective cancer detection. Chaudhury et al. [193] explored the integration of ViT and LSTM networks for breast cancer diagnosis, comparing ultrasonography and histology as diagnostic modalities. While traditional CNNs effectively extracted visual features, this study leveraged bidirectional encoder representations from Transformers, optimized for image processing. The integration of ViT and LSTM demonstrated significant potential in improving breast cancer diagnosis, providing a powerful tool for more precise and reliable healthcare decisions.

4.5. Large language models

LLMs, such as GPT, BERT, and their variants, are neural network models designed for processing and understanding human language at scale. LLMs, for example, have also been explored in many medical domains, such as diabetes diagnosis, where LSTM networks and chatbot-based medical support, such as the WizardLM-based DiabeTalk, have been investigated to improve classification accuracy and patient interaction [199]. LLMs are typically based on Transformer architectures, which rely on self-attention mechanisms to capture the relationships between words in a sequence. The self-attention computes a weighted sum of the values, with weights determined by the similarity between queries and keys. LLMs are trained using large corpora through masked language modeling for BERT or autoregressive prediction for GPT, optimizing the following cross-entropy loss:

$$L = - \sum_i \log p(w_i | w_{<i}) \quad (18)$$

where $p(w_i | w_{<i})$ is the probability of word w_i [77, 28, 200]. Among the types of advanced methods, GPT-4 Vision (GPT-4V) is a multi-modal LLM developed by OpenAI, extending the capabilities of GPT-4 by enabling it to process and generate both text and visual data. This integration of vision and language allows GPT-4V to perform a wide range of tasks involving the understanding and reasoning of images in combination with text [61, 201]. Another example is the generalist language model (GLaM), a sparse mixture-of-experts model designed by Google to provide efficient and scalable language modeling with significantly reduced computational cost compared to dense models like GPT-3. GLaM achieves this by activating only a subset of its parameters during each forward pass, making it more efficient in terms of memory and processing power while maintaining high performance [202]. Additionally, Llama-2-70b-chat is a version of the Llama-2 model, an open-source model developed by Meta (formerly Facebook) as part of their LLaMA series. Specifically, Llama-2-70b-chat is a dialogue-optimized model with 70 billion parameters, designed to generate natural and coherent text for conversation-like tasks. It builds on the success of the original LLaMA models and is optimized for chatbot and conversational applications [203, 204]. Figure 14 provides an overview of the key LLMs explored and analyzed in the context of cancer detection. Additionally, Table 15 provides a summary of several state-of-the-art studies that employed LLMs as the primary approach for cancer diagnosis.

The paper [200] introduced **CancerLLM**, a specialized LLM designed for the cancer domain to address the need for more focused and efficient models in healthcare (see Figure 15). The authors highlighted that while existing LLMs such as ClinicalCamel 70B and Llama3-OpenBioLLM 70B are large and computationally expensive, CancerLLM provided a more efficient alternative with 7 billion parameters and a Mistral-style architecture. They provided three datasets specifically designed for cancer phenotype extraction, cancer diagnosis generation, and cancer treatment plan generation. The model was pre-trained on over 2.6 million clinical notes and 500,000 pathology reports covering 17 cancer types and fine-tuned on these tasks. The findings demonstrated that CancerLLM significantly enhanced clinical AI systems, contributing to improved research and healthcare delivery in oncology. Wu et al. [202] proposed a liver cancer diagnosis assistant that combined large and small models to improve diagnostic accuracy, particularly for less experienced doctors in primary healthcare settings. The framework addressed limitations such as inadequate understanding of medical images, insufficient consideration of liver blood vessels, and inaccurate medical information extraction. Small models were optimized for precise perception, with specialized methods for liver tumor and vessel segmentation to enhance information extraction. The large model employed Chain-of-Thought technology to mimic the reasoning process of experienced doctors and utilized retrieval-augmented generation for responses based on reliable domain knowledge. Results showed improved segmentation performance and higher evaluation scores from doctors for the assistant's responses compared to control methods, making it a valuable tool for liver cancer diagnosis. Sun [205] focused on developing five-year survival prediction models for bladder cancer patients undergoing neoadjuvant chemotherapy and radical cystectomy. The study explored the feasibility of using LLMs, such as Vicuna and Dolly, to extract clinical descriptors from reports, which were then incorporated into a nomogram model. It also examined the impact of combining these descriptors with radiomics and DL features derived from CTU images, leveraging back-propagation neural networks (BPNNs). The models, developed and validated using data from 163 patients, included variations based on clinical descriptors (C), radiomics descriptors (R), DL descriptors (D), and their combinations. The performance of models using LLM-extracted descriptors was comparable to those using manually extracted descriptors, demonstrating the potential of LLMs in clinical information extraction for survival prediction. Deng et al. [206] proposed **GeneLLM**, a novel LLM designed

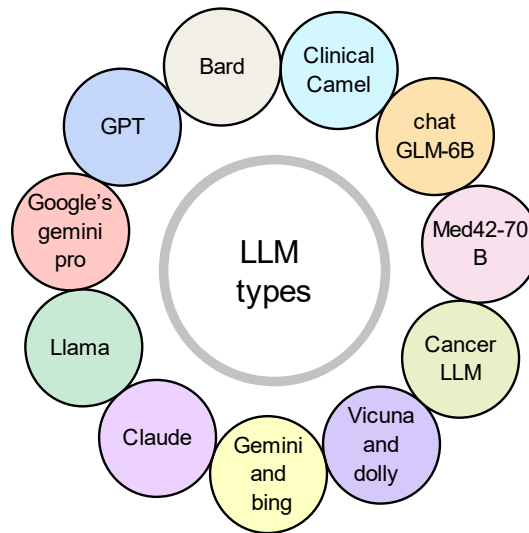


Figure 14: Type of LLM for cancer diagnosis. CancerLL M [200]; Vicuna and dolly [205]; GeneLLM [206]; Llama [207]; GPT [208]; Gemini and bing [208]; Claude and Bard [209]; Privacy-preserving LLM [210]; Off-the-shelf LLMs [211]; Google's Gemini-pro [212]; ClinicalCamel [207]; ChatGLM-6B [202].

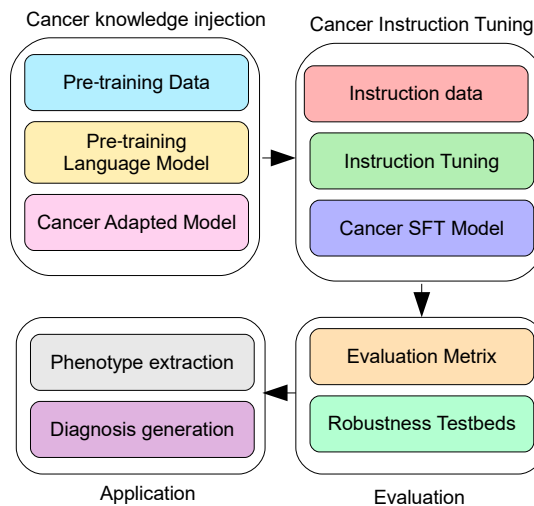


Figure 15: An example of a LLM in cancer domain [200]. The process of adapting an LLM for the cancer domain begins with pre-training a general-purpose language model on diverse datasets. Cancer-specific knowledge is then injected using specialized datasets, publications, and terminologies. Instruction data is created for domain-specific tasks like phenotype extraction and diagnosis generation. The model undergoes instruction tuning and supervised fine-tuning (SFT) to specialize in cancer-related applications. The resulting Cancer-SFT model is evaluated using metrics and robustness tests to ensure reliability. Finally, the model is applied in real-world scenarios, aiding in phenotype extraction, diagnostic insights, and treatment recommendations, enhancing precision and efficiency in cancer research and clinical workflows.

to directly interpret plasma cell-free RNA (cfRNA) sequences for cancer screening, bypassing traditional genome annotations. Unlike conventional methods reliant on bioinformatics tools to count known genes, GeneLLM identified cfRNA from previously unknown genes, termed "dark matters," which serve as pseudo-biomarkers for cancer detection. This approach not only improved detection accuracy but also made the process more accessible and cost-effective. The findings highlighted GeneLLM's potential to revolutionize biomarker discovery and enhance understanding of intercellular communication through novel RNA molecules. Chang et al. [207] investigated the use of open-source clinical LLMs (Llama-2-70b-chat, ClinicalCamel-70B, and Med42-70B) for classifying cancer stages, specifically extracting pathologic tumor-node-metastasis (TNM) staging information from unstructured clinical reports. Unlike traditional NLP approaches that require labor-intensive labeled datasets, this study demonstrated the feasibility of using LLMs without labeled training data. The experiments compared LLMs with a BERT-based model fine-tuned on labeled data. Results showed that while LLMs performed sub-optimally in Tumor (T) classification, they achieved comparable results in Metastasis (M) classification and outperformed in Node (N) classification when appropriate prompting strategies were applied. This demonstrated the potential of LLMs for efficiently extracting staging information for oncology patients from real-world pathology reports. Google's **Gemini** was also employed in the context of cancer detection by Lammert et al. [212], who developed

an advanced system named **MEREDITH** to address the limitations of LLMs in precision oncology. MEREDITH integrated PubMed clinical studies, trial databases, and oncology guidelines with LLMs to enhance the accuracy and relevance of treatment recommendations. The study evaluated the system using 10 fictional patient cases involving 7 tumor types and 59 molecular alterations, assessed by the Molecular Tumor Board (MTB) at the Center of Personalized Medicine (ZPMTUM). MEREDITH employed a retrieval-augmented generation system enhanced by Google's Gemini Pro, along with chain-of-thought prompting. Iterative improvements were made based on expert feedback from MTB, comparing LLM-generated recommendations to those annotated by clinical experts. The study concluded that incorporating expert feedback into LLM training significantly enhanced the model's alignment with clinical reasoning, presenting a promising tool for clinical decision support in precision oncology. Lee et al. [210] evaluated a privacy-preserving **FastChat-T5** for automating question answering from thyroid cancer surgical pathology reports. Eighty-four reports were analyzed by the LLM and two independent reviewers across 12 medical questions related to staging and recurrence risk. FastChat-T5 significantly reduced task completion time while maintaining accuracy comparable to human reviewers.

Sivarajkumar et al. [204] investigated the use of **LLAMA-2** to automate the extraction of treatment response information, particularly disease progression, from EHRs. Their study involved 1,953 primary lung cancer patients from the UPMC Hillman Cancer Center, using approximately 113,000 clinical notes. Disease progression was defined based on RECIST guidelines, with a gold standard dataset created from 50 manually annotated notes. The researchers fine-tuned LLAMA-2 and compared its performance to a traditional rule-based NLP system. The results highlighted the potential of LLMs to improve accuracy and scalability in treatment response assessments. Rajaganapathy et al. [213] applied **LLAMA-2** to automatically generate synoptic reports from 7,774 cancer-related pathology reports annotated with reference synoptic reports from Mayo Clinic EHRs. LLAMA-2 was fine-tuned to produce reports containing 22 unique data elements. The evaluation showed that fine-tuned LLMs effectively automated synoptic report generation, demonstrating their potential to enhance efficiency and accuracy in clinical documentation.

Multiple versions of ChatGPT have been utilized in LLM-based cancer detection and treatment. As examples, Cao et al. [208] evaluated the performance of **ChatGPT-3.5** (OpenAI), **Gemini** (Google), and **Bing** (Microsoft) in answering questions related to hepatocellular carcinoma (liver cancer). Their work assessed the accuracy, reliability, and readability of responses to 20 liver cancer-related questions concerning diagnosis and management. Six fellowship-trained physicians from three academic liver transplant centers evaluated the responses, categorizing them as accurate (all information true and relevant), inadequate (true but incomplete or irrelevant), or inaccurate (false information). Mean scores with standard deviations were recorded to determine overall accuracy and reliability, while readability was assessed using the Flesch Reading Ease Score and Flesch-Kincaid Grade Level. Choi et al. [214] explored the use of **GPT-4** for extracting clinical factors from breast cancer pathology and ultrasound reports. Using 2,931 patient records, they developed prompts for GPT to extract data more time- and cost-efficiently than manual methods. The work demonstrated that LLMs could significantly improve the efficiency of clinical data extraction. Matsuo et al. [215] evaluated **GPT-3.5 Turbo** for Tumor, node, and metastasis (TNM) classification in lung cancer radiology reports, focusing on multilingual capabilities in Japanese and English. The LLM achieved its highest accuracy when provided full TNM definitions in English, showcasing the relevance of LLMs in radiological applications. Deng et al. [216] assessed the performance of **ChatGPT-3.5**, ChatGPT-4.0, and Claude 2 in breast cancer clinical scenarios. ChatGPT-4.0 provided the most accurate and relevant responses, particularly in psychosocial support and treatment decision-making, outperforming other models and highlighting its potential in clinical oncology. Ferber et al. [61] tested **GPT-4V** for cancer histopathology tasks using in-context learning. The LLM matched or surpassed specialized neural networks in colorectal tissue classification, colon polyp subtyping, and breast tumor detection, demonstrating its potential for medical image analysis without domain-specific training. Sushil et al. [51] investigated zero-shot breast cancer pathology classification using **ChatGPT-4** and ChatGPT-3.5. ChatGPT-4 outperformed traditional models, particularly in tasks with label imbalance, highlighting LLMs as a viable alternative for reducing data annotation burdens. Shiraishi et al. [217] explored **LLMs** (GPT-4, Bard, and BingAI) for diagnosing skin lesions. Using prompts with lesion images, they evaluated LLMs in determining malignancy and specific diagnoses. The findings underscored their potential for assisting dermatology patients in seeking professional consultations. Similarly, Zhou et al. [209] compared the performance of LLM-powered chatbots in addressing colorectal cancer queries with oncology physicians. Eight chatbots, including **Claude 2.1**, ChatGPT-3.5, ChatGPT-4, and Doctor GPT, were tested on 150 questions, alongside responses from nine oncology physicians. Each response was scored for consistency with clinical guidelines. Claude 2.1 outperformed residents, fellows, and attendings in accuracy, while Doctor GPT also surpassed residents and fellows. Results indicated that LLMs can provide more accurate information on colorectal cancer than human physicians in certain cases.

Additionally, BERT has also been explored in the same context. Karim et al. [218] addressed challenges in utilizing biomedical data for cancer diagnosis and treatment. They introduced a domain-specific knowledge graph (KG), supported by the OncoNet Ontology (ONO), which integrated information from structured and unstructured sources. The KG, enriched with **BioBERT** and **SciBERT**, enabled semantic reasoning for cancer biomarker discovery and interactive question answering, fine-tuned using LLMs to incorporate the latest research.

Table 15: Summary of LLMs-based approaches in cancer diagnosis.

Ref	Model(s) used	Dataset	Contribution	Best result (%)	Limitation
[200]	CancerLLM	Cancer	LLM for cancer diagnosis and treatment recommendations.	F1: 95.52 Rec: 95.52	Depends on dataset quality and diversity.

Continued on next page

Ref	Model(s) used	Dataset	Contribution	Best result (%)	Limitation
[202]	ChatGLM-6B	Liver cancer	LLM for liver cancer diagnosis with domain-specific knowledge.	Acc: 99.50 Rec: 92.90	Constrained by integrated knowledge sources.
[204]	LLAMA-2	Lung cancer	LLM for detecting lung cancer treatment progression.	F1: 92.00 Spe: 91.00	Variability in patient records.
[205]	Vicuna and Dolly	Bladder cancer	LLM for survival predictions from clinical reports.	AUC: 89.00	Relies on clinical report quality.
[207]	Llama-2-70b-chat	Clinical text	LLM to classify cancer stages from clinical text.	Pre: 98.00 Pre: 94.00	Dependent on text data consistency.
[206]	GeneLLM	cfRNA sequencing	LLM for processing cfRNA reads for cancer screening.	Acc > 78.00 AUC>90.00	Requires extensive computational resources.
[209]	Claude 2.1	Colorectal cancer	LLM chatbots for responding to cancer queries.	Acc: 82.67	Limited by general knowledge base.
[213]	LLAMA-2	Pathology reports	LLM for summarizing cancer pathology reports.	F1: 94.00 Acc: 81.00	Summaries may miss clinical nuances.
[214]	GPT	Breast cancer	LLM for clinical information extraction from pathology reports.	Acc: 98.20	Report formatting variability.
[215]	GPT-3.5-turbo	Lung cancer	Multilingual LLM for lung cancer TNM staging classification.	Acc: 74.00	Variability in report language.
[216]	ChatGPT, and Claude2	Breast cancer	Comparison of ChatGPT and Claude2 for breast cancer scenarios.	Fleiss' kappa: 0.345	Requires further validation.
[218]	BioBERT, and SciBERT	Biomedical literature	LLM and KGs for cancer biomarker discovery.	Pre: 91.36 Rec: 90.75	Complex integration of KGs.
[219]	GPT-3.5 and GPT-4	Radiation oncology	LLM for decision support in radiation oncology.	Acc: 74.57	Needs real-world clinical validation.

5. Computational approaches

Advanced DL methods, including FL, RL, TL, Transformers, and LLMs, have become essential for addressing computationally intensive tasks, enabled by advancements in algorithms, computational power, and access to vast datasets. These methods tackle challenges such as scalability, privacy, and efficiency, unlocking applications previously unattainable. Modern DL architectures vary in layer connectivity and depth, with networks like ResNet evolving toward unprecedented scales, potentially reaching 1000 layers. Optimization strategies, such as SGD, fine-tune parameters to boost accuracy, while FL ensures privacy-preserving training across distributed datasets. Training large models like ResNet on datasets such as ImageNet, with over 14 million images, often requires tens of thousands of iterations and immense computational power, exceeding 10^{20} FLOPS. RL optimizes dynamic decision-making tasks, TL reduces labeled data requirements by leveraging pretrained models, and Transformers/LLMs excel in tasks requiring contextual and multi-modal analysis. Despite improvements in hardware like GPUs and memory bandwidth, rising DL complexity amplifies computational demands, particularly in networks with varying computation-to-bandwidth ratios. These advanced DL techniques are reshaping the landscape of AI, delivering scalable, efficient, and privacy-conscious solutions across diverse fields [220, 221].

5.1. CPU

Advanced deep learning (DL) methods, including FL, RL, TL, Transformers, and LLMs, often require a balance between computational power, memory, and adaptability, making the choice of hardware critical. Central processing unit (CPU) nodes are ideal for tasks that prioritize robust network connections, extensive memory, and storage capabilities, offering flexibility and ease of integration into diverse systems. While CPUs lack the raw computational throughput of specialized hardware like field-programmable gate arrays (FPGAs) and GPUs, they are well-suited for DL techniques like FL, where distributed training across nodes necessitates strong networking and memory resources. Similarly, CPUs can support RL for real-time decision-making and TL for adapting pretrained models to specific tasks without requiring immense computational loads. However, computational-intensive tasks such as fine-tuning Transformers and LLMs on large datasets often benefit from the parallel processing capabilities of GPUs or the customizability of FPGAs. Despite this, the adaptability and versatility of CPUs make them indispensable for many DL applications where network and memory demands outweigh the need for pure processing speed [222, 223].

5.2. GPU

Advanced DL methods, including FL, RL, TL, Transformers, and LLMs, often rely on GPUs for their ability to handle computationally intensive tasks with exceptional efficiency. GPUs excel in executing fundamental DL operations such as AFs, matrix multiplication, and convolutions due to their highly parallel computing capabilities. Modern GPUs, equipped with integrated high bandwidth memory (HBM) stacked memory, significantly boost bandwidth and optimize resource utilization, enabling dense linear algebra operations to outperform CPUs by 10–20 times. This makes GPUs indispensable for tasks like training DNNs, fine-tuning Transformers, and optimizing LLMs for large-scale datasets. For FL, their parallel processing power supports the aggregation of models from distributed nodes, while in RL, GPUs enable real-time learning and decision-making. TL also benefits from GPUs' speed in adapting pretrained models to new tasks, reducing training time. With up to sixty-four computational units, each featuring multiple single instruction, multiple data (SIMD) engines, GPUs achieve peak performances of 25 TFLOPS (fp16) and 10 TFLOPS (fp32), ensuring efficiency in both training and inference. The ability to combine addition and multiplication functions for vector operations and utilize inner product instructions further enhances GPU performance, making them a versatile and essential tool for advanced DL applications [224, 225].

5.3. FPGA

Advanced DL methods, including FL, RL, TL, Transformers, and LLMs, benefit significantly from FPGA technology, particularly in inference acceleration tasks where efficiency and customization are paramount. Unlike GPUs, which offer high floating-point performance, FPGAs excel in minimizing unnecessary functions and overhead, delivering low-latency and energy-efficient solutions. Their ability to dynamically reconfigure array characteristics in real-time and support custom designs makes them highly adaptable for specialized DL operations. FPGAs achieve superior performance per watt through strategies like implementing custom high-performance hardware, pruned networks, and reduced arithmetic precision, often outperforming GPUs and CPUs in these areas. For tasks such as CNN inference, FPGAs deliver over 15 TOPs in peak performance, reaching more than 80% efficiency with 8-bit accuracy. Additionally, pruning techniques, particularly in LSTM models, enable significant model size reductions up to 20 times facilitating optimal deployment in resource-constrained environments. Recent advancements in lowering arithmetic precision to 8-bit fixed-point or custom floating-point formats further enhance FPGA performance, making them ideal for applications requiring highly efficient and tailored solutions, such as in federated learning or LLMs deployed at edge devices [226, 227].

6. Research challenges and future directions

6.1. Challenges

DL is a widely used and highly effective method for training AI systems with large datasets, but it also presents significant challenges that require innovative solutions. These challenges include issues like data privacy, computational costs, limited labeled data, and model interpretability. Advanced DL techniques offer promising alternatives to address these difficulties. FL tackles privacy concerns by enabling collaborative model training across decentralized datasets without sharing sensitive data. RL optimizes decision-making in complex, dynamic environments, making it suitable for tasks like personalized treatment planning. TL mitigates the need for extensive labeled data by leveraging pretrained models to adapt to specific tasks with smaller datasets. Additionally, Transformers and LLMs have revolutionized AI by improving the scalability, accuracy, and interpretability of models in tasks like NLP understanding and medical data analysis. Adopting these advanced approaches not only addresses the limitations of traditional DL methods but also enhances the effectiveness and deployment of AI systems across diverse applications.

- (a) **Training data:** In DL, training data is critical for robust model performance, but data insufficiency remains a challenge. FL addresses this by training models across decentralized data without sharing sensitive information; however, ensuring data privacy, managing communication overhead, and addressing heterogeneity across devices remain key challenges. TL leverages knowledge from related tasks to improve performance on limited datasets, but it often struggles with negative transfer when source and target tasks are not closely related. Transformers, pivotal in modern AI, excel in processing sequential data but require extensive training data, computational resources, and are prone to overfitting on smaller datasets. RL enhances model adaptability through trial-and-error, yet suffers from sample inefficiency and exploration challenges. LLMs face hurdles like data bias, resource intensity, and ensuring generalization across diverse tasks. Overcoming these challenges necessitates innovative strategies in data simulation, optimization, and efficient architecture design.
- (b) **Imbalanced data:** Imbalanced data, where one class significantly outweighs another, poses challenges for training DL models, particularly in maintaining predictive accuracy across all classes. FL can exacerbate this issue when data imbalance occurs across distributed nodes, making global model updates less effective and complicating convergence. TL offers a solution by using pre-trained models from balanced datasets, which can be fine-tuned to improve performance on minority classes. However, the relevance of source domains remains critical. RL, while adaptive, struggles with reward sparsity and policy optimization in imbalanced datasets, further amplifying bias toward majority classes. Transformers and LLMs, although powerful, require balanced data for effective learning and risk significant bias amplification in imbalanced settings, particularly when fine-tuned without addressing class disparities.
- (c) **Interpretability of data:** Interpretability of data is a crucial challenge in DL as models grow in complexity. FL, while preserving data privacy, limits transparency due to distributed data storage, making it harder to understand how local data influences global models. TL, though effective, raises questions about the relevance and transferability of learned features, particularly when adapting to tasks with differing data distributions. RL models face interpretability issues in understanding decision-making processes, especially when reward structures are complex or sparsely distributed. Transformers and LLMs present significant challenges due to their vast number of parameters and opaque attention mechanisms, making it difficult to discern why specific predictions are made. The added complexity of federated, reinforcement, and transfer learning setups, combined with the expansive architectures of transformers and LLMs, exacerbates these interpretability concerns.
- (d) **Uncertainty scaling:** Uncertainty scaling poses significant challenges in FL, TL, RL, Transformers, and LLMs, adding complexities that hinder reliable deployment. Confidence scores, crucial for robust predictions, are often poorly calibrated across these domains. FL and TL face added difficulties due to heterogeneous data distributions across clients or tasks, intensifying uncertainty quantification challenges. In RL, the reliance on cumulative rewards makes the confidence in exploration-exploitation trade-offs unreliable, complicating policy optimization. Transformers and LLMs, while successful, frequently produce overconfident predictions due to softmax-based probabilities, particularly when generalizing to unseen or out-of-distribution data. These challenges are further amplified in critical fields such as healthcare and autonomous systems, where poorly scaled uncertainties can result in life-threatening decisions or system failures.

- (e) **Overfitting:** Data overfitting is a prevalent issue in DL models during training, caused by the complex correlations among a large number of parameters. This overfitting reduces the model's effectiveness on new, unseen data and is a challenge not limited to any single field but common across various tasks, including FL, TL, RL, Transformers, and LLMs. In FL, the decentralized nature and heterogeneous client data exacerbate overfitting risks. Similarly, TL struggles with overfitting when the source and target domains have limited similarity. In RL, the sparse reward structure and high-dimensional state-action spaces often lead to policies overfitting the training environment. Transformers and LLMs face overfitting challenges due to their immense parameter spaces and reliance on pretraining finetuning paradigms, particularly when adapting to domain-specific tasks.
- (f) **Unified assessment:** In numerous studies, there is a notable absence of comprehensive details concerning the technical facets of the experiments conducted. The choice of measurement indicators and baseline methods often seems random, leading to a non-standardized evaluation process. Researchers primarily focus on metrics such as accuracy, sensitivity, or specificity of DL networks. However, Unified Assessment poses additional challenges across advanced methodologies. For FL, standardizing evaluations is difficult due to data heterogeneity, privacy concerns, and inconsistent benchmarks for data. RL struggles with variability in reward structures, task complexity, and cross-environment benchmarking. TL lacks clarity in reporting domain adaptation success and the influence of pre-trained models. Transformers face challenges in scalability, computational overhead, and variations in results across implementations. LLMs complicate assessment with issues of fine-tuning effectiveness, interpretability, and resource-intensive evaluations. A standardized framework addressing these challenges is vital for cancer detection.
- (g) **High computational requirements:** Transformers, particularly ViTs, are computationally intensive and require significant GPU/TPU resources for training and inference. This makes it difficult to deploy these models in real-time clinical settings, especially in resource-constrained environments. Similarly, FL amplifies computational demands due to frequent communication overheads between clients and servers, as well as the need to handle non-IID data across devices. RL is hindered by high computational costs associated with iterative policy optimization and simulation-based training, particularly in complex environments. TL also faces challenges when fine-tuning large pre-trained models on domain-specific datasets, which often requires extensive computational resources. Transformers exacerbate the problem with their quadratic complexity concerning input sequence length, making them unsuitable for low-resource scenarios. LLMs demand immense memory and processing power during both training and inference, further complicating their integration into clinical workflows. Addressing these challenges is critical for scalable deployment in healthcare.

6.2. Future directions

As advanced DL methods represent a significant leap in modern AI techniques, current and future research focuses heavily on their application in cancer diagnosis. Despite extensive research efforts in this field, the use of these methods is still in its early stages, offering vast potential for future development. The complexity of cancer diagnosis arises not only from the variety of types and detection methods but also from handling complex medical data, including radiological images and genetic analyses. To overcome these challenges, AI systems require advanced capabilities in analysis, decision-making, tool utilization, and memory management. Consequently, researchers have identified several key aspects that need to be addressed in systems based on advanced DL methods for cancer diagnosis.

- (a) **TL:** TL will continue to advance by addressing challenges in negative transfer, where knowledge from a pretrained model adversely impacts target tasks. Research is focusing on improving domain adaptation techniques to ensure efficient knowledge transfer across diverse datasets. TL in multitask learning is another promising area, enabling simultaneous optimization of multiple related tasks. The development of scalable and lightweight TL models for deployment on edge devices is also a key focus. Additionally, incorporating TL into continual learning frameworks will allow models to adapt incrementally to new tasks, ensuring long-term usability without catastrophic forgetting.
- (b) **FL:** FL is poised to expand in privacy-preserving applications through advancements in differential privacy and homomorphic encryption, ensuring secure model training on sensitive data like healthcare records. A major future direction includes adaptive FL frameworks that can handle non-IID data and address client variability. FL in edge computing is also expected to grow, enabling decentralized AI systems on low-power devices for real-time applications. Additionally, the integration of FL with emerging technologies like blockchain for secure data sharing and quantum computing for accelerated training promises to redefine its scalability and efficiency in large-scale deployments.
- (c) **RL:** RL is moving toward more sample-efficient algorithms to reduce training time, making it suitable for real-time applications such as computer network [228], and healthcare. A key future direction is the integration of RL with deep learning architectures, like Transformers, for solving complex, high-dimensional problems. Multi-agent RL is also gaining traction, enabling collaboration and competition among agents in dynamic environments. Furthermore, RL is anticipated to play a pivotal role in optimizing autonomous systems, such as self-driving cars and energy management. Bridging RL with unsupervised and semi-supervised learning will enhance its adaptability in scenarios with limited labeled data.
- (d) **Transformers and LLM:** The future of Transformers and LLMs is closely tied to advancements in retrieval-augmented generation (RAG) [229], which combines LLMs with external knowledge retrieval systems. RAG enables LLMs to access and utilize vast databases, reducing the dependency on model size by dynamically fetching relevant information. Future research will focus on optimizing retrieval mechanisms for domain-specific tasks, improving both speed and accuracy. Additionally, integrating

RAG with real-time knowledge updates ensures that models remain current and relevant without extensive retraining. The development of privacy-preserving RAG systems, particularly for sensitive domains like healthcare, will be crucial. RAG's ability to enhance interpretability by linking model outputs to specific knowledge sources also addresses transparency and accountability challenges, paving the way for its broader adoption in fields like personalized medicine, legal analysis, and scientific research.

- (e) **Hybrid approaches:** Future hybrid methods in advanced deep learning promise to revolutionize AI by combining the strengths of techniques such as FL, RL, TL, Transformers, and RAG. For instance, FL and TL can work together to deploy privacy-preserving, personalized models across decentralized systems, especially in healthcare and edge computing. RL integrated with Transformers can enhance sequential decision-making in applications like robotics and conversational agents, while TL combined with RAG enables domain-specific LLMs to incorporate real-time knowledge dynamically. Additionally, FL and RL hybrids can optimize resource allocation in decentralized networks, ensuring privacy and efficiency. Transformers coupled with multimodal learning techniques will further enhance cross-modal understanding for applications in autonomous vehicles and medical diagnostics. By strategically integrating these methods, hybrid approaches will create scalable, efficient, and context-aware AI systems, addressing real-world challenges in personalized healthcare, smart cities, and knowledge-intensive fields like law and medicine.
- (f) **Blockchain for data security:** In the context of cancer detection, the transition from traditional models to advanced DL methods, such as FL, RL, TL, Transformers, LLMs, is driven by the need for improved prediction accuracy, scalability, and real-time data processing of heterogeneous datasets. Traditional models, which relied on centralized datasets, posed significant privacy and security risks, making them unsuitable for handling sensitive patient data. Advanced methods like FL, integrated with blockchain, enable decentralized model training while ensuring secure, tamper-proof data sharing and patient confidentiality. RL enhances decision-making in dynamic scenarios, such as personalized treatment plans and diagnostic workflows, with blockchain providing secure logging of decision-making processes and auditability. TL, when paired with blockchain, enables efficient adaptation of pretrained models to cancer datasets, ensuring data provenance and reducing risks of tampered inputs. Transformers and LLMs deliver exceptional accuracy and contextual understanding for cancer diagnostics, with blockchain enhancing transparency and traceability in multimodal data integration and model updates. Together, these technologies ensure secure, distributed, and precise systems tailored to the complex challenges of cancer detection.
- (g) **Interpretability and scalability:** The application of advanced DL techniques, such as FL, RL, TL, Transformers, and LLMs, holds transformative potential for cancer detection. These methods can improve interpretability by providing clearer insights into patterns and anomalies in medical images or genetic data, making diagnostic results more actionable for physicians. LLMs and Transformers excel in multimodal data analysis, enabling better differentiation between malignant and normal tissues, while FL ensures privacy-preserving collaboration across decentralized datasets. Scalability remains a critical future direction, particularly in integrating these techniques with large, heterogeneous datasets to support diverse cancer types and clinical scenarios. Advanced architectures, such as lightweight LLMs and optimized FL frameworks, can address the challenges of computational efficiency and resource constraints. Future research should prioritize improving interpretability to enhance physician trust and understanding, alongside developing scalable models that deliver precise and personalized cancer diagnosis at population-wide levels.

7. Conclusion

In this comprehensive review, we have explored the transformative potential of advanced DL methodologies, such as RL, FL, TL, Transformers, and LLMs, in enhancing cancer detection and diagnosis. These techniques represent significant progress in overcoming longstanding challenges in medical applications, such as data privacy, model scalability, and the scarcity of labeled datasets. RL has shown promise in optimizing diagnostic and treatment pathways, offering dynamic learning capabilities that adapt to real-time clinical scenarios. By leveraging reward-based mechanisms, RL has demonstrated its utility in tasks ranging from tumor localization to treatment decision-making. FL, on the other hand, provides a privacy-preserving framework for collaborative model training across decentralized datasets, enabling the inclusion of diverse data while addressing privacy concerns. Its application in cancer diagnosis highlights the growing trend toward ethical AI deployment in healthcare. TL continues to mitigate the challenge of limited labeled data by enabling the adaptation of pretrained models to specific cancer datasets. This approach not only enhances model performance but also significantly reduces the computational costs associated with training from scratch. The introduction of Transformer-based models and LLMs has further revolutionized the field by enabling complex, context-aware analysis of medical data, including imaging, genomics, and unstructured text. Their ability to process vast datasets and deliver contextually rich predictions exemplifies the potential of cutting-edge NLP and vision models in oncology.

The review also addresses critical technical challenges, including data imbalance and generalizability issues, by discussing advanced solutions like data augmentation, ensemble methods, and cost-sensitive learning. These approaches ensure that AI models maintain robustness across diverse cancer types and clinical conditions. Furthermore, the incorporation of evaluation metrics and datasets provides a robust foundation for assessing model performance and identifying areas for future improvement. Despite these advancements, several challenges remain. Issues such as the interpretability of complex DL models, the high computational demands of training, and the ethical implications of AI deployment in clinical settings must be addressed to fully realize the potential of these technologies. Future research directions should focus on integrating DL techniques with emerging technologies, such as quantum computing and edge AI, to further enhance efficiency and scalability. In conclusion, the integration of advanced DL techniques into cancer detection and diagnosis is reshaping the landscape of healthcare. By addressing both technical and ethical challenges, these methodologies hold the promise of improving diagnostic accuracy, personalizing treatment plans, and ultimately enhancing patient

outcomes health condition. This review serves as a foundational resource for researchers and practitioners, highlighting the current state, challenges, and future directions in applying advanced DL in oncology.

References

- [1] A. K.-y. Lam, Squamous cell carcinoma of thyroid: a unique type of cancer in world health organization classification, *Endocrine-related cancer* 27 (6) (2020) R177–R192.
- [2] M.-r. Kwon, I. Youn, M. Y. Lee, H.-A. Lee, Diagnostic performance of artificial intelligence–based computer-aided detection software for automated breast ultrasound, *Academic Radiology* 31 (2) (2024) 480–491.
- [3] K. A. Tran, O. Kondrashova, A. Bradley, E. D. Williams, J. V. Pearson, N. Waddell, Deep learning in cancer diagnosis, prognosis and treatment selection, *Genome Medicine* 13 (1) (2021) 1–17.
- [4] B. Jiang, L. Bao, S. He, X. Chen, Z. Jin, Y. Ye, Deep learning applications in breast cancer histopathological imaging: diagnosis, treatment, and prognosis, *Breast Cancer Research* 26 (1) (2024) 137.
- [5] Y. Xie, W.-Y. Meng, R.-Z. Li, Y.-W. Wang, X. Qian, C. Chan, Z.-F. Yu, X.-X. Fan, H.-D. Pan, C. Xie, et al., Early lung cancer diagnostic biomarker discovery by machine learning methods, *Translational oncology* 14 (1) (2021) 100907.
- [6] S. Lal, A. K. Chanchal, J. Kini, G. K. Upadhyay, FPGA implementation of deep learning architecture for kidney cancer detection from histopathological images, *Multimedia Tools and Applications* (2024) 1–19.
- [7] K. Das, C. J. Cockerell, A. Patil, P. Pietkiewicz, M. Giuliani, S. Grabbe, M. Goldust, Machine learning and its application in skin cancer, *International Journal of Environmental Research and Public Health* 18 (24) (2021) 13409.
- [8] M. Jawahar, L. J. Anbarasi, S. Narayanan, A. H. Gandomi, An attention-based deep learning for acute lymphoblastic leukemia classification, *Scientific Reports* 14 (1) (2024) 17447.
- [9] Y. Habchi, Y. Himeur, H. Kheddar, A. Boukabou, S. Atalla, A. Chouchane, A. Ouamane, W. Mansoor, AI in thyroid cancer diagnosis: Techniques, trends, and future directions, *Systems* 11 (10) (2023) 519.
- [10] S. K. Mathivanan, S. Sonaimuthu, S. Murugesan, H. Rajadurai, B. D. Shivhare, M. A. Shah, Employing deep learning and transfer learning for accurate brain tumor detection, *Scientific Reports* 14 (1) (2024) 7232.
- [11] A. Ajit, K. Acharya, A. Samanta, A review of convolutional neural networks, in: 2020 international conference on emerging trends in information technology and engineering (ic-ETITE), IEEE, 2020, pp. 1–5.
- [12] A. Auriemma Citarella, L. Di Biasi, F. De Marco, G. Tortora, Entail: yet another amyloid fibrils classifier, *BMC bioinformatics* 23 (1) (2022) 517.
- [13] A. C. Mazari, H. Kheddar, Deep learning-and transfer learning-based models for covid-19 detection using radiography images, in: 2023 International Conference on Advances in Electronics, Control and Communication Systems (ICAEECS), IEEE, 2023, pp. 1–4.
- [14] Y. Himeur, S. Al-Maadeed, H. Kheddar, N. Al-Maadeed, K. Abualsaud, A. Mohamed, T. Khattab, Video surveillance using deep transfer learning and deep domain adaptation: Towards better generalization, *Engineering Applications of Artificial Intelligence* 119 (2023) 105698.
- [15] Y. Himeur, I. Varlamis, H. Kheddar, A. Amira, S. Atalla, Y. Singh, F. Bensaali, W. Mansoor, Federated learning for computer vision, *arXiv preprint arXiv:2308.13558* (2023).
- [16] H. Kheddar, M. Hemis, Y. Himeur, Automatic speech recognition using advanced deep learning approaches: A survey, *Information Fusion* (2024) 102422.
- [17] S. K. Zhou, H. N. Le, K. Luu, H. V. Nguyen, N. Ayache, Deep reinforcement learning in medical imaging: A literature review, *Medical image analysis* 73 (2021) 102193.
- [18] N. Djeflal, H. Kheddar, D. Addou, A. C. Mazari, Y. Himeur, Automatic speech recognition with BERT and CTC transformers: A review, in: 2023 2nd International Conference on Electronics, Energy and Measurement (IC2EM), Vol. 1, IEEE, 2023, pp. 1–8.
- [19] D. P. Panagoulas, M. Virvou, G. A. Tsihrintzis, Evaluating LLM-Generated Multimodal Diagnosis from Medical Images and Symptom Analysis, *arXiv preprint arXiv:2402.01730* (2024).
- [20] Y. Habchi, H. Kheddar, Y. Himeur, A. Boukabou, A. Chouchane, A. Ouamane, S. Atalla, W. Mansoor, Machine learning and vision transformers for thyroid carcinoma diagnosis: A review, *arXiv preprint arXiv:2403.13843* (2024).
- [21] H. M. Rai, J. Yoo, A comprehensive analysis of recent advancements in cancer detection using machine learning and deep learning models for improved diagnostics, *Journal of Cancer Research and Clinical Oncology* 149 (15) (2023) 14365–14408.
- [22] S. Sharma, K. Guleria, A comprehensive review on federated learning based models for healthcare applications, *Artificial Intelligence in Medicine* 146 (2023) 102691.
- [23] S. Atasever, N. Azginoglu, D. S. Terzi, R. Terzi, A comprehensive survey of deep learning research on medical image analysis with focus on transfer learning, *Clinical imaging* 94 (2023) 18–41.
- [24] H. T. Gayap, M. A. Akhloufi, Deep machine learning for medical diagnosis, application to lung cancer detection: a review, *BioMedInformatics* 4 (1) (2024) 236–284.
- [25] A. Carriero, L. Groenhoff, E. Vologina, P. Basile, M. Albera, Deep learning in breast cancer imaging: State of the art and recent advancements in early 2024, *Diagnostics* 14 (8) (2024) 848.
- [26] S. Nerella, S. Bandyopadhyay, J. Zhang, M. Contreras, S. Siegel, A. Bumin, B. Silva, J. Sena, B. Shickel, A. Bihorac, et al., Transformers and large language models in healthcare: A review, *Artificial Intelligence in Medicine* (2024) 102900.
- [27] M. N. Al-Hamadani, M. A. Fadhel, L. Alzubaidi, B. Harangi, Reinforcement learning algorithms and applications in healthcare and robotics: A comprehensive and systematic review, *Sensors* 24 (8) (2024) 2461.
- [28] Z. A. Nazi, W. Peng, Large language models in healthcare and medical domain: A review, in: *Informatics*, Vol. 11, MDPI, 2024, p. 57.
- [29] X. Jiang, S. Wang, Y. Zhang, Vision transformer promotes cancer diagnosis: A comprehensive review, *Expert Systems with Applications* 252 (2024) 124113.
- [30] K. N. Ryu, W. Jin, J. S. Park, Radiography, MRI, ct, bone scan, and pet-ct, in: *Osteonecrosis*, Springer, 2025, pp. 243–261.
- [31] F. Piccialli, V. Di Somma, F. Giampaolo, S. Cuomo, G. Fortino, A survey on deep learning in medicine: Why, how and when?, *Information Fusion* 66 (2021) 111–137.
- [32] H. Zhang, Y. Qie, Applying deep learning to medical imaging: a review, *Applied Sciences* 13 (18) (2023) 10521.
- [33] H. Kheddar, M. Hemis, Y. Himeur, D. Megias, A. Amira, Deep learning for steganalysis of diverse data types: A review of methods, taxonomy, challenges and future directions, *Neurocomputing* (2024) 127528.
- [34] M. Hemis, H. Kheddar, S. Bourouis, N. Saleem, Deep learning techniques for hand vein biometrics: A comprehensive review, *Information Fusion* (2024) 102716.
- [35] M. Bal-Ghaoui, M. H. E. Y. Alaoui, A. Jilbab, A. Bourouhou, Approaching cross-disease features for improved classification of thyroid and breast cancer in ultrasound images, in: 2023 3rd International Conference on Innovative Research in Applied Science, Engineering and Technology (IRASET), IEEE, 2023, pp. 1–5.
- [36] N. Bibi, M. Sikandar, I. Ud Din, A. Almogren, S. Ali, IoMT-based automated detection and classification of leukemia using deep learning, *Journal of healthcare engineering* 2020 (2020) 1–12.

- [37] M. Mohammed, H. Mwambi, I. B. Mboya, M. K. Elbashir, B. Omolo, A stacking ensemble deep learning approach to cancer type classification based on TCGA data, *Scientific reports* 11 (1) (2021) 15626.
- [38] P. Agarwal, A. Yadav, P. Mathur, Breast cancer prediction on breakhis dataset using deep CNN and transfer learning model, in: *Data Engineering for Smart Systems: Proceedings of SSIC 2021*, Springer, 2022, pp. 77–88.
- [39] E. Gomathi, M. Jayasheela, M. Thamarai, M. Geetha, Skin cancer detection using dual optimization based deep learning network, *Biomedical Signal Processing and Control* 84 (2023) 104968.
- [40] N. Y. Gharaibeh, R. De Fazio, B. Al-Naami, A.-R. Al-Hinnawi, P. Visconti, Automated lung cancer diagnosis applying butterworth filtering, bi-level feature extraction, and sparse convolutional neural network to luna 16 CT images, *Journal of Imaging* 10 (7) (2024).
- [41] J. C. Cai, H. Nakai, S. Kuanar, A. T. Froemming, C. W. Bolan, A. Kawashima, H. Takahashi, L. A. Mynderse, C. D. Dora, M. R. Humphreys, et al., Fully automated deep learning model to detect clinically significant prostate cancer at MRI, *Radiology* 312 (2) (2024) e232635.
- [42] A. Santhoshi, A. Muthukumaravel, Optimizing deep learning algorithms for colorectal tumor identification via noise removal, in: *2024 International Conference on Knowledge Engineering and Communication Systems (ICKECS)*, Vol. 1, IEEE, 2024, pp. 1–6.
- [43] H. Wang, E. Ahn, J. Kim, A multi-resolution self-supervised learning framework for semantic segmentation in histopathology, *Pattern Recognition* 155 (2024) 110621.
- [44] A. M. Mostafa, M. Zakariah, E. A. Aldakheel, Brain tumor segmentation using deep learning on MRI images, *Diagnostics* 13 (9) (2023) 1562.
- [45] A. Dutta, Using machine learning to identify the risk factors of pancreatic cancer from the nih plco dataset (2023).
- [46] J. M. Johnson, T. M. Khoshgoftaar, Survey on deep learning with class imbalance, *Journal of big data* 6 (1) (2019) 1–54.
- [47] L. Han, Y. Huang, H. Dou, S. Wang, S. Ahamad, H. Luo, Q. Liu, J. Fan, J. Zhang, Semi-supervised segmentation of lesion from breast ultrasound images with attentional generative adversarial network, *Computer methods and programs in biomedicine* 189 (2020) 105275.
- [48] M. N. Q. Bhuiyan, M. Shamsujjoha, S. H. Ripon, F. H. Proma, F. Khan, Transfer learning and supervised classifier based prediction model for breast cancer, in: *Big Data Analytics for Intelligent Healthcare Management*, Elsevier, 2019, pp. 59–86.
- [49] S. Pati, U. Baid, B. Edwards, M. Sheller, S.-H. Wang, G. A. Reina, P. Foley, A. Gruzdev, D. Karkada, C. Davatzikos, et al., Federated learning enables big data for rare cancer boundary detection, *Nature communications* 13 (1) (2022) 7346.
- [50] J. An, Y. Wang, Q. Cai, G. Zhao, S. Dooper, G. Litjens, Z. Gao, Transformer-based weakly supervised learning for whole slide lung cancer image classification, *IEEE Journal of Biomedical and Health Informatics* (2024).
- [51] M. Sushil, T. Zack, D. Mandair, Z. Zheng, A. Wali, Y.-N. Yu, Y. Quan, A. J. Butte, A comparative study of zero-shot inference with large language models and supervised modeling in breast cancer pathology classification, *Research Square* (2024).
- [52] X. Liu, C. Yoo, F. Xing, H. Oh, G. El Fakhri, J.-W. Kang, J. Woo, et al., Deep unsupervised domain adaptation: A review of recent advances and perspectives, *APSIPA Transactions on Signal and Information Processing* 11 (1) (2022).
- [53] K. Raza, N. K. Singh, A tour of unsupervised deep learning for medical image analysis, *Current Medical Imaging* 17 (9) (2021) 1059–1077.
- [54] B. Yuan, D. Yang, B. E. Rothberg, H. Chang, T. Xu, Unsupervised and supervised learning with neural network for human transcriptome analysis and cancer diagnosis, *Scientific Reports* 10 (1) (2020) 19106.
- [55] F. Silva, T. Pereira, J. Morgado, J. Frade, J. Mendes, C. Freitas, E. Negrao, B. F. De Lima, M. C. Da Silva, A. J. Madureira, et al., EGFR assessment in lung cancer CT images: analysis of local and holistic regions of interest using deep unsupervised transfer learning, *IEEE Access* 9 (2021) 58667–58676.
- [56] C. I. Bercea, B. Wiestler, D. Rueckert, S. Albarqouni, Feddis: Disentangled federated learning for unsupervised brain pathology segmentation, *arXiv preprint arXiv:2103.03705* (2021).
- [57] J. N. Stember, H. Shalu, Unsupervised deep clustering and reinforcement learning can accurately segment MRI brain tumors with very small training sets, in: *International Symposium on Intelligent Informatics*, Springer, 2022, pp. 255–270.
- [58] O. Pina, V. Vilaplana, Unsupervised domain adaptation for multi-stain cell detection in breast cancer with transformers, in: *Proceedings of the IEEE/CVF Conference on Computer Vision and Pattern Recognition*, 2024, pp. 5066–5074.
- [59] H. S. Jung, H. Lee, Y. S. Woo, S. Y. Baek, J. H. Kim, Expansive data, extensive model: Investigating discussion topics around llm through unsupervised machine learning in academic papers and news, *Plos one* 19 (5) (2024) e0304680.
- [60] M. Grootendorst, BERTopic: Neural topic modeling with a class-based tf-idf procedure, *arXiv preprint arXiv:2203.05794* (2022).
- [61] D. Ferber, G. Wölflein, I. C. Wiest, M. Liger, S. Sainath, N. G. Laleh, O. S. El Nahhas, G. Müller-Franzes, D. Jäger, D. Truhn, et al., In-context learning enables multimodal large language models to classify cancer pathology images, *arXiv preprint arXiv:2403.07407* (2024).
- [62] H. Huang, R. Wu, Y. Li, C. Peng, Self-supervised transfer learning based on domain adaptation for benign-malignant lung nodule classification on thoracic ct, *IEEE Journal of Biomedical and Health Informatics* 26 (8) (2022) 3860–3871.
- [63] S. Dadgar, M. Neshat, Comparative hybrid deep convolutional learning framework with transfer learning for diagnosis of lung cancer, in: *International Conference on Soft Computing and Pattern Recognition*, Springer, 2022, pp. 296–305.
- [64] T. A. Shaikh, R. Ali, M. S. Beg, Transfer learning privileged information fuels cad diagnosis of breast cancer, *Machine Vision and Applications* 31 (1) (2020) 9.
- [65] Y. Zhang, Z. Li, X. Han, S. Ding, J. Li, J. Wang, S. Ying, J. Shi, Pseudo-data based self-supervised federated learning for classification of histopathological images, *IEEE Transactions on Medical Imaging* (2023).
- [66] L. Liu, K. Fan, M. Yang, Federated learning: a deep learning model based on RESNET18 dual path for lung nodule detection, *Multimedia Tools and Applications* 82 (11) (2023) 17437–17450.
- [67] S. Kumbhare, A. B. Kathole, S. Shinde, Federated learning aided breast cancer detection with intelligent heuristic-based deep learning framework, *Biomedical Signal Processing and Control* 86 (2023) 105080.
- [68] L. S. Garia, M. Hariharan, Vision transformers for breast cancer classification from thermal images, in: *Robotics, Control and Computer Vision: Select Proceedings of ICRCCV 2022*, Springer, 2023, pp. 177–185.
- [69] F. Shi, B. Chen, Q. Cao, Y. Wei, Q. Zhou, R. Zhang, Y. Zhou, W. Yang, X. Wang, R. Fan, et al., Semi-supervised deep transfer learning for benign-malignant diagnosis of pulmonary nodules in chest CT images, *IEEE Transactions on medical imaging* 41 (4) (2021) 771–781.
- [70] N. Thungprue, N. Tamronganunsakul, M. Hongchukiat, K. Sumetpipat, T. Leeboonngam, Using semi-supervised transfer learning for classification of solar lentigo, lentigo maligna, and lentigo maligna melanoma, in: *2022 14th Biomedical Engineering International Conference (BMEiCON)*, IEEE, 2022, pp. 1–5.
- [71] K. H. Leung, S. P. Rowe, M. S. Sadaghiani, J. P. Leal, E. Mena, P. L. Choyke, Y. Du, M. G. Pomper, Deep semisupervised transfer learning for fully automated whole-body tumor quantification and prognosis of cancer on PET/CT, *Journal of Nuclear Medicine* 65 (4) (2024) 643–650.
- [72] W. Wang, R. Jiang, N. Cui, Q. Li, F. Yuan, Z. Xiao, Semi-supervised vision transformer with adaptive token sampling for breast cancer classification, *Frontiers in Pharmacology* 13 (2022) 929755.
- [73] X. Yang, Z. Song, I. King, Z. Xu, A survey on deep semi-supervised learning, *IEEE Transactions on Knowledge and Data Engineering* (2022).
- [74] T. Bdaire, N. Navab, S. Albarqouni, FedPerL: Semi-supervised peer learning for skin lesion classification, in: *International Conference on Medical Image Computing and Computer-Assisted Intervention*, Springer, 2021, pp. 336–346.
- [75] C. Barata, V. Rotemberg, N. C. Codella, P. Tschandl, C. Rinner, B. N. Akay, Z. Apalla, G. Argenziano, A. Halpern, A. Lallas, et al., A reinforcement learning model for ai-based decision support in skin cancer, *Nature Medicine* 29 (8) (2023) 1941–1946.
- [76] S. Kumari, A. Das, S. K. Roy, I. Joshi, P. Singh, Leveraging task-specific knowledge from llm for semi-supervised 3d medical image segmentation, *arXiv preprint arXiv:2407.05088* (2024).

- [77] H. Kheddar, Transformers and large language models for efficient intrusion detection systems: A comprehensive survey, arXiv preprint arXiv:2408.07583 (2024).
- [78] H. Kheddar, D. W. Dawoud, A. I. Awad, Y. Himeur, M. K. Khan, Reinforcement-learning-based intrusion detection in communication networks: A review, *IEEE Communications Surveys & Tutorials* (2024).
- [79] R. Khajuria, A. Sarwar, Active reinforcement learning based approach for localization of target roi (region of interest) in cervical cell images, *Multimedia Tools and Applications* (2024) 1–13.
- [80] S. Luo, Lung cancer classification using reinforcement learning-based ensemble learning, *International Journal of Advanced Computer Science and Applications* (IJACSA) 14 (8) (2023).
- [81] Y. Dahdouh, A. Anouar Boudhir, M. Ben Ahmed, A new approach using deep learning and reinforcement learning in healthcare: skin cancer classification, *International journal of electrical and computer engineering systems* 14 (5) (2023) 557–564.
- [82] E. Pesce, S. J. Withey, P.-P. Ypsilantis, R. Bakewell, V. Goh, G. Montana, Learning to detect chest radiographs containing pulmonary lesions using visual attention networks, *Medical image analysis* 53 (2019) 26–38.
- [83] B. Zhao, J. Zhang, D. Ye, J. Cao, X. Han, Q. Fu, W. Yang, Rlogist: fast observation strategy on whole-slide images with deep reinforcement learning, in: *Proceedings of the AAAI Conference on Artificial Intelligence*, Vol. 37, 2023, pp. 3570–3578.
- [84] R. P. Kumar, K. Venkatraman, C. Jawahar, B. Harish, S. Bharathraj, K. Mukesh, Attention-guided residual network for skin lesion classification using deep reinforcement learning, in: *2023 International Conference on Integrated Intelligence and Communication Systems (ICIICS)*, IEEE, 2023, pp. 1–7.
- [85] P. Petousis, S. X. Han, W. Hsu, A. A. Bui, Generating reward functions using irl towards individualized cancer screening, in: *International Workshop on Artificial Intelligence in Health*, Springer, 2018, pp. 213–227.
- [86] P. Petousis, A. Winter, W. Speier, D. R. Aberle, W. Hsu, A. A. Bui, Using sequential decision making to improve lung cancer screening performance, *Ieee Access* 7 (2019) 119403–119419.
- [87] G. Renith, A. Senthilselvi, Automated skin cancer diagnosis and localization using deep reinforcement learning, *IETE Journal of Research* (2024) 1–15.
- [88] S. Arora, M. Lamba, 3d brain image based tumor classification using ensemble of reinforcement transfer-based belief neural networks, *Multimedia Tools and Applications* (2024) 1–28.
- [89] C. Xu, Y. Song, D. Zhang, L. K. Bittencourt, S. H. Tirumani, S. Li, Spatiotemporal knowledge teacher–student reinforcement learning to detect liver tumors without contrast agents, *Medical Image Analysis* 90 (2023) 102980.
- [90] G. Tao, H. Li, J. Huang, C. Han, J. Chen, G. Ruan, W. Huang, Y. Hu, T. Dan, B. Zhang, et al., SeqSeg: a sequential method to achieve nasopharyngeal carcinoma segmentation free from background dominance, *Medical Image Analysis* 78 (2022) 102381.
- [91] P. Praneeth, A. D. Lakshmi, H. Tekchandani, S. Verma, N. D. Londhe, RL2NdgsNet: Reinforcement learning based efficient classifier for mediastinal lymph nodes malignancy detection in CT images, in: *2022 13th International Conference on Computing Communication and Networking Technologies (ICCCNT)*, IEEE, 2022, pp. 1–5.
- [92] Z. Liu, C. Yao, H. Yu, T. Wu, Deep reinforcement learning with its application for lung cancer detection in medical internet of things, *Future Generation Computer Systems* 97 (2019) 1–9.
- [93] P. Balaprakash, R. Egele, M. Salim, S. Wild, V. Vishwanath, F. Xia, T. Brettin, R. Stevens, Scalable reinforcement-learning-based neural architecture search for cancer deep learning research, in: *Proceedings of the international conference for high performance computing, networking, storage and analysis*, 2019, pp. 1–33.
- [94] U. A. Usmani, J. Watada, J. Jaafar, I. A. Aziz, A. Roy, A reinforcement learning algorithm for automated detection of skin lesions, *Applied Sciences* 11 (20) (2021) 9367.
- [95] G. Maicas, A. P. Bradley, J. C. Nascimento, I. Reid, G. Carneiro, Pre and post-hoc diagnosis and interpretation of malignancy from breast DCE-MRI, *Medical image analysis* 58 (2019) 101562.
- [96] R. Huang, Q. Ying, Z. Lin, Z. Zheng, L. Tan, G. Tang, Q. Zhang, M. Luo, X. Yi, P. Liu, et al., Extracting keyframes of breast ultrasound video using deep reinforcement learning, *Medical Image Analysis* 80 (2022) 102490.
- [97] J. Balajee, U. K. B. Hariitha, A. S. Reddy, K. Mounika, K. S. Kumar, Pulmonary chest nodule detection through adaptive reinforcement learning model (arlm), in: *2023 Second International Conference on Electrical, Electronics, Information and Communication Technologies (ICEEICT)*, IEEE, 2023, pp. 01–05.
- [98] Q. Zhang, X. Liu, Y. Wang, Detection of benign and malignant thyroid nodules: an reinforcement region selection network framework, in: *2023 5th International Conference on Machine Learning, Big Data and Business Intelligence (MLBDBI)*, IEEE, 2023, pp. 1–9.
- [99] S. Narad, K. Reddy, Efficient model for prediction of non-small cells lung cancer via deep q-learning, in: *Congress on Intelligent Systems*, Springer, 2023, pp. 403–413.
- [100] N. Thakur, P. Kumar, A. Kumar, Reinforcement learning (RL)-based semantic segmentation and attention based backpropagation convolutional neural network (ABB-CNN) for breast cancer identification and classification using mammogram images, *Neural Computing and Applications* (2024) 1–27.
- [101] A. Heidari, D. Javaheri, S. Toumaj, N. J. Navimipour, M. Rezaei, M. Unal, A new lung cancer detection method based on the chest CT images using federated learning and blockchain systems, *Artificial Intelligence in Medicine* 141 (2023) 102572.
- [102] B. L. Y. Agbley, J. P. Li, A. U. Haq, E. K. Bankas, C. B. Mawuli, S. Ahmad, S. Khan, A. R. Khan, Federated fusion of magnified histopathological images for breast tumor classification in the internet of medical things, *IEEE Journal of Biomedical and Health Informatics* (2023).
- [103] Y. Lan, L. Xie, X. Cai, L. Wang, A many-objective evolutionary algorithm based on integrated strategy for skin cancer detection, *KSII Transactions on Internet and Information Systems (TIIS)* 16 (1) (2022) 80–96.
- [104] M. A. Mohammed, A. Lakhan, K. H. Abdulkareem, B. Garcia-Zapirain, Federated auto-encoder and xgboost schemes for multi-omics cancer detection in distributed fog computing paradigm, *Chemometrics and Intelligent Laboratory Systems* 241 (2023) 104932.
- [105] A. H. Omran, S. Y. Mohammed, M. Aljanabi, Detecting data poisoning attacks in federated learning for healthcare applications using deep learning, *Iraqi Journal for Computer Science and Mathematics* 4 (4) (2023) 225–237.
- [106] G. N. Gunesli, M. Bilal, S. E. A. Raza, N. M. Rajpoot, A Federated Learning Approach to Tumor Detection in Colon Histology Images, *Journal of Medical Systems* 47 (1) (2023) 99.
- [107] H. AlSalman, M. S. Al-Rakhani, T. Alfakih, M. M. Hassan, Federated Learning Approach for Breast Cancer Detection Based on DCNN, *IEEE Access* (2024).
- [108] V. Jindal, V. Kukreja, D. P. Singh, S. Vats, S. Mehta, Modernizing Lung Cancer Detection: The Federated Learning CNN Approach, in: *2023 4th IEEE Global Conference for Advancement in Technology (GCAT)*, IEEE, 2023, pp. 1–6.
- [109] A. Vibith, J. Christ, GBDTMO: as new option for early-stage breast cancer detection and classification using machine learning, *Automatika: časopis za automatiku, mjerenje, elektroniku, računarstvo i komunikacije* 64 (4) (2023) 858–867.
- [110] Y. Supriya, R. Chengoden, Breast cancer prediction using shapely and game theory in federated learning environment, *IEEE Access* (2024).
- [111] S. U. Salma, M. S. Sakib, N. Yasaar, M. M. M. Alvee, M. T. Reza, M. Z. Parvez, Privacy focused classification of prostate cancer using federated learning, in: *International Conference on Information Technology and Applications*, Springer, 2022, pp. 265–281.
- [112] K. R. Kanjula, A. R. Datla, T. Chen, M. F. Kabir, An edge internet of things framework for machine learning-based skin cancer detection models, in: *2023 International Conference on Machine Learning and Applications (ICMLA)*, IEEE, 2023, pp. 2167–2173.
- [113] F. Wagner, Z. Li, P. Saha, K. Kamnitsas, Post-deployment adaptation with access to source data via federated learning and source-target remote gradient alignment, in: *International Workshop on Machine Learning in Medical Imaging*, Springer, 2023, pp. 253–263.

- [114] B. J. Ayekai, C. Wenyu, G. E. S. Addai, A. W. Xornam, K. S. Mawuena, C. B. Mawuli, D. Kulevome, B. L. Agbley, R. E. Turkson, E. E. Kuupole, Personalized federated learning for histopathological prediction of lung cancer, in: 2023 20th International Computer Conference on Wavelet Active Media Technology and Information Processing (ICCWAMTIP), IEEE, 2023, pp. 1–7.
- [115] E. Gad, M. Abou Khatwa, M. A. Elattar, S. Selim, A Novel Approach to Breast Cancer Segmentation Using U-Net Model with Attention Mechanisms and FedProx, in: Annual Conference on Medical Image Understanding and Analysis, Springer, 2023, pp. 310–324.
- [116] X. Lessage, L. Collier, C.-H. B. Van Ouytsel, A. Legay, S. Mahmoudi, P. Massonet, Secure federated learning applied to medical imaging with fully homomorphic encryption, in: 2024 IEEE 3rd International Conference on AI in Cybersecurity (ICAIC), IEEE, 2024, pp. 1–12.
- [117] F. Kong, X. Wang, J. Xiang, S. Yang, X. Wang, M. Yue, J. Zhang, J. Zhao, X. Han, Y. Dong, et al., Federated attention consistent learning models for prostate cancer diagnosis and gleason grading, Computational and Structural Biotechnology Journal 23 (2024) 1439–1449.
- [118] L. Qiu, J. Cheng, H. Gao, W. Xiong, H. Ren, Federated semi-supervised learning for medical image segmentation via pseudo-label denoising, IEEE journal of biomedical and health informatics 27 (10) (2023) 4672–4683.
- [119] J. L. Salmeron, I. Arévalo, A privacy-preserving, distributed and cooperative fcm-based learning approach for cancer research, in: Rough Sets: International Joint Conference, IJCRS 2020, Havana, Cuba, June 29–July 3, 2020, Proceedings, Springer, 2020, pp. 477–487.
- [120] S. Iqbal, A. N. Qureshi, M. Alhussein, K. Aurangzeb, K. Javeed, R. Ali Naqvi, Privacy-preserving collaborative ai for distributed deep learning with cross-sectional data, Multimedia Tools and Applications (2023) 1–23.
- [121] H. Zhu, G. Han, J. Hou, X. Liu, Y. Ma, Knowledge sharing for pulmonary nodule detection in medical cyber-physical systems, IEEE Journal of Biomedical and Health Informatics 27 (2) (2022) 625–635.
- [122] K. F. Zubair Nafis, S. Maisha Tarannum, K. Haque Charu, M. H. Kabir Mehedi, A. Alim Rasel, Comparative analysis of federated learning and centralized approach for detecting different lung diseases, in: Proceedings of the 2023 9th international conference on computer technology applications, 2023, pp. 60–66.
- [123] S. Dagli, K. Dedhia, V. Sawant, A proposed solution to build a breast cancer detection model on confidential patient data using federated learning, in: 2021 IEEE Bombay Section Signature Conference (IBSSC), IEEE, 2021, pp. 1–6.
- [124] C. Yan, X. Zeng, R. Xi, A. Ahmed, M. Hou, M. H. Tunio, PLA—A Privacy-Embedded Lightweight and Efficient Automated Breast Cancer Accurate Diagnosis Framework for the Internet of Medical Things, Electronics 12 (24) (2023) 4923.
- [125] G. Mostafa, M. S. Hamidi, D. M. Farid, Detecting lung cancer with federated and transfer learning, in: 2023 26th International Conference on Computer and Information Technology (ICCIT), IEEE, 2023, pp. 1–6.
- [126] C.-H. Hsiao, F. Y.-S. Lin, T.-L. Sun, Y.-Y. Liao, C.-H. Wu, Y.-C. Lai, H.-P. Wu, P.-R. Liu, B.-R. Xiao, C.-H. Chen, et al., Precision and Robust Models on Healthcare Institution Federated Learning for Predicting HCC on Portal Venous CT Images, IEEE Journal of Biomedical and Health Informatics (2024).
- [127] A. Jiménez-Sánchez, M. Tardy, M. A. G. Ballester, D. Mateus, G. Piella, Memory-aware curriculum federated learning for breast cancer classification, Computer Methods and Programs in Biomedicine 229 (2023) 107318.
- [128] M. Sikandar, I. U. Din, A. Almogren, Integrating generative AI and federated learning for privacy preserved sequence-based stomach adenocarcinoma detection, IEEE Transactions on Consumer Electronics (2024).
- [129] Y. N. Tan, P. D. Lam, V. P. Tinh, D.-D. Le, N. H. Nam, T. A. Khoa, Joint federated learning using deep segmentation and the gaussian mixture model for breast cancer tumors, IEEE Access (2024).
- [130] S. Bhadauriya, T. Merothiya, S. C. Yadav, M. ChandraPrabha, Detection of brain tumour using CNN in federated machine learning, in: 2023 5th International Conference on Advances in Computing, Communication Control and Networking (ICAC3N), IEEE, 2023, pp. 653–658.
- [131] N. K. Trivedi, S. Jain, S. Kaswan, V. Jain, Federated Learning Empowered Breast Cancer Detection in Images: A YOLO and ResNet-50 Fusion Approach, in: 2024 International Conference on Computational Intelligence and Computing Applications (ICCICA), Vol. 1, IEEE, 2024, pp. 24–29.
- [132] Y. Habchi, H. Kheddar, Y. Himeur, A. Boukabou, S. Atalla, W. Mansoor, H. Al-Ahmad, Deep transfer learning for kidney cancer diagnosis, arXiv preprint arXiv:2408.04318 (2024).
- [133] S. S. Sohail, Y. Himeur, H. Kheddar, A. Amira, F. Fadli, S. Atalla, A. Copiaco, W. Mansoor, Advancing 3d point cloud understanding through deep transfer learning: A comprehensive survey, Information Fusion (2024) 102601.
- [134] H. Kheddar, Y. Himeur, S. Al-Maadeed, A. Amira, F. Bensaali, Deep transfer learning for automatic speech recognition: Towards better generalization, Knowledge-Based Systems 277 (2023) 110851.
- [135] H. Kheddar, Y. Himeur, A. I. Awad, Deep transfer learning for intrusion detection in industrial control networks: A comprehensive review, Journal of Network and Computer Applications 220 (2023) 103760.
- [136] H. Aljuaid, N. Alturki, N. Alsubaie, L. Cavallaro, A. Liotta, Computer-aided diagnosis for breast cancer classification using deep neural networks and transfer learning, Computer Methods and Programs in Biomedicine 223 (2022) 106951.
- [137] M. M. Kalbhor, S. V. Shinde, Cervical cancer diagnosis using convolution neural network: feature learning and transfer learning approaches, Soft Computing (2023) 1–11.
- [138] K. Bansal, R. Bathla, Y. Kumar, Deep transfer learning techniques with hybrid optimization in early prediction and diagnosis of different types of oral cancer, Soft Computing 26 (21) (2022) 11153–11184.
- [139] G. Ayana, J. Park, J.-W. Jeong, S.-w. Choe, A novel multistage transfer learning for ultrasound breast cancer image classification, Diagnostics 12 (1) (2022) 135.
- [140] Z. Rong, D. Lingyun, L. Jinxing, G. Ying, Diagnostic classification of lung cancer using deep transfer learning technology and multi-omics data, Chinese Journal of Electronics 30 (5) (2021) 843–852.
- [141] S. Mehmood, T. M. Ghazal, M. A. Khan, M. Zubair, M. T. Naseem, T. Faiz, M. Ahmad, Malignancy detection in lung and colon histopathology images using transfer learning with class selective image processing, IEEE Access 10 (2022) 25657–25668.
- [142] H. Zhou, K. Wang, J. Tian, Online transfer learning for differential diagnosis of benign and malignant thyroid nodules with ultrasound images, IEEE Transactions on Biomedical Engineering 67 (10) (2020) 2773–2780.
- [143] S. Khan, N. Islam, S. Jan, I. U. Din, J. J. C. Rodrigues, A novel deep learning based framework for the detection and classification of breast cancer using transfer learning, Pattern Recognition Letters 125 (2019) 1–6.
- [144] A. Saber, M. Sakr, O. M. Abo-Seida, A. Keshk, H. Chen, A novel deep-learning model for automatic detection and classification of breast cancer using the transfer-learning technique, IEEE Access 9 (2021) 71194–71209.
- [145] V. Anand, S. Gupta, A. Altameem, S. R. Nayak, R. C. Poonia, A. K. J. Saudagar, An enhanced transfer learning based classification for diagnosis of skin cancer, Diagnostics 12 (7) (2022) 1628.
- [146] H. M. Balaha, A. E.-S. Hassan, Skin cancer diagnosis based on deep transfer learning and sparrow search algorithm, Neural Computing and Applications 35 (1) (2023) 815–853.
- [147] A. Pati, M. Parhi, B. K. Pattanayak, D. Singh, V. Singh, S. Kadry, Y. Nam, B.-G. Kang, Breast cancer diagnosis based on IoT and deep transfer learning enabled by fog computing, Diagnostics 13 (13) (2023) 2191.
- [148] A. Faghihi, M. Fathollahi, R. Rajabi, Diagnosis of skin cancer using VGG16 and VGG19 based transfer learning models, Multimedia Tools and Applications 83 (19) (2024) 57495–57510.
- [149] R. Rai, D. S. Sisodia, Real-time data augmentation based transfer learning model for breast cancer diagnosis using histopathological images, in: Advances in Biomedical Engineering and Technology: Select Proceedings of ICBEST 2018, Springer, 2021, pp. 473–488.
- [150] S. Deepak, P. Ameer, Brain tumor classification using deep CNN features via transfer learning, Computers in biology and medicine 111 (2019) 103345.

- [151] K. S. Rao, P. V. Terlapu, D. Jayaram, K. K. Raju, G. K. Kumar, R. Pemula, V. Gopalachari, S. Rakesh, Intelligent ultrasound imaging for enhanced breast cancer diagnosis: Ensemble transfer learning strategies, *IEEE Access* (2024).
- [152] Y. Celik, M. Talo, O. Yildirim, M. Karabatak, U. R. Acharya, Automated invasive ductal carcinoma detection based using deep transfer learning with whole-slide images, *Pattern Recognition Letters* 133 (2020) 232–239.
- [153] Y. Chen, X. Qin, J. Xiong, S. Xu, J. Shi, H. Lv, L. Li, H. Xing, Q. Zhang, Deep transfer learning for histopathological diagnosis of cervical cancer using convolutional neural networks with visualization schemes, *Journal of Medical Imaging and Health Informatics* 10 (2) (2020) 391–400.
- [154] N. A. Samee, A. A. Alhussan, V. F. Ghoneim, G. Atteia, R. Alkanhel, M. A. Al-Antari, Y. M. Kadah, A hybrid deep transfer learning of CNN -based LR-PCA for breast lesion diagnosis via medical breast mammograms, *Sensors* 22 (13) (2022) 4938.
- [155] N. A. Samee, N. F. Mahmoud, G. Atteia, H. A. Abdallah, M. Alabdulhafith, M. S. Al-Gaashani, S. Ahmad, M. S. A. Muthanna, Classification framework for medical diagnosis of brain tumor with an effective hybrid transfer learning model, *Diagnostics* 12 (10) (2022) 2541.
- [156] S. Aziz, K. Munir, A. Raza, M. S. Almutairi, S. Nawaz, IVNet: Transfer learning based diagnosis of breast cancer grading using histopathological images of infected cells, *IEEE Access* 11 (2023) 127880–127894.
- [157] L. Alzubaidi, M. Al-Amidie, A. Al-Asadi, A. J. Humaidi, O. Al-Shamma, M. A. Fadhel, J. Zhang, J. Santamaría, Y. Duan, Novel transfer learning approach for medical imaging with limited labeled data, *Cancers* 13 (7) (2021) 1590.
- [158] M. T. Mali, E. Hancer, R. Samet, Z. Yildirim, N. Nemati, Detection of colorectal cancer with vision transformers, in: *2022 Innovations in Intelligent Systems and Applications Conference (ASYU)*, IEEE, 2022, pp. 1–6.
- [159] Q. Abbas, Y. Daadaa, U. Rashid, M. E. Ibrahim, Assist-dermo: A lightweight separable vision transformer model for multiclass skin lesion classification, *Diagnostics* 13 (15) (2023) 2531.
- [160] T. Gulsoy, E. B. Kablan, Diagnosis of lung cancer based on CT scans using vision transformers, in: *2023 14th International Conference on Electrical and Electronics Engineering (ELECO)*, IEEE, 2023, pp. 1–5.
- [161] I. Pacal, Maxcervixt: A novel lightweight vision transformer-based approach for precise cervical cancer detection, *Knowledge-Based Systems* 289 (2024) 111482.
- [162] G. Ayana, H. Barki, S.-w. Choe, Pathological insights: Enhanced vision transformers for the early detection of colorectal cancer, *Cancers* 16 (7) (2024) 1441.
- [163] Z. Zhou, S. Qiu, Y. Wang, M. Zhou, X. Chen, M. Hu, Q. Li, Y. Lu, Swin-spectral transformer for cholangiocarcinoma hyperspectral image segmentation, in: *2021 14th International Congress on Image and Signal Processing, BioMedical Engineering and Informatics (CISP-BMEI)*, IEEE, 2021, pp. 1–6.
- [164] C. Zhao, R. Shuai, L. Ma, W. Liu, M. Wu, Improving cervical cancer classification with imbalanced datasets combining taming transformers with t2t-vit, *Multimedia tools and applications* 81 (17) (2022) 24265–24300.
- [165] L. Wang, J. Liu, P. Jiang, D. Cao, B. Pang, Lgvit: Local-global vision transformer for breast cancer histopathological image classification, in: *ICASSP 2023-2023 IEEE International Conference on Acoustics, Speech and Signal Processing (ICASSP)*, IEEE, 2023, pp. 1–5.
- [166] R. J. Chen, R. G. Krishnan, Self-supervised vision transformers learn visual concepts in histopathology, *arXiv preprint arXiv:2203.00585* (2022).
- [167] S. Tabatabaei, K. Rezaee, M. Zhu, Attention transformer mechanism and fusion-based deep learning architecture for MRI brain tumor classification system, *Biomedical Signal Processing and Control* 86 (2023) 105119.
- [168] L. Chen, H. Ge, J. Li, Crossformer: Multi-scale cross-attention for polyp segmentation, *IET Image Processing* 17 (12) (2023) 3441–3452.
- [169] A. Sriwastawa, J. A. Arul Jothi, Vision transformer and its variants for image classification in digital breast cancer histopathology: A comparative study, *Multimedia Tools and Applications* 83 (13) (2024) 39731–39753.
- [170] K. Ikromjanov, S. Bhattacharjee, Y.-B. Hwang, R. I. Sumon, H.-C. Kim, H.-K. Choi, Whole slide image analysis and detection of prostate cancer using vision transformers, in: *2022 international conference on artificial intelligence in information and communication (ICAIC)*, IEEE, 2022, pp. 399–402.
- [171] S. Tummala, S. Kadry, S. A. C. Bukhari, H. T. Rauf, Classification of brain tumor from magnetic resonance imaging using vision transformers ensembling, *Current Oncology* 29 (10) (2022) 7498–7511.
- [172] E. Pachetti, S. Colantonio, M. A. Pascali, On the effectiveness of 3D vision transformers for the prediction of prostate cancer aggressiveness, in: *International Conference on Image Analysis and Processing*, Springer, 2022, pp. 317–328.
- [173] J. Sun, B. Wu, T. Zhao, L. Gao, K. Xie, T. Lin, J. Sui, X. Li, X. Wu, X. Ni, Classification for thyroid nodule using vit with contrastive learning in ultrasound images, *Computers in biology and medicine* 152 (2023) 106444.
- [174] X. Chen, K. Zhang, N. Abdoli, P. W. Gilley, X. Wang, H. Liu, B. Zheng, Y. Qiu, Transformers improve breast cancer diagnosis from unregistered multi-view mammograms, *Diagnostics* 12 (7) (2022) 1549.
- [175] G. Yang, S. Luo, P. Greer, A novel vision transformer model for skin cancer classification, *Neural Processing Letters* 55 (7) (2023) 9335–9351.
- [176] G. Ayana, S.-w. Choe, Vision transformers-based transfer learning for breast mass classification from multiple diagnostic modalities, *Journal of Electrical Engineering & Technology* (2024) 1–20.
- [177] R. R. Nejad, S. Hooshmand, HViT4Lung: hybrid vision transformers augmented by transfer learning to enhance lung cancer diagnosis, in: *2023 5th International Conference on Bio-engineering for Smart Technologies (BioSMART)*, IEEE, 2023, pp. 1–7.
- [178] S. Hossain, A. Chakrabarty, T. R. Gadekallu, M. Alazab, M. J. Piran, Vision transformers, ensemble model, and transfer learning leveraging explainable ai for brain tumor detection and classification, *IEEE Journal of Biomedical and Health Informatics* 28 (3) (2023) 1261–1272.
- [179] J. Yang, A. Rusak, A. Belozubov, Enhancing brain tumor classification using data-efficient image transformer, in: *2024 International Russian Smart Industry Conference (SmartIndustryCon)*, IEEE, 2024, pp. 339–343.
- [180] Z. Zhou, G. Sun, L. Yu, S. Tian, G. Xiao, J. Wang, S. Zhou, Rfia-net: Rich CNN -transformer network based on asymmetric fusion feature aggregation to classify stage i multimodality oesophageal cancer images, *Engineering Applications of Artificial Intelligence* 118 (2023) 105703.
- [181] C. Xin, Z. Liu, K. Zhao, L. Miao, Y. Ma, X. Zhu, Q. Zhou, S. Wang, L. Li, F. Yang, et al., An improved transformer network for skin cancer classification, *Computers in Biology and Medicine* 149 (2022) 105939.
- [182] T. Zhang, Y. Feng, Y. Zhao, G. Fan, A. Yang, S. Lyu, P. Zhang, F. Song, C. Ma, Y. Sun, et al., Msht: Multi-stage hybrid transformer for the rose image analysis of pancreatic cancer, *IEEE Journal of Biomedical and Health Informatics* 27 (4) (2023) 1946–1957.
- [183] P. Yin, B. Yu, C. Jiang, H. Chen, Pyramid tokens-to-token vision transformer for thyroid pathology image classification, in: *2022 Eleventh International Conference on image processing theory, tools and applications (IPTA)*, IEEE, 2022, pp. 1–6.
- [184] S. J. Wagner, D. Reisenbüchler, N. P. West, J. M. Niehues, J. Zhu, S. Foersch, G. P. Veldhuizen, P. Quirke, H. I. Grabsch, P. A. van den Brandt, et al., Transformer-based biomarker prediction from colorectal cancer histology: A large-scale multicentric study, *Cancer Cell* 41 (9) (2023) 1650–1661.
- [185] A. Alotaibi, T. Alafif, F. Alkhilaiwi, Y. Alatawi, H. Althobaiti, A. Alrefaei, Y. Hawsawi, T. Nguyen, Vit-deit: An ensemble model for breast cancer histopathological images classification, in: *2023 1st International Conference on Advanced Innovations in Smart Cities (ICAISC)*, IEEE, 2023, pp. 1–6.
- [186] Y. Gulzar, S. A. Khan, Skin lesion segmentation based on vision transformers and convolutional neural networks—a comparative study, *Applied Sciences* 12 (12) (2022) 5990.
- [187] S. S. Boudouh, M. Bouakkaz, Advancing precision in breast cancer detection: a fusion of vision transformers and CNNs for calcification mammography classification, *Applied Intelligence* (2024) 1–14.
- [188] G. J. Ferdous, K. A. Sathi, M. A. Hossain, M. M. Hoque, M. A. A. Dewan, Lcdeit: A linear complexity data-efficient image transformer for MRI brain tumor classification, *IEEE Access* 11 (2023) 20337–20350.
- [189] S. M. H. Hashemi, L. Safari, A. D. Taromi, Realism in action: Anomaly-aware diagnosis of brain tumors from medical images using YOLOv8 and DeiT, *arXiv preprint arXiv:2401.03302* (2024).

- [190] S. Ayas, Multiclass skin lesion classification in dermoscopic images using Swin transformer model, *Neural Computing and Applications* 35 (9) (2023) 6713–6722.
- [191] I. Pacal, A novel Swin transformer approach utilizing residual multi-layer perceptron for diagnosing brain tumors in MRI images, *International Journal of Machine Learning and Cybernetics* (2024) 1–19.
- [192] S. Tummala, J. Kim, S. Kadry, Breast-net: Multi-class classification of breast cancer from histopathological images using ensemble of Swin transformers, *Mathematics* 10 (21) (2022) 4109.
- [193] S. Chaudhury, K. Sau, N. Shelke, Transforming breast cancer image classification with vision transformers and lstm integration, in: 2024 IEEE International Students' Conference on Electrical, Electronics and Computer Science (SCEECS), IEEE, 2024, pp. 1–8.
- [194] D. Gai, J. Zhang, Y. Xiao, W. Min, Y. Zhong, Y. Zhong, Rmtf-net: Residual mix transformer fusion net for 2d brain tumor segmentation, *Brain Sciences* 12 (9) (2022) 1145.
- [195] S. Basu, M. Gupta, P. Rana, P. Gupta, C. Arora, Radformer: Transformers with global–local attention for interpretable and accurate gallbladder cancer detection, *Medical Image Analysis* 83 (2023) 102676.
- [196] H. Cai, X. Feng, R. Yin, Y. Zhao, L. Guo, X. Fan, J. Liao, Mist: multiple instance learning network based on Swin transformer for whole slide image classification of colorectal adenomas, *The Journal of Pathology* 259 (2) (2023) 125–135.
- [197] Z. Tu, H. Talebi, H. Zhang, F. Yang, P. Milanfar, A. Bovik, Y. Li, Maxvit: Multi-axis vision transformer, in: *European conference on computer vision*, Springer, 2022, pp. 459–479.
- [198] H. Barzekar, Y. Patel, L. Tong, Z. Yu, Multinet with transformers: a model for cancer diagnosis using images, *arXiv preprint arXiv:2301.09007* (2023).
- [199] D. Rossi, A. A. Citarella, F. De Marco, L. Di Biasi, G. Tortora, Comparative analysis of diabetes diagnosis: We-lstm networks and wizardlm-powered diabetalk chatbot, in: 2024 IEEE International Conference on Bioinformatics and Biomedicine (BIBM), IEEE, 2024, pp. 6859–6866.
- [200] M. Li, A. Blaes, S. Johnson, H. Liu, H. Xu, R. Zhang, Cancerllm: A large language model in cancer domain, *arXiv preprint arXiv:2406.10459* (2024).
- [201] N. Naik, A. Khandelwal, M. Joshi, M. Atre, H. Wright, K. Kannan, S. Hill, G. Mamidipudi, G. Srinivasa, C. Bifulco, et al., Applying large language models for causal structure learning in non small cell lung cancer, in: 2024 IEEE 12th International Conference on Healthcare Informatics (ICHI), IEEE, 2024, pp. 688–693.
- [202] X. Wu, G. Li, X. Wang, Z. Xu, Y. Wang, J. Xian, X. Wang, G. Li, K. Yuan, Diagnosis assistant for liver cancer utilizing a large language model with three types of knowledge, *arXiv preprint arXiv:2406.18039* (2024).
- [203] C.-H. Change, M. M. Lucas, G. Lu-Yao, C. C. Yang, Classifying cancer stage with open-source clinical large language models, in: 2024 IEEE 12th International Conference on Healthcare Informatics (ICHI), IEEE, 2024, pp. 76–82.
- [204] S. Sivarajkumar, S. Edupuganti, M. Bhattacharya, D. Lazris, M. Davis, Y. Huang, Y. Wang, Automating the detection of treatment progression in patients with lung cancer using large language models. (2024).
- [205] D. Sun, L. Hadjiiski, J. Gormley, H.-P. Chan, E. M. Caoili, R. Cohan, A. Alva, R. Mihalcea, C. Zhou, V. Gulani, Large language model-assisted information extraction from clinical reports for survival prediction of bladder cancer patients, in: *Medical Imaging 2024: Computer-Aided Diagnosis*, Vol. 12927, SPIE, 2024, pp. 449–454.
- [206] S. Deng, L. Sha, Y. Jin, T. Zhou, C. Wang, Q. Liu, H. Guo, C. Xiong, Y. Xue, X. Li, et al., Genellm: A large cfRNA language model for cancer screening from raw reads, *bioRxiv* (2024) 2024–06.
- [207] C.-H. Chang, M. M. Lucas, G. Lu-Yao, C. C. Yang, Classifying cancer stage with open-source clinical large language models, *arXiv preprint arXiv:2404.01589* (2024).
- [208] J. J. Cao, D. H. Kwon, T. T. Ghaziani, P. Kwo, G. Tse, A. Kesselman, A. Kamaya, J. R. Tse, Large language models' responses to liver cancer surveillance, diagnosis, and management questions: accuracy, reliability, readability, *Abdominal Radiology* (2024) 1–9.
- [209] S. Zhou, X. Luo, C. Chen, H. Jiang, C. Yang, G. Ran, J. Yu, C. Yin, The performance of large language model powered chatbots compared to oncology physicians on colorectal cancer queries, *International Journal of Surgery* (2024) 10–1097.
- [210] D. Lee, A. Vaid, K. Menon, R. Freeman, D. Matteson, M. Marin, G. Nadkarni, Development of a privacy preserving large language model for automated data extraction from thyroid cancer pathology reports, *medRxiv* (2023) 2023–11.
- [211] P. Manjunath, B. Lerner, T. Dunn, Towards interactive and interpretable image retrieval-based diagnosis: Enhancing brain tumor classification with llm explanations and latent structure preservation, in: *International Conference on Artificial Intelligence in Medicine*, Springer, 2024, pp. 335–349.
- [212] J. Lammert, T. F. Dreyer, A. M. Lörsch, J. Jung, S. Lange, N. Pfarr, A. Durner, M. B. Kiechle, U. A. Schatz, S. Mathes, et al., Large language models for precision oncology: Clinical decision support through expert-guided learning. (2024).
- [213] S. Rajaganapathy, S. Chowdhury, V. Buchner, Z. He, X. Jiang, P. Yang, J. R. Cerhan, N. Zong, Synoptic reporting by summarizing cancer pathology reports using large language models, *medRxiv* (2024) 2024–04.
- [214] H. S. Choi, J. Y. Song, K. H. Shin, J. H. Chang, B.-S. Jang, Developing prompts from large language model for extracting clinical information from pathology and ultrasound reports in breast cancer, *Radiation Oncology Journal* 41 (3) (2023) 209.
- [215] H. Matsuo, M. Nishio, T. Matsunaga, K. Fujimoto, T. Murakami, Exploring multilingual large language models for enhanced tnm classification of radiology report in lung cancer staging, *arXiv preprint arXiv:2406.06591* (2024).
- [216] L. Deng, T. Wang, Z. Zhai, W. Tao, J. Li, Y. Zhao, S. Luo, J. Xu, et al., Evaluation of large language models in breast cancer clinical scenarios: a comparative analysis based on chatgpt-3.5, chatgpt-4.0, and claude2, *International Journal of Surgery* 110 (4) (2024) 1941–1950.
- [217] M. Shiraiishi, K. Kanayama, R. Yang, M. Okazaki, Preliminary evaluation of the potential of commercially available large language models in diagnosing skin tumours, *Clinical and Experimental Dermatology* (2023) 114430.
- [218] M. R. Karim, L. M. Comet, M. Shajalal, O. Beyan, D. Rebholz-Schuhmann, S. Decker, From large language models to knowledge graphs for biomarker discovery in cancer, *arXiv preprint arXiv:2310.08365* (2023).
- [219] F. Putz, M. Haderlein, S. Lettmaier, S. Semrau, R. Fietkau, Y. Huang, Exploring the capabilities and limitations of large language models for radiation oncology decision support, *International Journal of Radiation Oncology, Biology, Physics* 118 (4) (2024) 900–904.
- [220] A. Darwish, A. E. Hassanien, S. Das, A survey of swarm and evolutionary computing approaches for deep learning, *Artificial intelligence review* 53 (2020) 1767–1812.
- [221] W. Cui, A. Aouidate, S. Wang, Q. Yu, Y. Li, S. Yuan, Discovering anti-cancer drugs via computational methods, *Frontiers in pharmacology* 11 (2020) 733.
- [222] M. Biswas, V. Kuppli, L. Saba, D. R. Edla, H. S. Suri, E. Cuadrado-Godia, J. R. Laird, R. T. Marinho, J. M. Sanches, A. Nicolaidis, et al., State-of-the-art review on deep learning in medical imaging, *Frontiers in Bioscience-Landmark* 24 (3) (2019) 380–406.
- [223] A. Paszke, S. Gross, F. Massa, A. Lerer, J. Bradbury, G. Chanan, T. Killeen, Z. Lin, N. Gimelshein, L. Antiga, et al., Pytorch: An imperative style, high-performance deep learning library, *Advances in neural information processing systems* 32 (2019).
- [224] E. Gianniti, L. Zhang, D. Ardagna, Performance prediction of GPU-based deep learning applications, in: 2018 30th International Symposium on Computer Architecture and High Performance Computing (SBAC-PAD), IEEE, 2018, pp. 167–170.
- [225] S. Hossain, D.-j. Lee, Deep learning-based real-time multiple-object detection and tracking from aerial imagery via a flying robot with GPU-based embedded devices, *Sensors* 19 (15) (2019) 3371.
- [226] T. Wang, C. Wang, X. Zhou, H. Chen, An overview of FPGA based deep learning accelerators: challenges and opportunities, in: 2019 IEEE 21st International Conference on High Performance Computing and Communications; IEEE 17th International Conference on Smart City; IEEE 5th International Conference on Data Science and Systems (HPCC/SmartCity/DSS), IEEE, 2019, pp. 1674–1681.

- [227] A. Namburu, D. Sumathi, R. Raut, R. H. Jhaveri, R. K. Dhanaraj, N. Subbulakshmi, B. Balusamy, FPGA-based deep learning models for analysing corona using chest X-ray images, *Mobile Information Systems 2022* (2022) 1–14.
- [228] A. Gueriani, H. Kheddar, A. C. Mazari, Deep reinforcement learning for intrusion detection in IoT: A survey, in: *2023 2nd International Conference on Electronics, Energy and Measurement (IC2EM)*, Vol. 1, IEEE, 2023, pp. 1–7.
- [229] P. Lewis, E. Perez, A. Piktus, F. Petroni, V. Karpukhin, N. Goyal, H. Küttler, M. Lewis, W.-t. Yih, T. Rocktäschel, et al., Retrieval-augmented generation for knowledge-intensive NLP tasks, *Advances in Neural Information Processing Systems 33* (2020) 9459–9474.